100p.

N64-17700
CODE-1
CR-55927

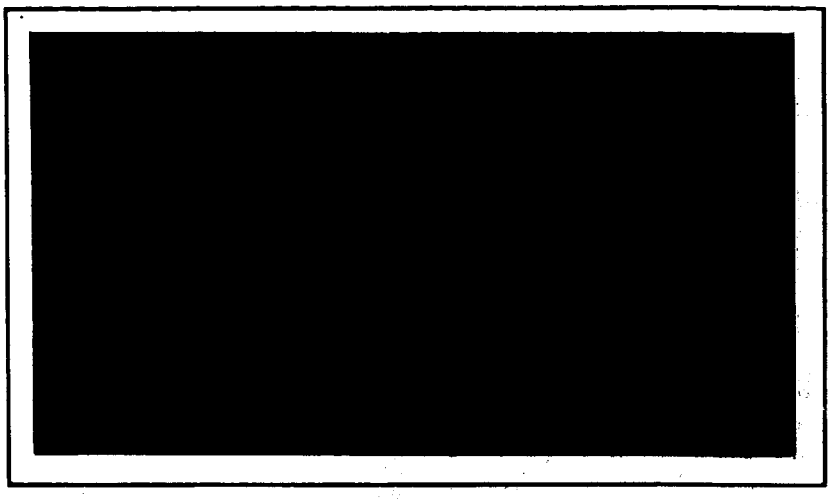

OTS PRICE

XEROX $ 8.60 ph

MICROFILM $ 3.20 mf

REPUBLIC
AVIATION CORPORATION

RAC-1333
(SSD-1027)
17 June 1963

SYNCHRONOUS METEOROLOGICAL SATELLITE (SMS) STUDY.

Volume 6:

System Synthesis and Evaluation

RAC 1333

Prepared for

NATIONAL AERONAUTICS AND SPACE ADMINISTRATION
Goddard Space Flight Center
Greenbelt, Maryland

under
Contract No. NAS5-3189

REPUBLIC AVIATION CORPORATION
Farmingdale, L.I., N.Y.

FOREWORD

This final report on Contract NAS 5-3189 is presented by Republic Aviation Corporation to the Goddard Space Flight Center of the National Aeronautics and Space Administration and consists of the seven volumes listed below. The period of the contract work was February through May, 1963.

The sub-titles of the seven volumes of this report are:

1 Summary and Conclusions

2 Configurations and Systems

3 Meteorological Sensors

4 Attitude and Station Control

5 Communications, Power Supply, and Thermal Control

6 System Synthesis and Evaluation

7 Classified Supplement on Sensors and Control

Except for Volume 7, all of these are unclassified. Volume 7 contains only that information on specific subsystems which had to be separated from the other material because of its present security classification. Some of these items may later be cleared for use in unclassified systems.

Volumes 3, 4, and 5 present detailed surveys and analyses of subsystems and related technical problems as indicated by their titles.

In Volume 2, several combinations of subsystems are reviewed as complete spacecraft systems, including required structure and integration. These combinations were selected primarily as examples of systems feasible within different mass limits, and are associated with the boosters to be available.

Volume 6 outlines methods and procedures for synthesizing and evaluating system combinations which are in addition to those presented in Volume 2.

Volume 1 presents an overall summary and the principal conclusions of the study.

TABLE OF CONTENTS

TABLE OF CONTENTS (Cont'd)

LIST OF ILLUSTRATIONS

LIST OF ILLUSTRATIONS (Continued)

LIST OF ILLUSTRATIONS (Continued)

LIST OF ILLUSTRATIONS (Continued)

SECTION 1 - INTRODUCTION

The purpose of this volume is to summarize the results of a parametric study of the Synchronous Meteorological Satellite (SMS) and to permit the user to develop configurations to fit his selected requirements. The basic parameter used to determine any configuration is sensor resolution.

By following the design steps outlined, the weight of a spacecraft configuration may be derived. It is emphasized that the weights obtained are the relative values of different configurations arrived at by following the same procedures. The actual weight value of a given configuration would depend on a detailed preliminary design.

Certain subsystems will be found to be insensitive to changes in resolution; these are discussed in Section 4. Subsystems which do change with resolution (sensitive subsystems) are described in Section 5. The step-by-step procedure to arrive at a configuration is presented in Section 6.

SECTION 2 - APPLICATION OF DESIGN PROCEDURES

The procedures outlined in this volume are applicable to 3-axis stabilized spacecraft in the approximate weight range of 400 to 1000 lb. Their purpose is to accomplish the following:

(1) Formulate a logical approach to the synthesis of an SMS spacecraft

(2) Relate system performance to vehicle size

(3) Permit a rough comparison of system configurations

(4) Provide a means of assessing the results of parameter variation

This volume is not intended to permit a detailed preliminary design, although it can serve as the framework for such. Its main utility is that it will permit a designer to select or assume certain basic parameters, and then, using this volume, to relate these assumptions to a final vehicle size and system performance, which can then be compared to those of other configurations.

Certain configurations and subsystems are excluded from consideration because of their special requirements. These are as follows:

(1) Spin-Stabilized Satellites. The requirements for image motion compensation and pointing of a narrow field camera influence the design to such an extent that this type of satellite is better considered separately

(2) Active Thermal Control Subsystems. The complexity of such devices and the nonavailability of hardware justifies this exclusion. The use of passive or semiactive thermal control subsystems permits them to be considered as part of the structure

(3) Minimum-Weight Spacecraft (under 300 lb). Weight control is of such overriding importance for these vehicles that a generalized design approach is not considered adequate to indicate performance capability

(4) Nonequatorial Synchronous Orbit Spacecraft. Consideration of injection error correction, identification of sensor aiming points, and consideration of design variation with orbit inclination require a specific treatment which is not covered in this volume

The major components of the SMS system are shown in block form in Figure 2-1. The overall system includes the ground stations and the ultimate users of the weather information, such as the National Meteorological Center (NMC), Area Forecast Centers (AFC), and local weather offices. This volume is only concerned with the synthesis and integration of the SMS itself, and not with the related systems.

The major subsystems of the SMS are as follows:

(1) Meteorological Sensors. These are the critical payload of the spacecraft, providing the basic information-sensing function. The sensors include wide- and narrow-angle cameras for cloud cover detection and infrared sensors for heat budget measurements

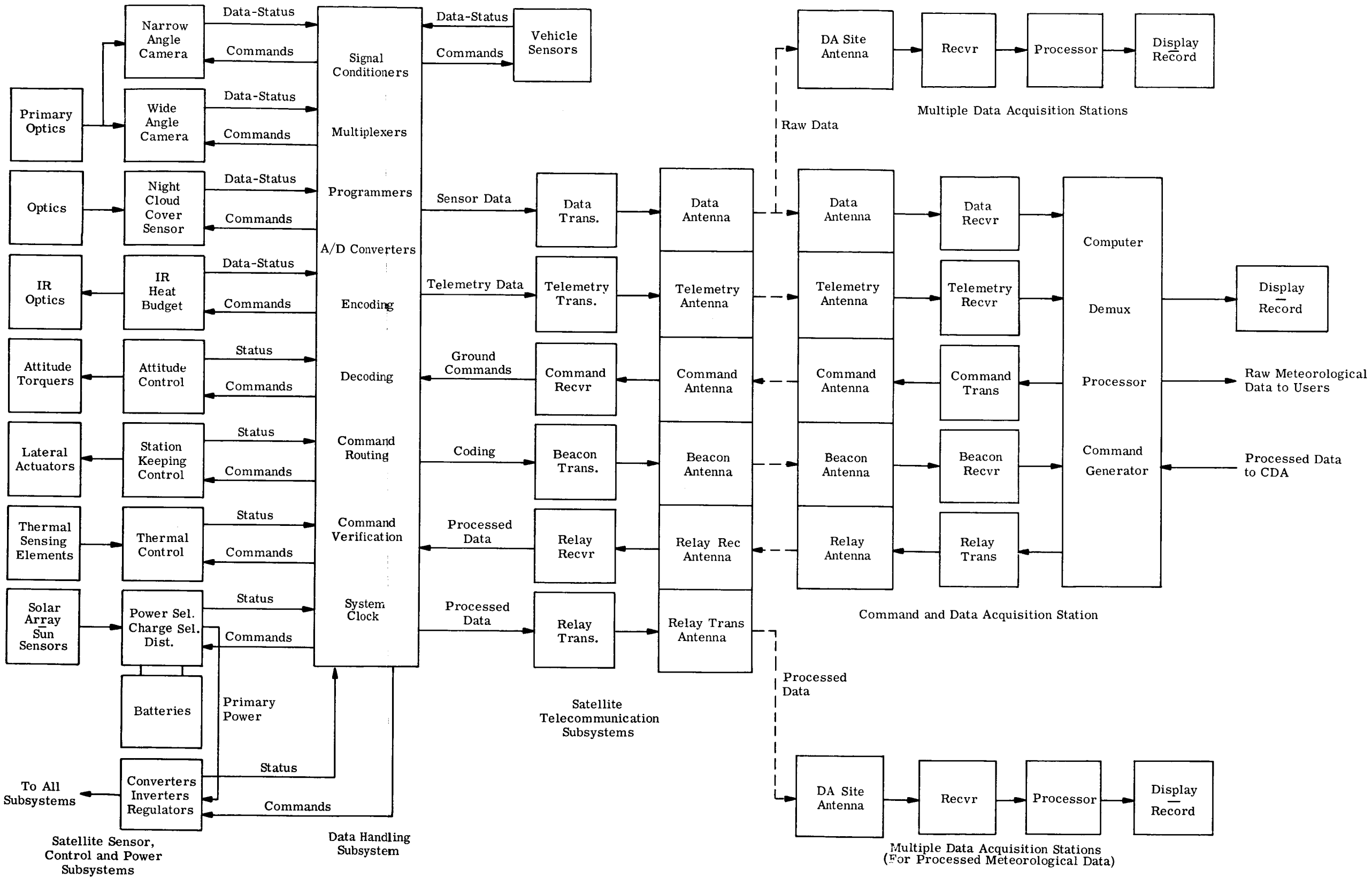

Figure 2-1. SMS System Block Diagram

(2) Guidance and Control. Provides for station-keeping and attitude control of the spacecraft

(3) Telecommunications. This subsystem includes telemetry, command, data transmission, communication relay, and tracking aids. It provides for monitoring spacecraft status, data transmission, relaying of processed meteorological data, and ground tracking of the spacecraft

(4) Data Handling. Provides for multiplexing, programming, encoding, decoding, verification, routing, conditioning, and timing of all information to and from the spacecraft

(5) Power. Provides the basic electrical power for all spacecraft subsystems

(6) Thermal control. Maintains the spacecraft within temperature design limits

(7) Structural Configuration. Provides the housing for all of the subsystems

The major components of the spacecraft subsystems are shown in tabular form in the following list:

Subsystem Components

Meteorological Sensors

Primary Optics
Scanning Mirror
Sensor Tubes (Vidicon and/or Image Orthicons)
Infrared Sensors
Gimbals and Drive Motors
Filters and Shutters
Amplifiers and Power Supplies

Guidance and Control

Horizon Sensors
Sun Sensors
Rate Gyros
Reaction and Constant-Speed Wheels
Gas and Bottles
Nozzles, Valves, Lines, and Regulators
Electronic Control Assembly

Telecommunications

Telemetry Data Transmitter
Sensor Data Transmitter
Tracking Beacon
Relay Receiver
Range and Range Rate (RARR) Transmitter-Receiver
Command Receiver
Antennas

Data Handling

- Commutators
- System Clock
- Coders and Decoders
- Signal Conditioners
- Storage Devices
- Command Verification, Programming, and Routing Logic

Power

- Solar Paddles and Drive Motors
- Batteries
- Control Electronics

Structural Configuration

- Basic Structure
- Thermal Control Devices
- Launch Vehicle-to-Spacecraft Adapter Ring

SECTION 3 - PRELIMINARY CONSIDERATIONS

A. INTERRELATIONSHIPS

There are several types of relationships that exist between the various subsystems of the SMS. Because of these relationships, the design of one subsystem more or less affects the design of related subsystems. It is important to have an understanding of these relationships during the design phase to simplify and facilitate the design procedure. The following paragraphs will qualitatively and briefly describe these relationships. Later sections of this volume will reduce these relationships to graphs and curves for design purposes.

Figure 3-1 illustrates the functional relationships that exist in the SMS system. When a request for meteorological information is received at the CDA station, the following sequence of events transpires:

(1) Telemetry and beacon data is examined to assess vehicle status, e.g., thermal and structural condition, subsystem operation, and attitude and position information

(2) Attitude and/or position commands, if required, are transmitted to the SMS and received through the command receiver

(3) These commands are verified through the SMS telemetry link

(4) Execute commands are transmitted to the SMS

(5) Desired attitude and/or position changes are verified through the telemetry and beacon links

(6) A command-verify-execute sequence is transmitted causing the sensors to commence data gathering

(7) Sensor data is passed through the SMS data handling and data link subsystems and transmitted to the CDA

(8) Processed sensor data is relayed through the SMS to the MDA stations

All of the seven SMS subsystems will be directly or indirectly involved in fullfilling this request for meteorological data. This, of course, is as it should be in an integrated, effective system. The meteorological sensors are the basic payload, and all other subsystems operate in support of them. In the same sense, the parameter specifications for all of the subsystems should directly or indirectly envolve from the characteristics of the meteorological sensors. However, not all subsystem components are affected to the same degree by a change in the meteorological sensor specifications. The degree of this dependence will now be discussed.

B. NON-SENSITIVE SUBSYSTEMS AND COMPONENTS

Certain subsystem components have a large degree of insensitivity to a change in the sensor specifications. For this reason, their design can be carried out for a large range of sensor parameters quite independently. These components, and a qualitative discussion of their relative independence, are as follows.

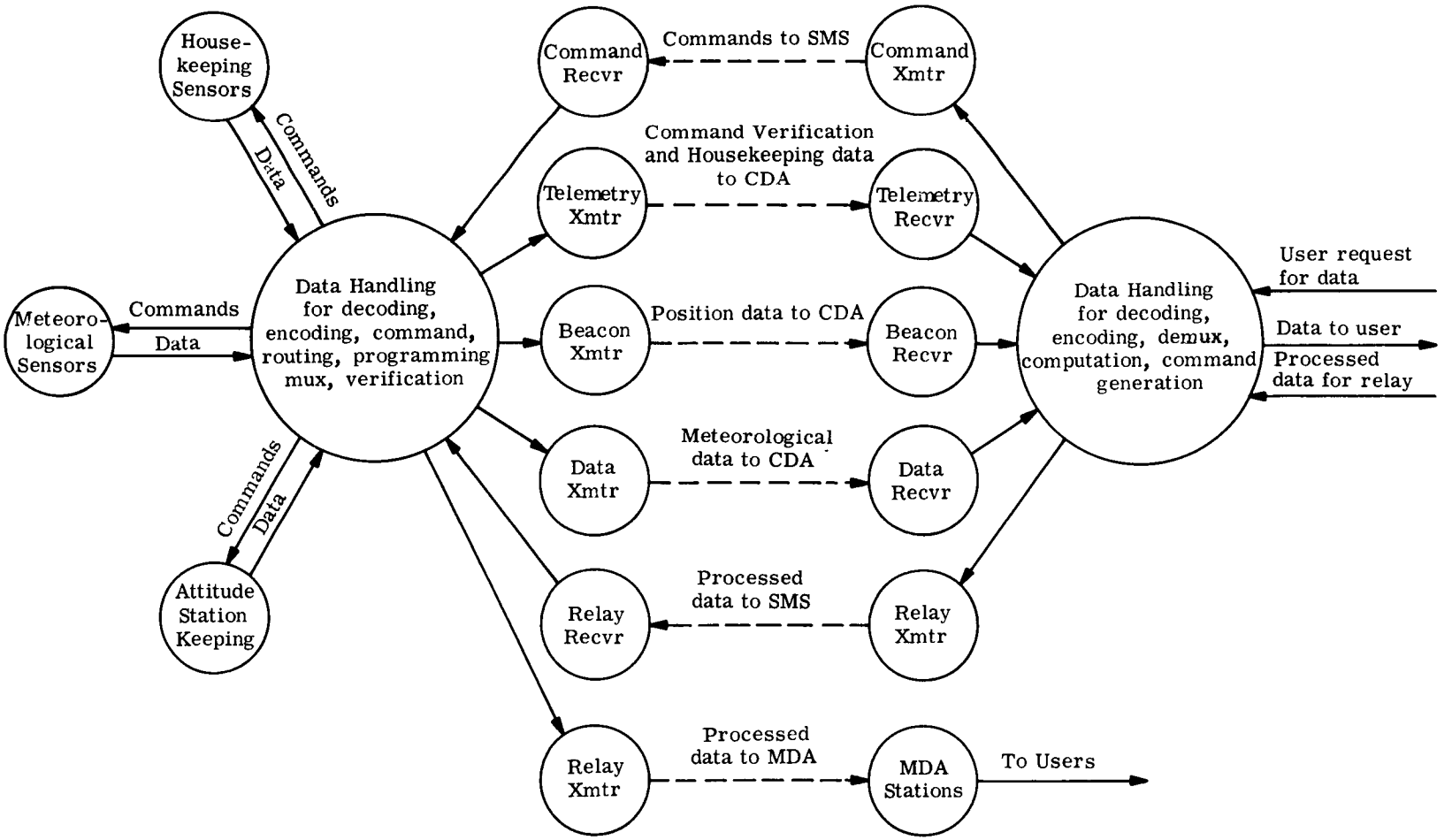

Figure 3-1. Functional Diagram - SMS System

1. Telemetry

The telemetry component of the telecommunications subsystem is considered to include only the amplifiers, modulators, output tubes, and antennas associated with the transmitter. All data processing, commutating, conditioning, etc., is done by the data handling subsystem. The major factors in telemetry transmitter design are the information bandwidth and link parameters. Since the SMS is in a stationary orbit, the link parameters are relatively invariant. For the same reason, the telemetry reporting cycle is not critical. Although an increase in sensor resolution presumably would result in a more complex vehicle and consequently greater telemetry requirements, the increased requirements can be handled by spreading out the time cycle. Thus, the telemetry transmitter can be made relatively insensitive over a wide range of sensor parameters.

2. Command

The command component of the telecommunications subsystem is considered here to include only the receivers and antennas, all data processing being done by the data handling subsystem. All the remarks made about the telemetry component apply as well to the command component. The receiver is designed around the required bandwidth and link parameters. An increase in the number of commands is handled by spreading out the time cycle, maintaining the bandwidth constant. It is assumed here that the command receiver will be designed to accommodate a PCM command system.

3. Tracking Aids

A tracking beacon is required during the ascent and orbiting phases. During ascent, a range and range rate system is desired. Once in orbit, the beacon merely has to provide a continuous, omnidirectional signal to permit the ground stations to track the SMS. Its specification is not directly related to the sensor resolution, and hence, it can be designed independently.

4. Relay Transmitter

The relay transmitter is determined by the link parameters and the nature of the processed information the CDA desires to relay. Although the basic content of some information may be determined by the sensor resolution, ground processing can reduce this dependence and permit relatively independent design of the relay transmitter. Processed data, such as weather maps, received from sources other than SMS may also be relayed.

5. Data Transmitter

This component includes only the amplifiers, modulator, output tubes, and antennas of the data link. All processing is done by the data handling subsystem. The determining factors in data transmitter design are the link parameters and the information bandwidth. The bandwidth required is a direct function of the sensor resolution, since no data storage is provided. The details of this relationship, along with tables, curves, and graphs, will be elaborated in Section 4, and a design procedure will be formulated.

C. SENSITIVE SUBSYSTEMS AND COMPONENTS

The following subsystems and components show differing degrees of sensitivity to the sensor resolution requirements. Changes in the sensors can affect the design of these subsystems. Hence, their design must be closely integrated.

1. Sensors

Variation in weight of the sensors is directly dependent on resolution. A major item is the weight of the optics. Selection of specific sensor tubes for cloud cover pictures will also introduce changes in physical size and power requirements, although the changes will not vary as widely with a change in resolution as does the weight of the optics.

2. Guidance and Control Subsystem

This subsystem, although not electrically connected to them, is strongly dependent on the sensors for its specifications. The relationship is complex, involving shutter speed, illumination level, system size, angular drift, etc. Section 4 will discuss in detail the relationship and design procedures.

3. Data Handling Subsystem

This subsystem is principally determined by the data, telemetry, command, and programming requirements. Depending on whether digital or analog techniques are used for the data, it becomes more or less dependent on the sensors. In some cases it may be possible to specify it, at least for a wide range of sensor parameters, independently of the sensors. The details of design and selection will be covered in Section 4.

4. Power Subsystem

Since this subsystem provides power for all the subsystems, it is strongly dependent on the sensor specifications. The nature of the SMS orbit greatly relieves its dependence on orbital parameters in two ways. First, the occult periods are very brief and occur infrequently, thus lessening the energy storage requirements. Second, the fixed position of the satellite relative to the Earth removes the need for sudden high peak powers during brief readout periods, as is the case with orbiting satellites. The sensitivity of the power subsystem to sensor parameters is further increased by the number of sensitive subsystems and components. Each change in sensor resolution is reflected several times in different sensitive subsystem power requirements. Design procedures will be detailed in Section 4.

5. Structural Subsystem

This subsystem reflects its dependence on the sensor resolution both directly and indirectly. Increased resolution requires a greater volume for the sensor optics, which affects the structure. At the same time, the sensitive subsystems will require greater volume, also placing demands on the structure. Also, the attitude subsystem is directly affected by the vehicle size and reflects again on the structure.

6. Thermal Control Subsystem

Increased sensor capability requires more power and more sensitive components. This, in turn, requires greater means for heat dissipation and closer temperature control for the more sensitive components.

SECTION 4 - NON-SENSITIVE SUBSYSTEMS AND COMPONENTS

Non-sensitive subsystems and components are defined as those whose weight and power requirements do not change materially with a change in sensor resolution. These subsystems and components, and their characteristics, are described in this section. They include:

(1) Sensor Data Transmitter
(2) Command Link
(3) Telemetry Link
(4) Tracking Aids
(5) Communications Relay Link
(6) Data Handling Subsystem

A. SENSOR DATA TRANSMITTER

1. Design Considerations

A suitable sensor data transmission component should possess the following characteristics:

(1) Transmission of sensor data information with minimum degradation

(2) A ground receiver signal-to-noise output ratio such that no apparent noise or picture degradation appears

(3) Use of the lowest necessary transmitter radiated power in order to achieve objectives (1) and (2) above. This will in turn define the DC input power drain

2. Component Restraints

The radio frequency allocations for this component have been discussed in Volume 5. The proposed FCC allocations for meteorological satellite service plus current design techniques indicate the use of a frequency range between 1700 and 2300 MC with preference for the range of 1700 to 1800 MC for the down link.

3. Design Procedure

The required transmitter power can be calculated from the following expression:

$$P_{T\ dbw} = \left[\alpha + C/N + L_o - G_T - G_R + P_n \right] \text{ in db} \qquad (1)$$

or by use of the nomograph Figure 4-1.

A typical design example will illustrate the design procedure. The following parameters are known:

(1) Carrier frequency, F = 1800 MC

(2) Sensor data maximum base bandwidth, B = 100 KC

(3) Free-space loss plus atmospheric losses (30° elevation angle), $\alpha = -189.5$ db

(4) Fading, line, polarization, and incidental losses, $L_o = -13$ db

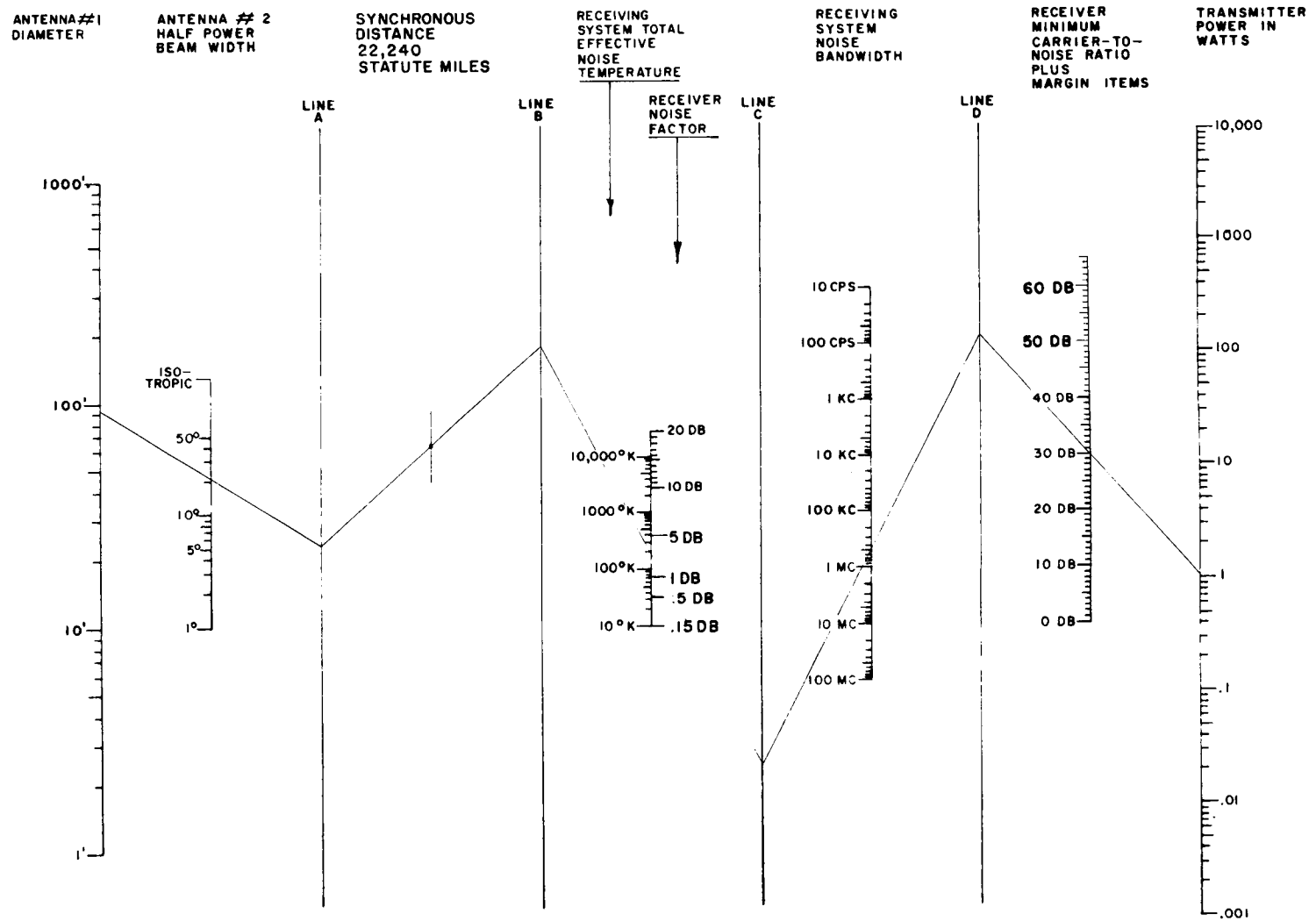

Figure 4-1. Satellite Communications Nomograph (Assumed Antenna Efficiency - 55%)

(5) Receiver total effective noise temperature, (NF = 1.8 db), T_e = +170°K

(6) Sensor output S/N = +40 db

(7) Required receiver S/N (for 1 db degradation of sensor S/N) = +46 db

(8) Satellite antenna gain for 21° beamwidth, G_T = + 18 db

(9) Ground antenna gain (85-ft diam.), G_R = +51 db

The unknowns in Eq (1) above require a knowledge of the ground receiver noise bandwidth, which in turn is a function of the type of transmission system employed.

The minimum receiver noise bandwidth for an SSB system is the same as the base bandwidth, B, while the output S/N is the same as the carrier C/N. For AM transmission, the minimum receiver noise or IF bandwidth is twice the base bandwidth or 2B, and the output S/N is the same as the input C/N, the same as for an SSB system.

In the case of an analog-transmission type FMFB system, the necessary transmitter power output (P_t), as well as the receiver noise bandwidth and required C/N ratio, can be obtained by observing the following procedure:

(1) A threshold C/N corresponding to a large modulation index is required. This can be obtained from Figure 4-2. Let the threshold C/N = 17 db

(2) The output S/N improvement above threshold can be determined:
S/N Improvement = Required receiver output S/N - Threshold C/N
= 46 db - 17 db
= 29 db

(3) The transmitter modulation index, m, for a given S/N improvement above threshold can be obtained from Figure 4-3. The transmitter modulation index, m_{RF} = 16.3 for a 29 db improvement ratio

(4) The optimum feedback factor, F, for an FMFB system can be obtained from Figure 4-4. Compare the transmitter modulation index against the receiver output S/N

For m_{RF} = 16.3 and S/N = 46 db,

F = 20 db or a voltage ratio of 10:1

(5) The IF amplifier modulation index is:

$$m_{IF} = \frac{M_{RF}}{F}$$

$$m_{IF} = \frac{16.3}{10} = 1.63$$

(6) The minimum receiver IF or noise bandwidth is:

$$B = 2\ (1 + m_{IF})$$

$$B = 2\ (1 + 1.6) = 0.52\ MC$$

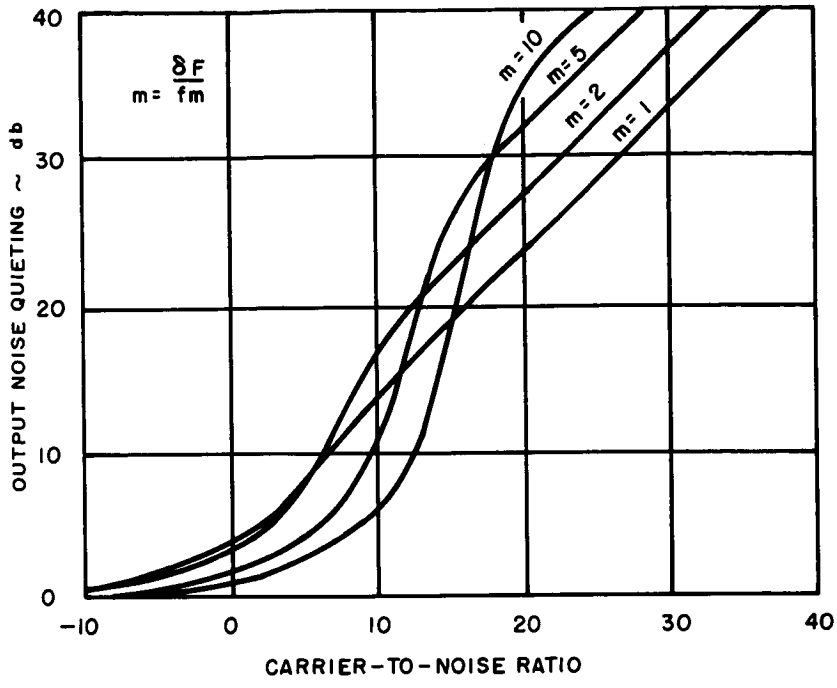

Figure 4-2. Typical FM Threshold Curves

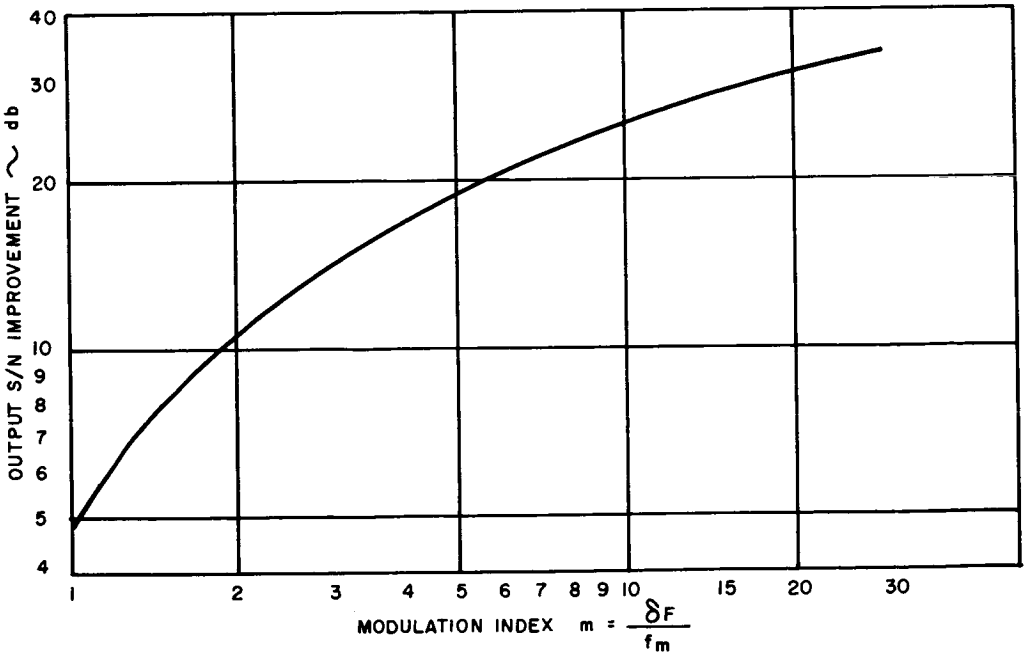

Figure 4-3. FM Improvement in db vs Modulation Index above Threshold

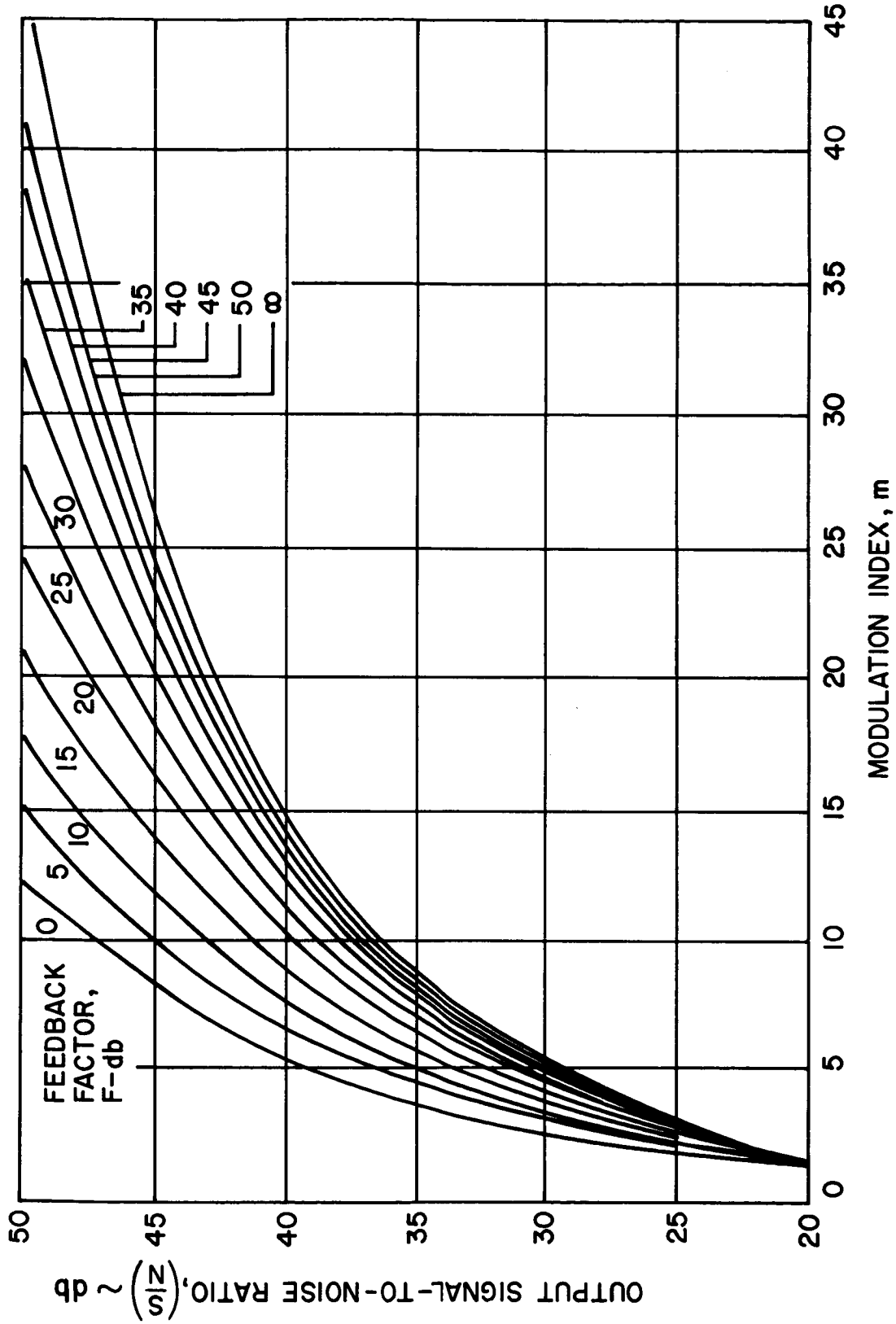

Figure 4-4. Design Parameters for Optimum Feedback FM Systems

(7) The receiver noise power for a given IF bandwidth (B) and total effective noise temperature (T_e) can be obtained from Figure 4-5.

For B = 0.52 MC and T_e = 170°K

P_n = - 149.3 dbw

(8) The required transmitter power can be calculated from

$$P_t = \alpha + C/N + L_o - G_R - G_r + P_n$$

$$= 189.5 + 17 + 13 - 51 - 149.3$$
$$= 1.2 \text{ dbw}$$
$$= 1.3 \text{ watts}$$

The same results can be obtained more readily by use of the nomograph Figure 4-1. The value of L_o should be added to the required C/N ratio.

The calculations for a digital-type transmission system, PCM - Bi phase, are as follows:

(1) The sampling rate is twice the base bandwidth:
Sampling rate = 100 KC x 2 = 200 KC

(2) The required number of bits to which each sample must be encoded in order not to degrade the required output S/N is:

$$db = 10.8 + 6n \text{ or } n = \frac{db - 10.8}{6}$$

$$n = \frac{46-10.8}{6} = 6 \text{ bits per sample}$$

(3) The resultant pulse or bit rate equals:
Bits per sample x Sampling rate

6 x 200 KC = 1,200,000 or 1.2×10^6 bits/sec

(4) The realizable practical video bandwidth is equal to the bit rate
Video bandwidth = Bit rate = 1.2 MC

(5) The IF bandwidth (B) required for both sidebands is
$B = 2 f_m$
= 2 x 1.2 MC = 2.4 MC

(6) The receiver noise power for a given IF bandwidth (B) and the total effective noise temperature (T_e) can be obtained from Figure 4-5.

For B = 2.4 MC and T_e = 170°K,

P_n = - 142.5 dbw

(7) The minimum C/N requirement is based upon the allowable error rate for the total number of bits in a single frame. The transmission time for each frame will be 10 seconds, resulting in a bit rate ten times the value of (3) above. The C/N value for any error rate can be obtained from Figure 4-6 for the PCM-PM Local Reference curve case

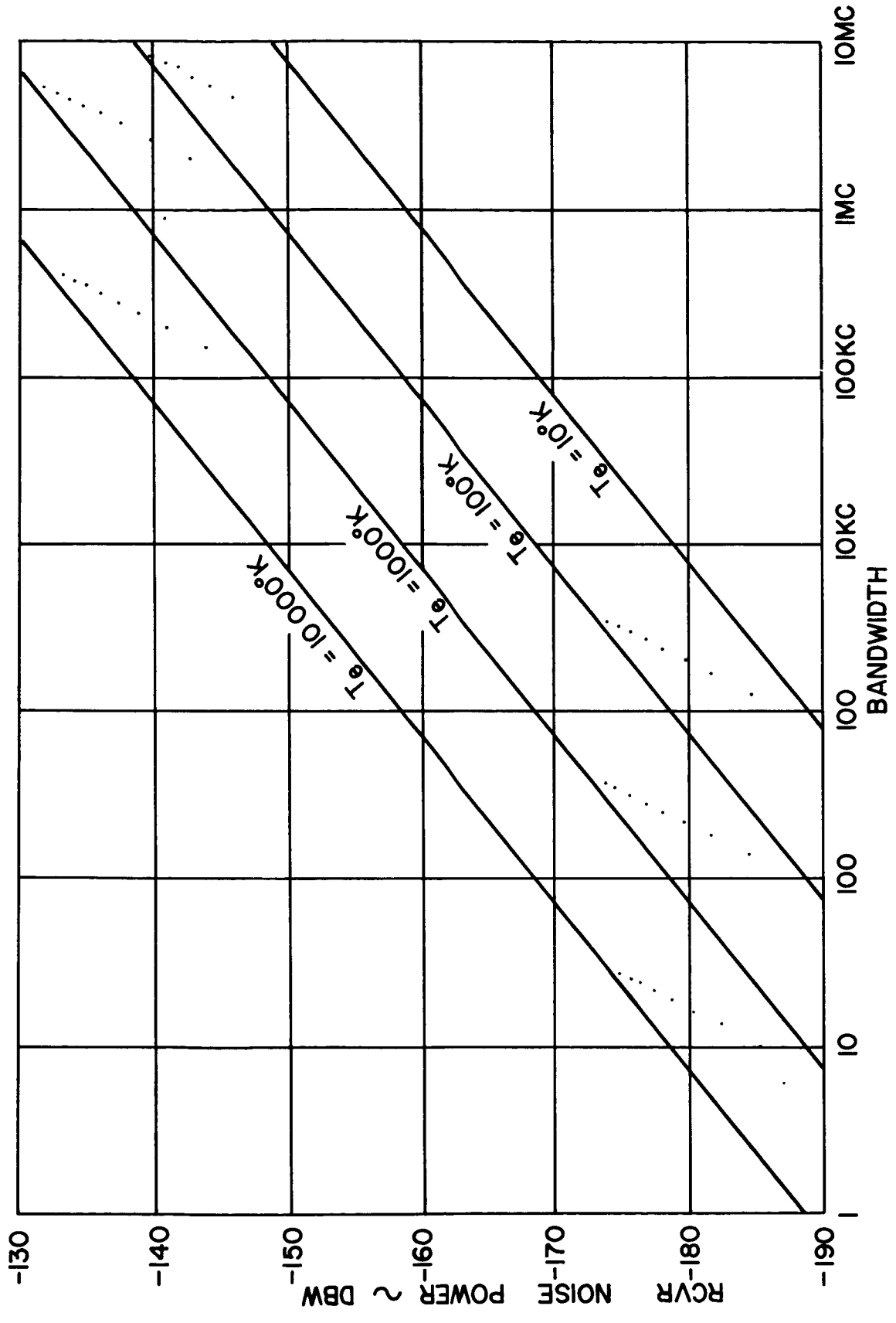

Figure 4-5. Receiver Noise Power vs Bandwidth for Various Total Effective Noise Temperature

Total bit rate = $10 \times 1.2 \times 10^6 = 1.2 \times 10^7$. The required C/N ratio for a 10^7 error rate, or approximately one bit error per picture, can be obtained from Figure 4-6 (12 db)

(8) The required transmitter power can be calculated from:

$$P_t = \alpha + C/N + L_o - G_R - G_t + P_n$$
$$= 189.5 + 12 + 13 - 51 - 81 - 142.5$$
$$= 3.0 \text{ dbw}$$
$$= 2.0 \text{ watts}$$

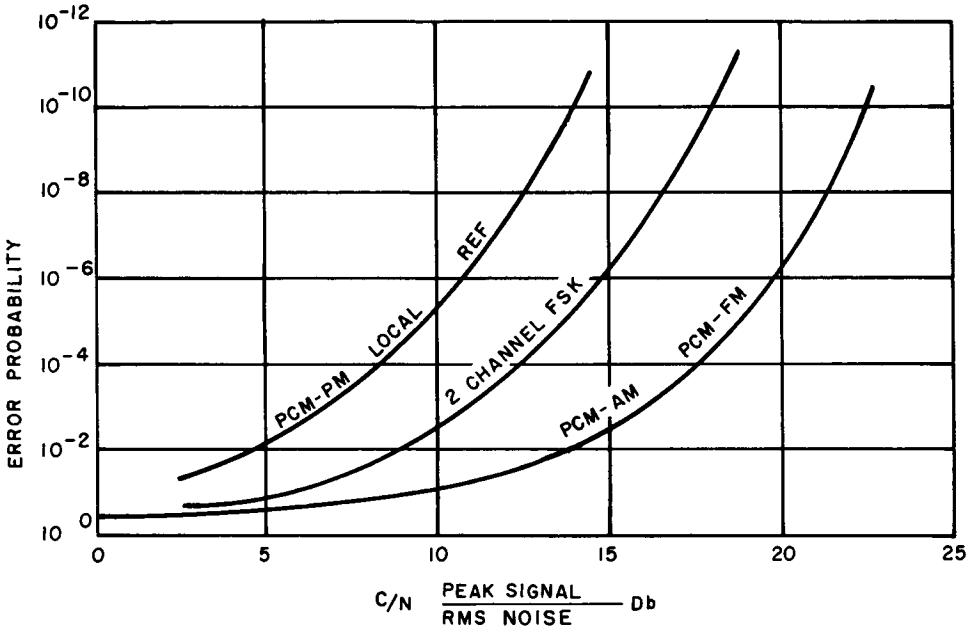

Figure 4-6. Error Probability

The weights and volumes of the items comprising the sensor data transmission link aboard the spacecraft are relatively non-sensitive for the given video bandwidth, 100 KC.

Table 4-1 gives the characteristics of these items for several feasible power outputs for a 3-axis stabilized satellite. The lower power output will result in a 6 db lower C/N ratio at the ground receiver.

TABLE 4-1
SENSOR DATA TRANSMITTER SIZE

Item	2.5-watt Transmitter		10-watt Transmitter	
	Weight (lb)	Volume ($in.^3$)	Weight (lb)	Volume ($in.^3$)
Output Stage (TWT)	1.5	20	1.8	41
Output Stage H. V. Supply	4.0	120	6.0	200
R. F. Driver	2.0	75	2.0	75
Parabolic Antenna	3.5	-	3.5	-
Total	11.0	215	13.3	316
Total Power	20 watts (50% duty cycle)		55 watts (50% duty cycle)	

B. COMMAND LINK

1. System Restraints

The preliminary draft of the NASA document "Standards for Tone Digital Command Systems" states that the ground command data transmission system shall be AM and operate in the 148 to 150 MC band.

In addition, all NASA command stations throughout the free world in conjunction with present or planned communications and meteorological satellites operate in the 148 MC band, with AM modulation.

2. Design Procedure

A satisfactory value of carrier-to-noise ratio, C/N, for command data reception in an AM-type system is 25 db.

The required ground transmitter power can be calculated from:

$$P_{T\ dbw} = \left[\alpha + C/N + L_o - G_T - G_R + P_n\right] \text{ in db}$$

or by use of the nomograph Figure 4-1.

Since this is an AM-type transmission, the output signal-to-noise ratio, S/N, is identical to the input carrier-to-noise ratio, C/N.

A typical design example will illustrate the design procedure. The following parameters are known:

(1) Carrier frequency, F = 148 MC

(2) Free-space loss plus atmospheric losses (30° elevation angle), α = 168 db

(3) Total effective noise temperature (Earth temp. of 290°K + cosmic noise contribution, from Figure 4-7, and 5 db NF), T_e = 1060°K

(4) Highest command subcarrier frequency = 11 KC

(5) Ground transmitter frequency drift = ±0.001% or ±1.48 KC

(6) Receiver local oscillator frequency drift = ±0.003% or ±3.5 KC

(7) Maximum doppler shift during transfer ellipse = -0.0034% or - 5 KC

(8) Based on the above, the receiver IF bandwidth, B = 50 KC

(9) Ground antenna gain (3 element helix), G_T = 20 db

(10) Satellite antenna gain, G_R = -3 db

(11) Diplexer loss + fading margin, L_o = 12 1/2 db

(12) C/N = 25 db

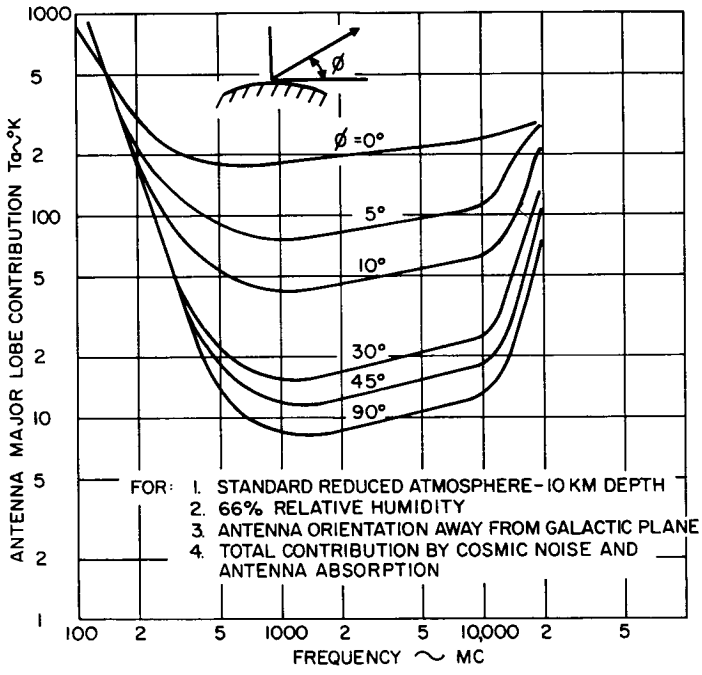

Figure 4-7. Equivalent Antenna Temperature vs Frequency

The receiver noise power for a 50 KC bandwidth and 1060°K noise temperature can be found from Figure 4-5:

P_n = 151.5 dbw

$P_T = \alpha + C/N + L_o - G_T - G_R + P_n$

= 168 + 25 + 12.5 - 20 + 3 - 151.5

= 37 dbw

P_T = 5000 watts

3. Other Characteristics

The weights and volumes of the command receiver link are non-sensitive. A suitable proportional factor for estimating the receiver weight is to use a value of 1 ounce per cubic inch of volume. Thus a 10 cubic inch receiver, which is a typical value, should weigh approximately 10 ounces. The turnstile antenna will weigh approximately 0.5 lb regardless of the satellite configuration.

C. TELEMETRY LINK

The factors from which the telemetry power can be determined are the telemetry information capacity in bits per second, the accuracy requirements of the voltages being telemetered, and the link parameters. These determine the IF bandwidth and the IF carrier-to-noise ratio, using Figure 4-8 and Table 4-2, respectively. Figure 4-8 shows the minimum telemetry bandwidth as specified by NASA.

TABLE 4-2
RMS ERROR vs SIGNAL NOISE RATIO

Telemetry Bit Detection Error	FM Receiver IF Carrier-to-Noise Ratio	Telemetry Signal Voltage Approximate RMS Error
1 error in 10^6 bits	12-15 db	0.1%
1 error in 10^3 bits	8-12 db	2%
1 error in 10 bits	3-5 db	20%

The minimum telemetry power required can then be found from Figure 4-9 which shown telemetry power versus IF bandwidth for various C/N ratios. This graph is based upon assumed values such as a receiver antenna gain of 14 db, an antenna temperature of 1000°K, no atmospheric losses, a polarization loss of 3 db, a pointing loss of 1 db, coupling losses of 0.8 db, and a receiver noise figure of 3 db. The transmitter antenna gain is assumed to be -3 db since it is an omnidirectional type that must function during tumbling. The telemetry antenna array would be a turnstile consisting of four monopole units, each 22 in. long, spaced 90° around the circumference of the SMS. The weight and volume of telemetry transmitter packages does not vary significantly for power output levels up to approximately 5 watts. An illustrative example of telemetry transmitter selection is given in the following:

Step 1: Select the information capacity of the telemetry system.
Example: 100 bits per second

Step 2: Determine receiver minumum IF bandwidth from Figure 4-8
Example: Referring to this graph, the minimum IF bandwidth for 100 bits per second is 150 cps.

Step 3: Select desired accuracy of voltages to be telemetered.
Example: Sun sensors may require accuracies to 0.1% for pitch or yaw.

Step 4: Determine carrier-to-noise ratio required from Table 4-2.
Example: Referring to this table, for an accuracy of 0.1%, the required carrier-to-noise ratio is 12 to 15 db. Assume a value of 13 db.

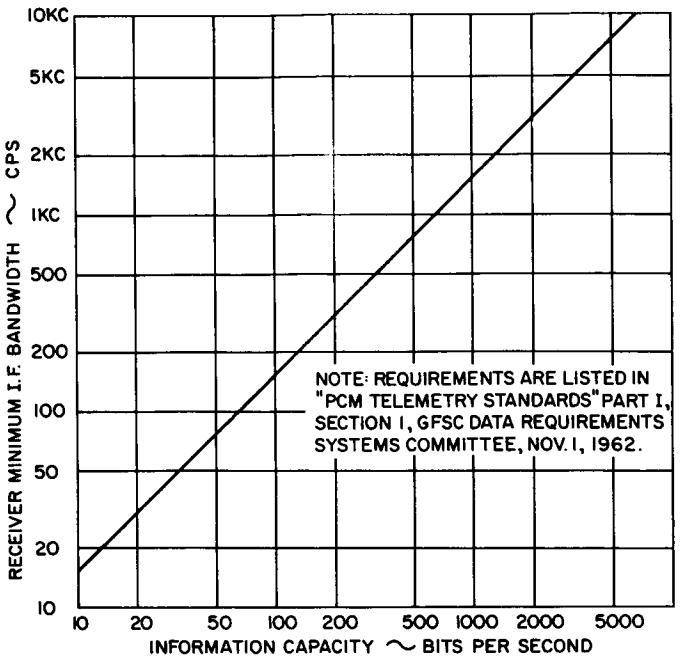

Figure 4-8. Minimum IF Bandwidth vs Bit Rate for PCM Telemetry

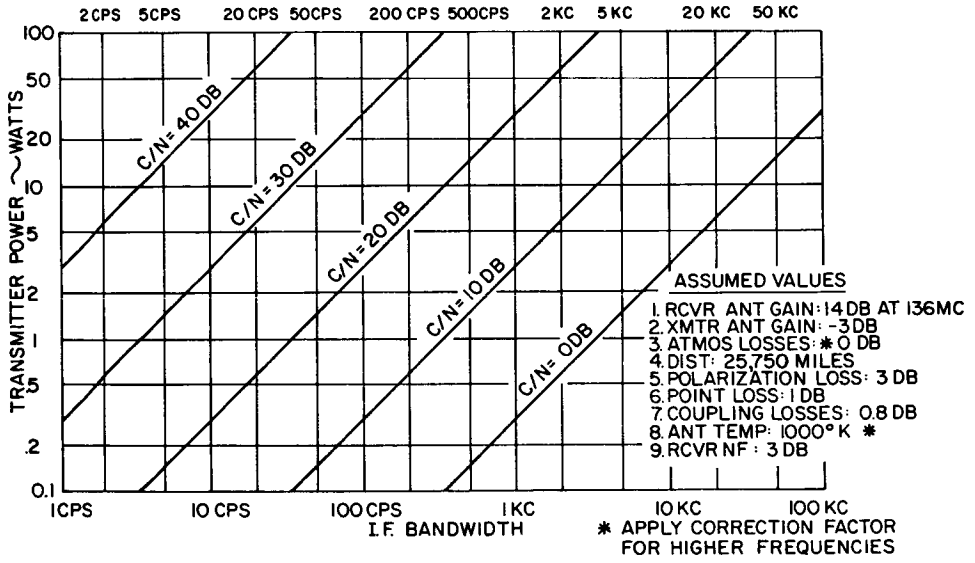

Figure 4-9. Telemetry Power vs Bandwidth for Various C/N (P_T vs B)

Step 5: When the minumum IF bandwidth and the carrier-to-noise ratio have been established, refer to Figure 4-9 to obtain the minimum telemetry power. Modify the power for different assumed values than those shown on the graph. Example: For an IF bandwidth of 150 cps and a carrier-to-noise ratio of 13 db, the telemetry power would be approximately 0.9 watts.

Step 6: Add a margin to the minimum telemetry power obtained in Step 5. Example: Adding a 3 db margin, the telemetry power of Step 5 would be increased to 1.8 watts.

Step 7: Weight and volume.
The weight and volume of a typical unit would be 1.5 lb and 23 cubic inches, respectively.

D. TRACKING AIDS

The tracking of the SMS during the early phases of launch and station acquisition would be performed by the Goddard Range and Range Rate (RARR) stations and Minitrack facilities. The RARR system requires the use of a frequency-coherent transponder system aboard the SMS. This is capable of operation with two types of transponders, one being at VHF frequencies (136-148 MC) and the other at S-Band frequencies (2270-1705 MC).

The following tabulation gives the approximate equipment accuracies and characteristics of each system:

RARR System	VHF	S-Band
Equipment Accuracy (approximately)		
Range	± 75 meters	± 15 meters
Range Rate	± 1 meter/sec	± 0.1 meter/sec
Angular Accuracy	Approx. 1°	Approx. 0.1°
Operating Distance	150-60,000 km	150-60,000 km
Frequency - Up Links	148.26 MC	2270.933 MC
Frequency - Down Links	136.11 MC	1705 MC
Highest Sidetone Frequency	20 KC	100 KC
Down Link Power	Up to 4 watts	Up to 2 watts
Down Link Antenna Gain	0 db	0 db
Ground Antenna Beamwidth	17°	2.5°

The VHF RARR system is not favored for future applications because a wide bandwidth is required for accurate measurements (up to 500 KC). This may not be available for allocation several years hence, so that the S-Band system would be preferable.

A VHF beacon at 136 MC is required for acquisition by the RARR ground station antennas. It is also used for tracking by Minitrack stations.

To conserve weight, it is desirable that the special instrumentation required for tracking measurements utilize as much of the existing equipment already on board (such as telemetry and sensor data transmitters) as is possible.

1. VHF Range and Range Rate System

The VHF system is intended for low weight satellites where the command and telemetry systems can be adapted for RARR measurements. Therefore, the design procedures given for the command and telemetry systems in subsections B and C would apply. Additional circuitry for making these units frequency-coherent would be required. However, this would not add significant weight or size to the telemetry and command systems already on board the SMS.

2. S-Band Range and Range Rate System

The S-Band transponder would use the sensor data transmitter of the SMS. This is feasible since there would be no sensor data transmissions when range and range rate measurement are required during the early phases of launch and station acquisition. The design procedures given for the sensor data transmitter in subsection A would apply.

An S-Band receiver for the transponder would be required in addition to the equipment already on board the SMS. This unit would be frequency-coherent and include a frequency-coherent driver for the sensor data transmitter. The S-Band receiver would be the same unit as described in the design procedure for the communications relay in subsection E, and its weight and size would not vary significantly with satellites of different capabilities.

An S-Band non-directional antenna is required for RARR measurements during launch and station acquisition when tumbling may occur. This would be used only during the early phases of operation, and the normal sensor data parabolic antenna would be used when the SMS is on station. A suitable design for a non-directional antenna would be a skirted dipole, 3/4 inches in diameter and 15 inches long, and with a weight of 0.5 lb. Its weight and size would not vary significantly with satellites of different capabilities.

3. VHF Beacon

The VHF beacon used for RARR acquisition and Minitrack station tracking could utilize the telemetry transmitter already on board. This would be placed in beacon mode by removing modulation and reducing carrier output to conserve power. Therefore, no additional weight or size would be required for the beacon.

E. COMMUNICATIONS RELAY LINK

The function of a relay system would be to rebroadcast processed meteorological information via the SMS to weather stations in various localities and to existing ground data-receiving stations. The important considerations in the design of the relay are the rate at which information is to be transmitted (baseband frequency) and the weight allotted for this function. Teleprinters operating at 60 to 100 wpm require baseband frequencies of up to 100 cps. High speed teleprinters require baseband frequencies of up to 750 cps while facsimile systems require the baseband frequencies shown in Figure 4-10. This graph shows the baseband frequency of a particular facsimile picture as a function of transmission time.

To conserve weight, it is desirable that the special instrumentation required for the relay function utilize the existing equipment already on board (such as the telemetry and sensor data transmitter). The transponder relay could therefore consist of the command receiver-telemetry transponder at VHF frequencies (see Figure 4-11) or an S-Band receiver-sensor data transmitter at S-Band frequencies (see Figure 4-12). The VHF relay is suitable for low information rates with baseband frequencies up to several KC. The S-Band relay is more suited to wideband data up to 100 KC. The selection of which relay system to use depends upon the weight allotted for this function.

The VHF relay could be part of the command-telemetry system with no additional weight required. It would thus be suitable for a low-weight SMS. The relayed information would be time-shared with telemetry and be limited to single-channel teletype or long readout time facsimile.

The S-Band relay would require an S-Band receiver in addition to the sensor data transmitter. The S-Band receiver would be a solid state unit weighing 3 lb, occupying a volume of 100 cubic inches, and consuming 3 watts. This unit would be the same as that used for range and range rate (RARR) measurements. The characteristics of the S-Band receiver would not vary significantly with satellites of different capabilities. S-Band receivers have been developed for other satellite programs such as EGO and are readily available. The sensor data transmitter would be time-shared or frequency-multiplexed for relay operation. Alternatively, with a wideband output stage such as TWT, separate drivers at different frequencies could be used for sensor data and relay transmissions. The S-Band relay would be suitable for medium and heavier SMS systems. An example of a power budget for the relay link is shown in Table 4-3.

TABLE 4-3
EXAMPLE OF S-BAND RELAY POWER BUDGET

A.	Ground-to-Spacecraft Link	
	Ground Transmitter Power (1 KW - 2200 MC)	+30 dbw
	Ground Antenna Gain (85-ft dia. parabolic)	+53 db
	Free-Space Loss (2300 MC at 25,750 miles)	-192 db
	Spacecraft Antenna Gain	+19 db
	Miscellaneous Losses	- 5 db
	Received Signal Power	-95 dbw
	S-Band Receiver NF	5 db
	S-Band Relay Antenna Temperature (t_a)	400°K

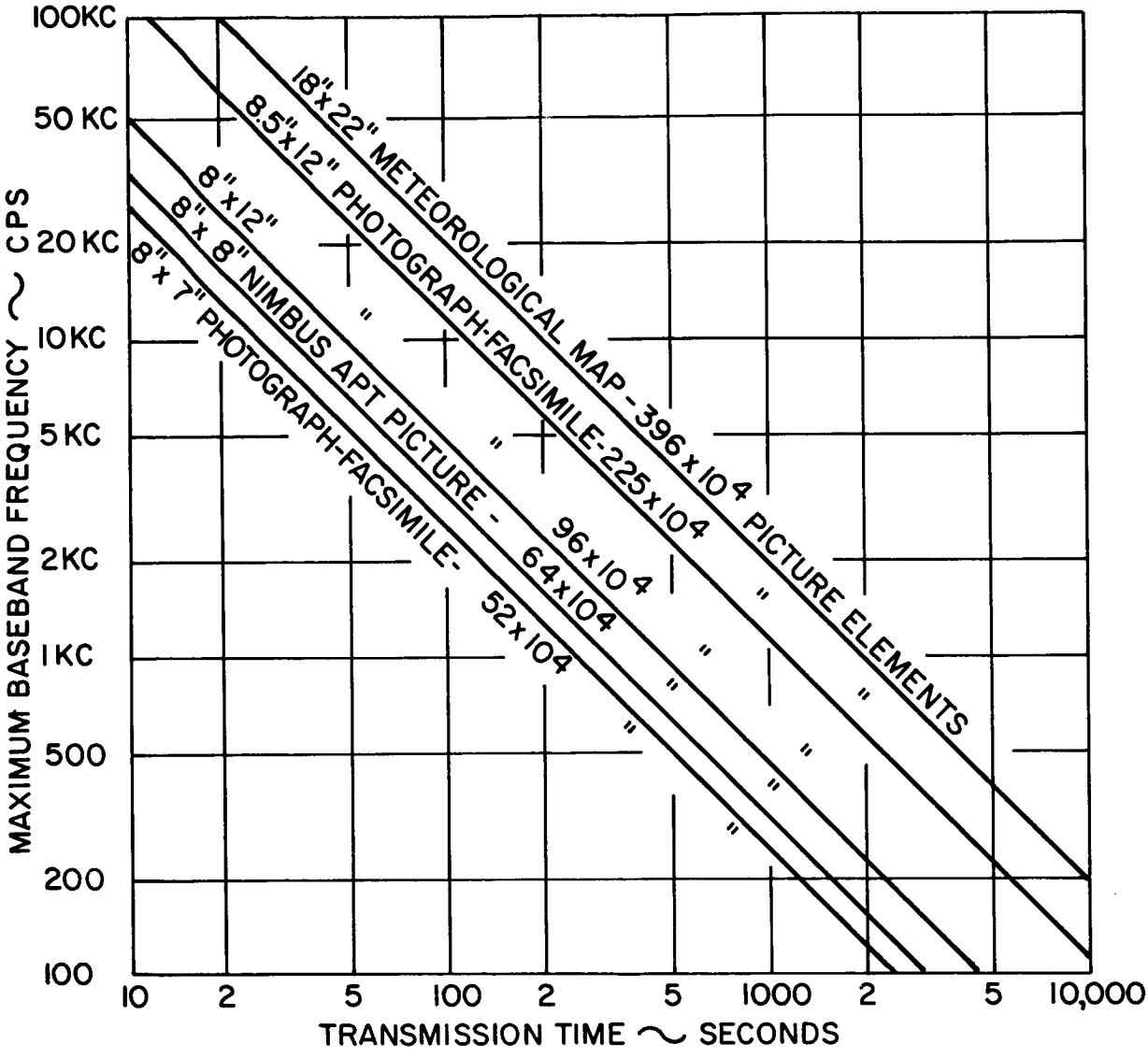

Figure 4-10. SMS Transponder Relay Baseband Frequency vs Transmission Time for Facsimile Pictures

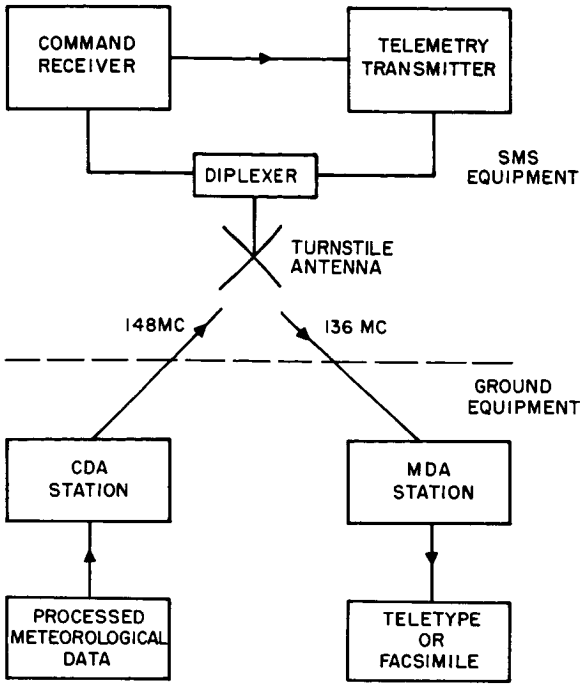

Figure 4-11. VHF Transponder Relay

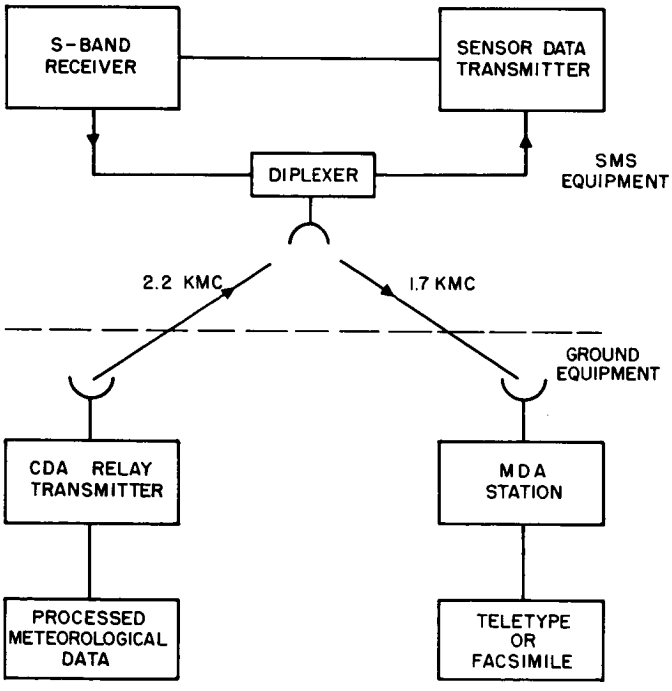

Figure 4-12. S-Band Transponder Relay

TABLE 4-3
EXAMPLE OF S-BAND RELAY POWER BUDGET (Cont'd)

A.	Ground-to-Spacecraft Link (Cont'd)		
	S-Band Receiver Temperature (t_r)	290 (NF-1) =	620°K
	Total Effective Temperature ($t_e = t_a + t_r$)		1020°K
	S-Band Relay Receiver Bandwidth		600 KC
	S-Band Relay Receiver Noise Power ($P_M = kt_e B$)		-140 dbw
	Received Carrier-to-Noise Ratio		+45 db
B.	Spacecraft-to-Ground Link		
	S-Band Relay Transmitter Output* (1 w at 1700 MC)		0 dbw
	Spacecraft Antenna Gain (21-in. dia.)		+17 db
	Free-Space Loss (1700 MC at 25,750 miles)		-190 db
	Miscellaneous Losses		-6 db
	Ground Antenna Gain (30-ft dia.)		+41 db
	Received Signal Power		-138 dbw
	Receiver NF		3.5 dbw
	Receiver Noise Temperature (t_r)	290 (NF-1) =	350°K
	Antenna Noise Temperature	t_a =	100°K
	Total Effective Noise Temperature ($t_e = t_r + t_a$)		450°K
	Baseband Frequency		0-1800 cps
	18 in. x 22 in. Facsimile Weather Map Transmission Time		1100 sec
	Subcarrier Frequency		3600 cps
	Highest Modulating Frequency	1800 + 3600 =	5400 cps
	Deviation Ratio		2
	RF Spectrum Bandwidth ($BW = 2(1 + D)f_m$) (for 99% energy)		32,000cps
	Receiver Noise Bandwidth		50 KC
	Receiver Noise Power ($N = K T_e B$)		-155 dbw
	Carrier-to-Noise Ratio		17 db
	Output Signal-to-Noise Ratio		24 db

* The S-Band relay transmitter output is assumed to be derived from the output stage of the sensor data transmitter. A wideband TWT output stage is assumed, and separate drivers are used for sensor data and relay transmissions. Therefore, relay transmissions can be obtained simultaneously with sensor data transmissions.

F. DATA HANDLING SUBSYSTEM

1. Command Link - Data Handling

The data handling portion of the command link shows a change of only eighteen commands out of a total of 100 in going from a minimum performance vehicle with 2200 picture elements per second to a maximum performance vehicle with 64,000 picture elements per second. This in itself represents no important change in requirement. The choice open to a designer then is whether to use a

PCM system alone, a Tone Digital System alone, or both. The considerations for making this choice are covered in Volume 5.

A command system using only a Tone Digital System will occupy 116 cubic inches, weigh 5.3 lb and consume 8.4 watts of power; a command system using only PCM will occupy 113 cubic inches, weigh 4.6 lb, and consume 6.3 watts of power; and a command system using both PCM and a Tone Digital System will occupy 210 cubic inches, weigh 8.8 lb, and consume 11.3 watts of power.

2. Telemetry Link - Data Handling

The data handling portion of the telemetry link shows a change in pulse rate of 20 pulses per second out of 200 pulses per second in going from a minimum performance vehicle with a sensor data output of 2200 picture elements per second to a maximum capability vehicle with a sensor data output of 64,000 picture elements per second. This is a negligible change in the system's requirement and will not affect the parameters of the telemetry data handling system. The telemetry data handling system will occupy 663 cubic inches, weigh 17.0 lb, and consume 17.1 watts of power.

3. Sensor Data Handling Subsystem

It has been determined that there is no strong reason for going to a digital transmission system for the video data. The only change in the sensor data handling subsystem occurs based on a systems decision as to whether to include the photo-interpreter data in the transmission. In the minimum case, any heat sensor data will go out on the telemetry link, while in the maximum case, as much as 43 seconds of channel time out of a half-hour will be devoted to heat-budget information on the sensor channel.

The estimated weight for the data handling portion of the sensor link is 2.5 lb. The size is estimated at 100 cubic inches, and the power requirement is 2 watts. If photo-interpreter data and sensor data are in the system, the change in video data information content has no bearing on the estimate. As the frequency requirements for the photo-interpreter data and/or the sensor data are reduced, there is a corresponding slight decrease in the size, weight, and power requirements. Removal of all heat-budget data transmission requirements permits slight additional savings. Further removal of the photo-interpreter data strips the data handling portion of all functions.

SECTION 5 - SENSITIVE SUBSYSTEMS AND COMPONENTS

A. METEOROLOGICAL SENSORS

This subsection discusses the major factors considered in determining the parameters of a visible sensor system for observing clouds from a synchronous altitude. Many considerations are involved, and the interrelationships between them are presented in parametric form by the use of tables, nomographs, and graphs. The range of parametric variation should fulfill the requirements of presently available configurations as well as any that may become practicable in the foreseeable future.

1. Design Considerations

a. Resolution Degradation off the Nadir

An imaging system in which the Earth is focused upon a plane sensor can be regarded as having the flat-faced sensor projected upon the curved Earth. Equally spaced scan lines on the sensor project on the Earth as unequally spaced lines, the spacing increasing as the distance from the nadir increases.

Figure 5-1 shows the increase in resolution element size as a function of the angle subtended at the center of the Earth. It can be seen that at 50° off the nadir, the resolution element is twice as large as at the nadir; at about 75°, it increases by a factor of 10.

b. Exposure Time

The allowable exposure time of the sensor is limited by the requirement of image immobilization during exposure. For a 3-axis stabilized vehicle, the ability of the attitude control system to reduce vehicle motion determines the exposure time. Figure 5-2 is a plot for a 3-axis stabilized vehicle which enables the control system rates to be specified. For example, if it is desired to have a 10-second exposure time and a 1-mile ground smear, the vehicle angular rates must be less than 2.5×10^{-4}° per second.

c. Illumination Variation

Volume 3 contains a detailed examination of the illumination levels expected at the sensor sensitive surface. From the vantage point of synchronous satellite, extremely wide variations of illumination are encountered. Daytime viewing conditions result in an illumination of approximately 5×10^3 foot-candles at the sensor from the tops of cumulonimbus clouds (albedo=0.7) at a 46,000-foot altitude. During nighttime viewing, the sensor illumination can be lower than 10^{-6} foot-candle. While this range of illumination is greater than nine orders of magnitude, it can be accommodated by techniques described in Volume 3, provided it does not occur in a single exposure.

No sensor yet devised has the ability to accommodate this range of illumination in one scene. Typical sensors (Vidicons, Image Orthicons) have a maximum dynamic range of between 35 to 1 and 100 to 1. (Certain special types, such as the SEC Vidicon and the Image Isocon, may range as high as 200 or 250 to 1.) Because a synchronous satellite is essentially stationary over a point on the equator, its field of view covers nearly half the Earth's surface. When it is

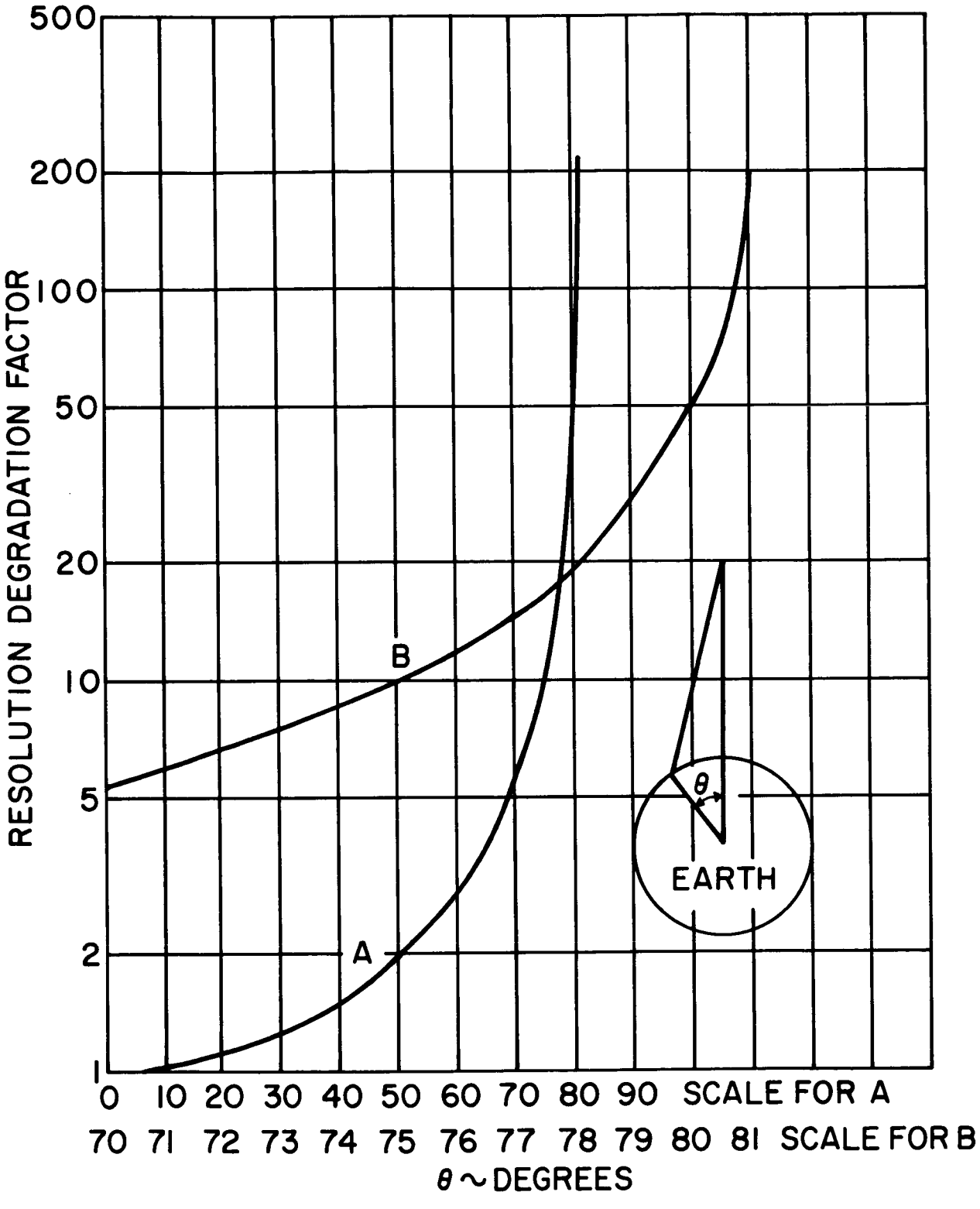

Figure 5-1. Resolution Degradation vs Angle off Nadir Normalized to Nadir

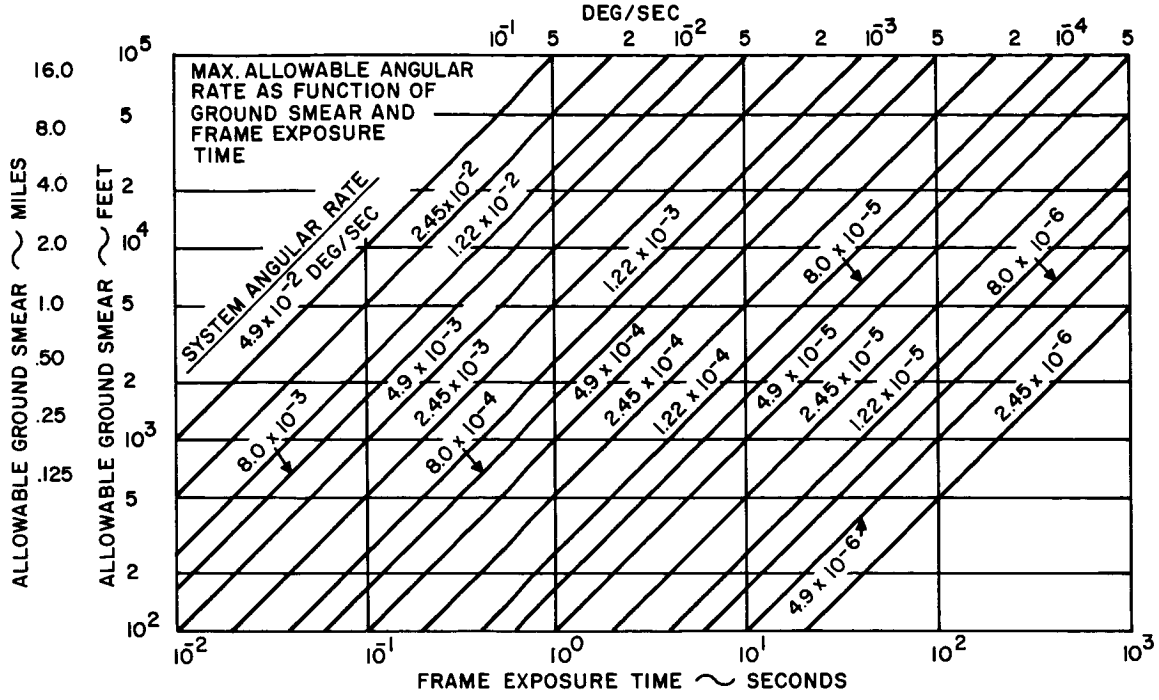

Figure 5-2. Minimum Allowable Angular Rate as a Function of Ground Smear and Frame Exposure Time

noon at the satellite subpoint, the entire disc of the Earth is illuminated by direct sunlight. Even under this condition, which occurs for a short period of time every 24 hours, the range of illumination at the sensor corresponds to sunrise at the west edge of the disc, to sunset at the east edge of the disc, and high noon at the satellite meridian. In general, some portion of the Earth's disc will be in sunlight for greater than 90% of the time, and the terminator (line of demarcation between day and night on the Earth) will be within the field of view.

Since the range of illumination levels is likely to be greater than the dynamic range capability of the sensor, the only practical method of viewing the complete Earth cloud cover is to use a mosaic of pictures with the illumination range in any one picture restricted to about two orders of magnitude. If a single picture of the full disc of the Earth is desired, the best obtainable would be one in which only the sunlit portion of the Earth is correctly exposed.

d. Sensor Selection

Volume 3 presents the results of an extensive survey of existing and planned visual sensors. Although many devices are described, the choice narrows to two (Vidicon and Image Orthicon) which are sufficiently advanced to accommodate the SMS. The Vidicon can, within the limits of present technology, be used for daytime viewing. The Image Orthicon is suitable for both day and night viewing, but not without penalties in size, weight, power, complexity, and reliability. Another device, intermediate between the Vidicon

and the Image Orthicon with respect to resolution, sensitivity, and complexity, is the SEC Vidicon. It may fill in the gap between the other two in the next few years.

A fourth device, the Image Isocon, promises a substantial improvement over the Image Orthicon, in signal-to-noise ratio and dynamic range performance at the cost of increased operating complexity. If further development is carried out over the next few years and this tube becomes fully operational, it may well supplant the Image Orthicon in such applications as the SMS program.

Finally, while no tube available today approaches the low light-level capability of the Intensifier Image Orthicon, its drastic fall-off in resolution at higher light levels, together with its large size and high voltage, renders this sensor unacceptable for the cloud cover system. Image Orthicons with even average sensitivity provide adequate resolution, with 1 second exposure periods, under near starlight scene illumination conditions.

In the paragraphs that follow, an attempt is made not only to select a sensor but also to predict its performance. In any such attempt, it is most desirable to be armed with experimental data closely related to the intended application. It is expected that in an SMS system the method of using the sensor will be different enough from conventional TV that judicious use of existing data will be mandatory. This is not to say that existing data is of no use; rather, it should be treated as a foundation upon which extensions can be built. Strong emphasis must also be placed on the techniques by which existing data were obtained to assess with confidence their applicability to situations for which the original measurements were not intended.

There are many differences between conventional TV systems and those for use in the SMS. The most important is that conventional TV uses a multiple-scan, high frame rate presentation and displays the information on a monitor. Continuous imaging upon the sensor is used, as is simultaneous readout. In the SMS application, a single scan will be used, the scan rate will be drastically reduced, and sequential exposure and readout is contemplated. In conventional multiple-frame systems, integration of signal and noise takes place in both the monitor phosphor and in the observer's mind, resulting in adequate visual pictures obtained with electrical signal-to-noise ratios on the order of 0.1. Comparable performance in a single-frame exposure requires a signal-to-noise ratio of about 20, or 200 times greater. Some compensation is provided, however, since slow scan operation results in higher signal-to-noise ratios than in conventional scan rates. In addition, other benefits accrue from low frame rates. Longer photocathode exposure times are available, permitting image integration to occur and thus build up a given charge pattern with lower light levels. Because readout beam velocity is lower, the beam current required to discharge a given target charge is reduced. This results in a potentially increased resolution because of reduced beam cross section and refined electron beam optics, as well as less beam noise (since beam noise is directly related to beam current). By using a slow scan, the video bandwidth is reduced, and techniques such as Target Feedback Control can be applied that are extremely difficult to use under standard rates (Volume 3). Reduced video bandwidth of itself permits higher signal-to-noise ratios by filtering the noise spectrum and also by allowing higher input impedances to develop larger signals.

While the above describes the trends taken by various effects, the quantitative results of their combined effects has not been measured, and there is no substitute for experimental verification. Experiments in slow scan operation of Image Orthicons have been made at several astronomical observatories, but caution must be used in applying the results. Here, point sources of light (stars) are being viewed. The signal-to-noise ratio required for threshold detection of point sources is lower than for extended sources (such as clouds). The sensors used were cooled to temperatures not anticipated in the SMS. The camera systems were not designed for automatic, unattended operation. Finally, many results were obtained by a combination of target integration and photographic film integration.

From the above discussion and by judicial use of existing data, it is postulated that sensor performance be estimated as follows: Resolution versus illumination for conventional TV systems is used to determine resolution for a specific photocathode illumination. For a slow scan system with 10-second frame time and simultaneous exposure and scan, the illumination required by the SMS sensor is reduced by a factor of ten, and the resolution is increased by 50%. A further modification of illumination can be made if scene contrast is less than 100%. The illumination increase required for a particular scene contrast is obtained from Figure 5-3, which is based on the performance of an ideal imaging device. These modifying factors are judged to be obtainable, and are probably on the conservative side.

Considering the Vidicon and the Image Orthicon as potential sensors, the choice between them is not a difficult one to make if the mission objectives and constraints are defined. For night viewing, only the Image Orthicon can be used. Figure 5-4 is a plot of limiting resolution vs. photocathode illumination for typical Image Orthicons operated in a conventional manner. From this figure, a selection can be made on the basis of resolution and light level. Other factors, of course, are involved. The spectral characteristics of the photocathode should match those of the scene to be viewed. For night viewing, it is desirable to have a high efficiency photocathode with infrared response such as the S-20. Also, if high sensitivity is to be achieved by target integration, it is necessary to use thin film metal oxide targets.

The Vidicon signal-to-dark current ratios for several tubes are plotted in Figure 5-5. The limiting source of noise in well designed Vidicon camera systems is in the video amplifier. However, there is another source of noise in the tube itself, the dark current, which can exceed the video amplifier noise current in some tubes. If slow scan is used, or long exposure times are contemplated, a tube should be selected that exhibits good storage and low dark current. It should be recognized that dark current of itself is not a noise contribution, but rather, noise stems from the variations of dark current. Dark current is indicative of these variations and is therefore used as a measure of noise for the purposes of Figure 5-5.

Another factor of prime importance to the meteorologist is the gray scale rendition in a picture. Figure 5-6 is a plot of the S/N ratio required to resolve a given number of gray steps, each step related to the next by a factor of 1.414. Present thin-film Image Orthicons can reproduce 8 or 9 gray steps. Vidicons are capable of about 9 or 10 gray steps. Estimates for improved tubes run as high as 13 or 14 steps.

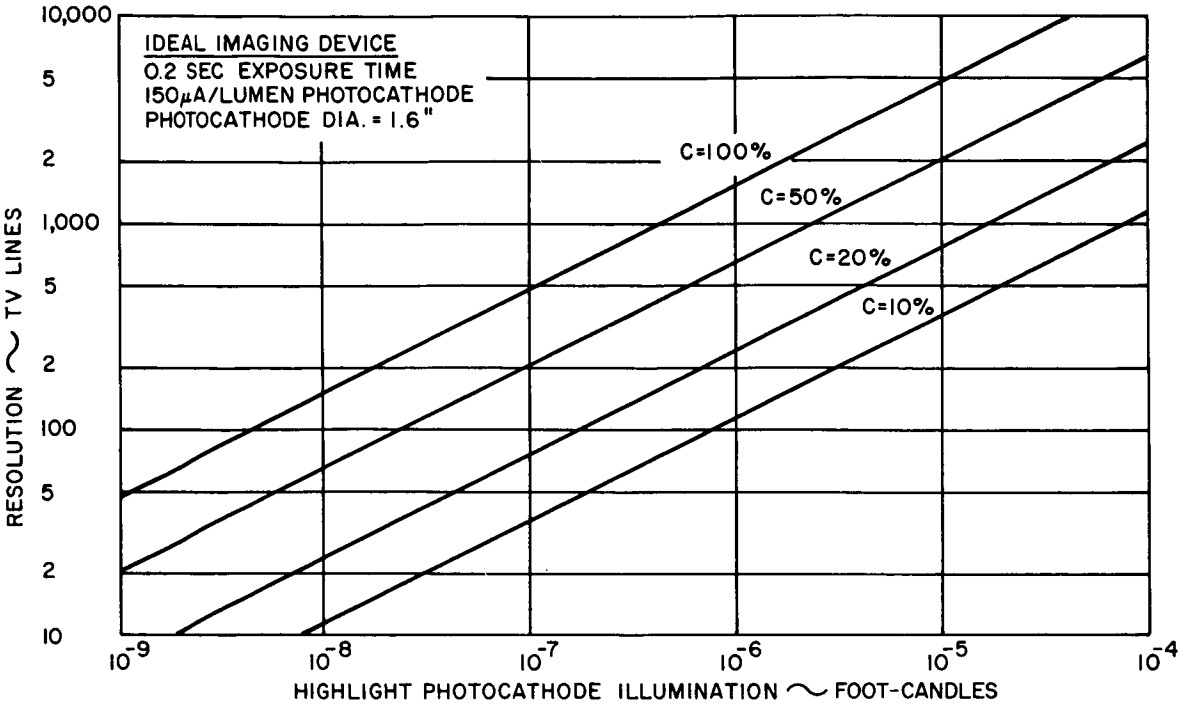

Figure 5-3. Effect of Contrast on Resolution

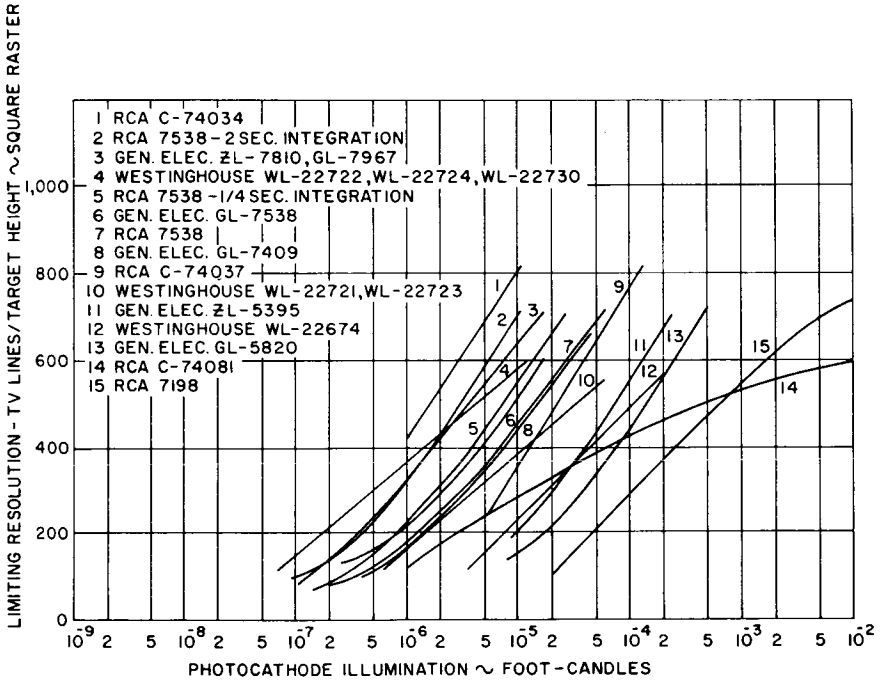

Figure 5-4. Typical Resolution - Sensitivity Characteristics of Image Orthicons

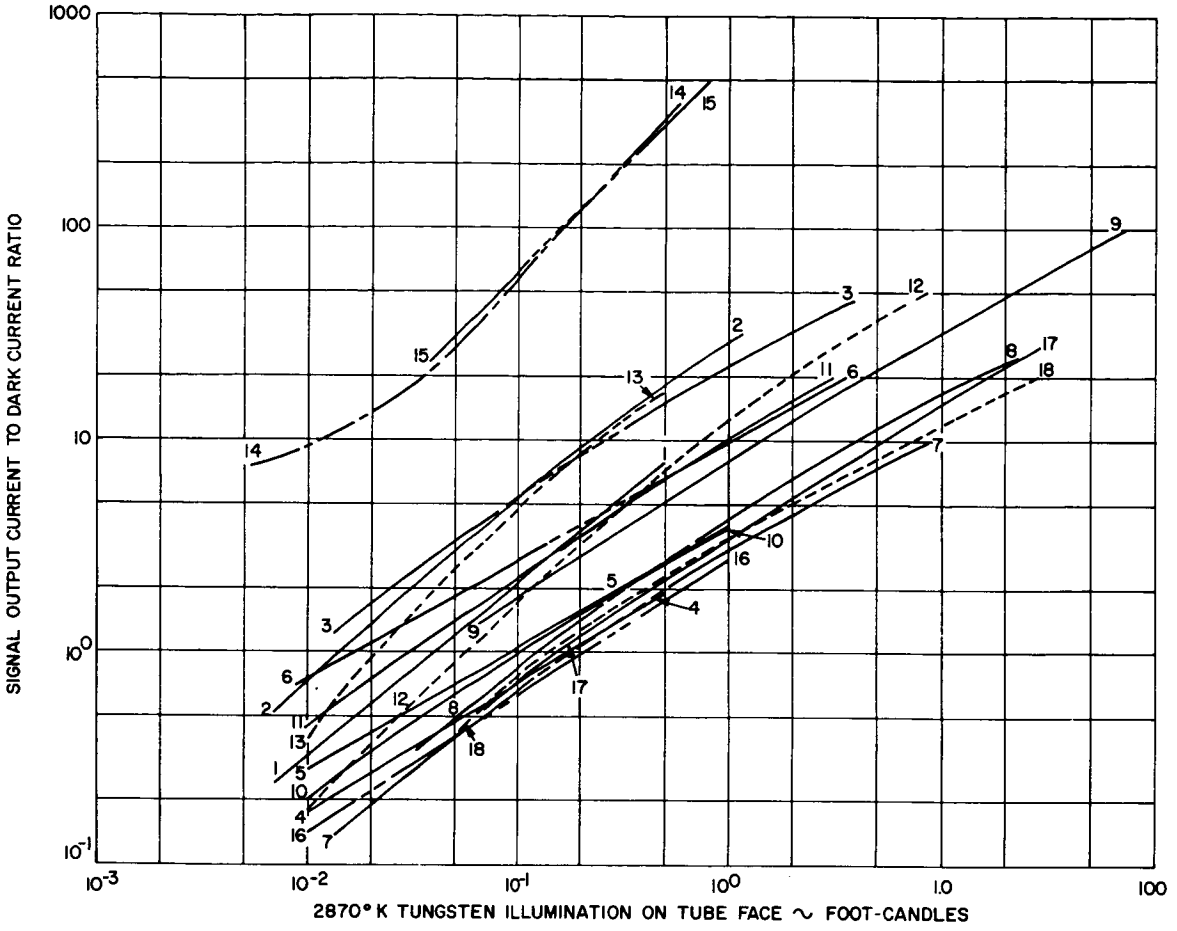

			DARK CURRENT (MICROAMPERES)	=
1	THE MACHLETT LAB, INC.	ML 7351A		0.08
2	"	"		0.02
3	"	"		0.008
4	RCA	7735A		0.02
5	"	"		0.10
6	"	"		0.02
7	"	8051		0.05
8	"	"		0.02
9	"	"		0.005
10	"	8134		0.10
11	"	2084A, 7262A, 7263A, 8134 & 7697		0.02
12	"	DEV TYPE C-73496		0.02
13	"	" " C-74078		0.02
14	WESTINGHOUSE	WX 4915		0.002
15	"	7290		0.0002
16	RCA	4427		0.05
17	"	7038		0.02
18	"	6326		0.02

Figure 5-5. Vidicon Signal to Dark Current Characteristics

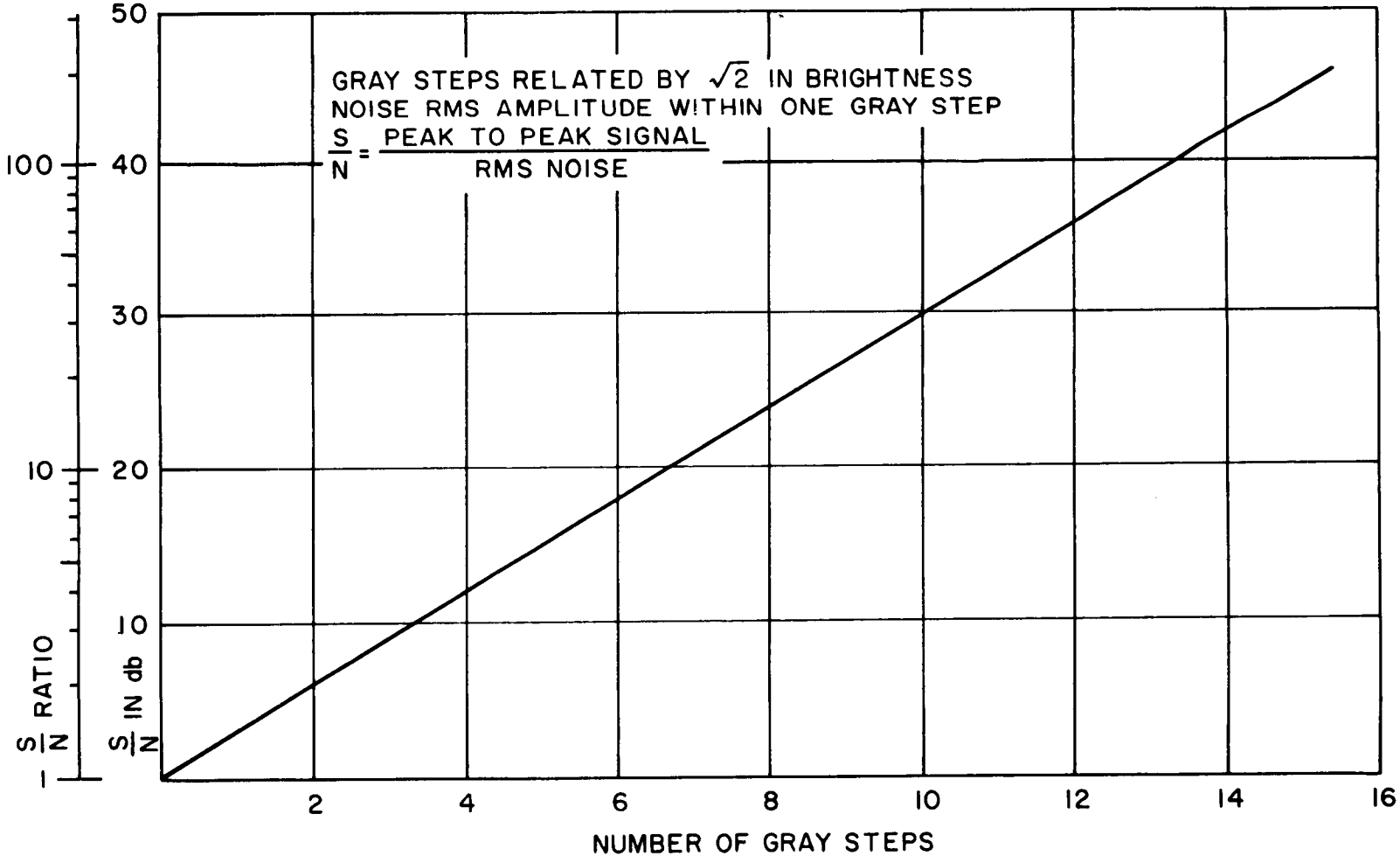

Figure 5-6. Gray Scale vs Signal-to-Noise Ratio

e. Optical-Sensor-Illumination Relationships

Figure 5-7 is a combined presentation of the relationships between scene illumination, scene reflectivity, lens efficiency, photocathode illumination, and typical sensor resolution. Perhaps the best method of describing its utility is to illustrate its use in a typical example. Consider that for a specific condition it is determined that the illumination on the scene is expected to be 1 millifoot-candle (corresponding roughly to quarter-Moon conditions) and that at least 500-line resolution is desired. Inspection of the sensor characteristics shows that, if the scene illumination is 5×10^{-5} foot-candle, the following Image Orthicons can be used: WL-22724, GL-7967, and C-74034. The intersection of 5×10^{-5} photocathode foot-candle and 10^{-3} scene foot-candle occurs at a multiplier constant of 0.005. This multiplier constant is achieved for an f/4.5 lens and scene reflectivity of 0.4, or an f/5.3 lens and scene reflectivity of 0.6, which is typical of stratos- and nimbus-type clouds. The tube data plotted has been modified by increasing resolution by 50%.

f. Earth Coverage and Resolution

Figure 5-8 is a nomograph that relates sensor resolution, sensor size, ground resolution at the nadir, Earth coverage, and lens focal length. It is designed to be used with the central scale (ground coverage) as a pivot point for a straightedge. Typical examples will be used to describe its use. Suppose that a 1-in. Vidicon is to be used to cover the full Earth disc in one picture. A straightedge placed between 0.44 in. picture height and 8000 miles ground coverage shows that a 1.2-in. focal length lens is required. Pivoting the straightedge about 8000 miles indicates that a 10-mile ground resolution can be achieved with 800 TV lines of resolution per picture height. Another example that can be worked out on this nomograph is that a 3000-line resolution is required to achieve a 1-mile ground resolution with a coverage of 3000 miles. If a 3-in. Image Orthicon were available for this, it would require the use of a 9-in. focal length lens.

g. Optical System Weight

Volume 3 is concerned with the optical considerations involved in the SMS. Figure 5-9 depicts the weight of an optical system as a function of the aperture diameter. The aperture can be obtained by using the relationship:

$$D = \frac{\text{Focal length}}{\text{f/number}}$$

The weight of the optical system can now be approximated with the aid of Figure 5-9.

h. Readout Time and Transmission Rate

After the determination of ground resolution and coverage has been made, the trade-off of readout time and transmission rate can be obtained by using Figure 5-10. This figure is a nomograph that has been designed with the center scale as a pivot point. A straightedge placed between known values of ground resolution and ground coverage will intersect the center scale. Pivoting

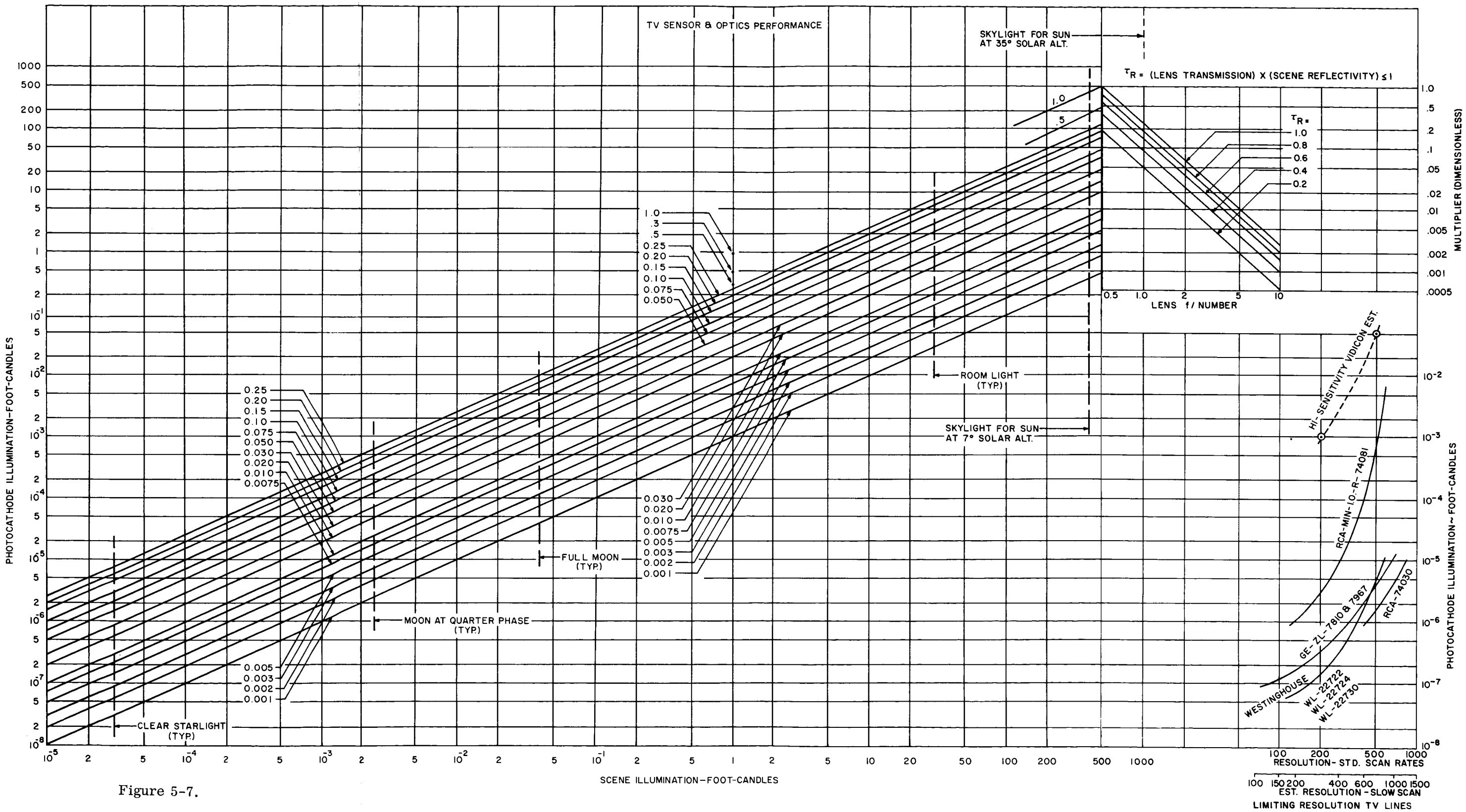

Figure 5-7.

Combined Relationship of Sensor-Illumination-Optical Factors

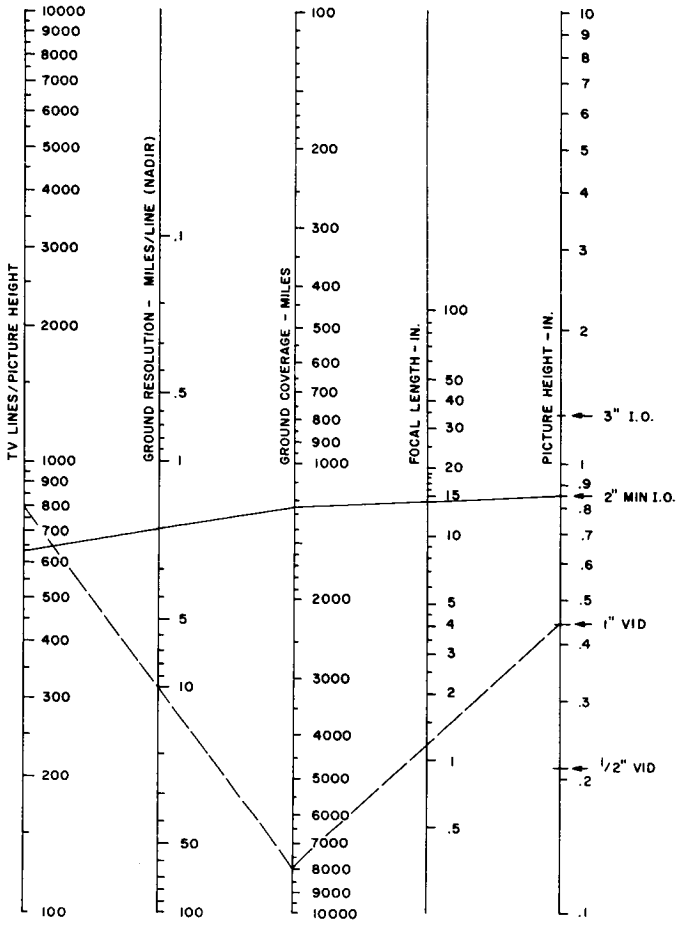

Figure 5-8. Optical Sensor Parameters - Single Frame Coverage

the straightedge about this point enables one to determine the transmission rate (in picture elements per second) corresponding to a given readout time. In a straightforward analog communication system, the baseband frequency bandwidth required is approximately half the transmission rate, since one frequency cycle corresponds to two picture elements. For example, the disc of the Earth can be covered with 1-mile nadir resolution in a system transmitting 6.4×10^6 picture elements per second and using a readout time of 10 seconds. Figure 5-8 can be used to determine that accomplishing this in one frame requires a sensor resolution of 8000 lines per picture height, assuming a square raster.

If a mosaic of pictures is to be used for large area coverage, several additional considerations are involved. If the maximum capability of the sensor is most efficiently used, a square raster is required. To cover an area that lies in a square inscribed within the disc of the Earth, suitable overlap of individual pictures must be allowed to ensure complete coverage. The percentage of overlap will vary with the system and is influenced by vehicle stability and the pointing accuracy of the sensor system. If coverage of the disc of the Earth with a resolution greater than that allowed by one picture is required, a mosaic can be used. Here also, overlap should be considered.

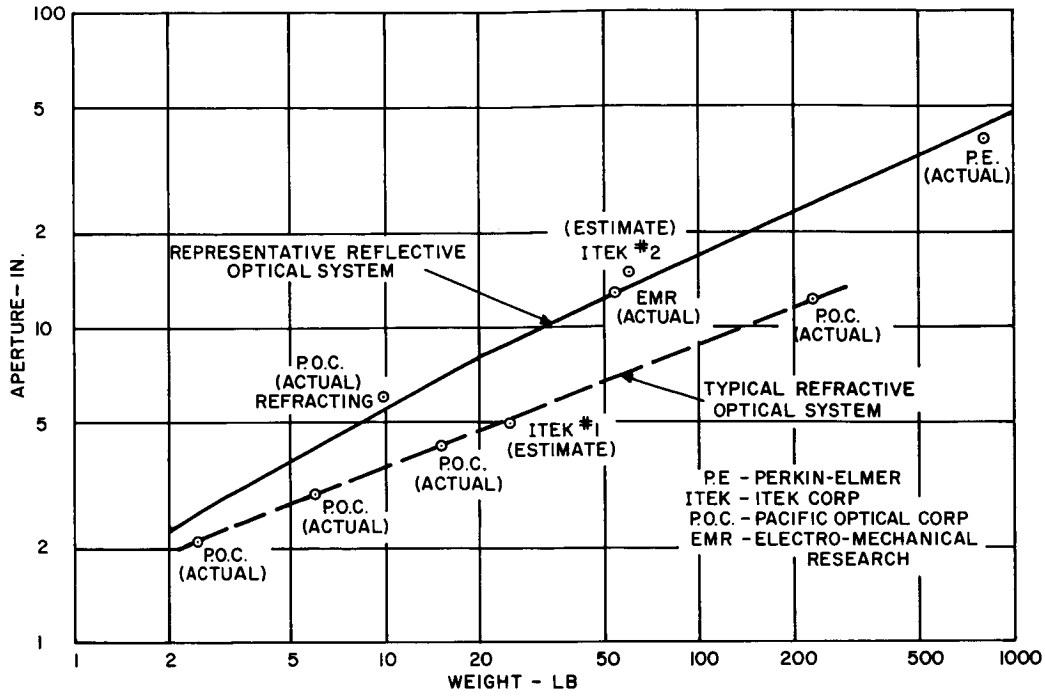

Figure 5-9. Optical System Weight vs Aperture

There is another factor to be considered. One might be tempted to increase ground resolution by covering the Earth with two pictures. However, nothing is gained in this situation, since the size of each frame is identical to that in the one-frame case. The same situation applies for three-picture coverage of the Earth. With four pictures, it is possible to increase ground resolution by a factor of two (linear dimension). But again, five-picture coverage is no better than four-picture coverage. It can be seen that improvement is achieved only when the number of frames is a perfect numerical square, i.e., 1, 4, 16, 25, 36, etc. When this series reaches 49 pictures, another factor arises. With 49 frames, 4 will be in the corners of the Earth disc-circumscribed square and can be eliminated since they contain no useful information. Therefore, the above series continues as 45, 60, and 77. All intermediate numbers offer no improvement over the next lowest allowable ones from the series.

i. Size, Power, and Weight

It is well recognized that size, power, and weight are of prime importance in satellite systems. It is likewise axiomatic that increased performance is accompanied by increased penalties in these parameters. Trade-offs are necessitated in the face of the conflicting requirements of maximum performance and reliability on the one hand, and minimum complexity, size, weight, and power on the other. While consideration was given to these parameters during the course of the SMS study program, there was insufficient time and available data to fully exploit them. Another complication is the current unavailability of an Image Orthicon camera system for satellite use. Presently available Image Orthicon camera systems would require modifications to be compatible with

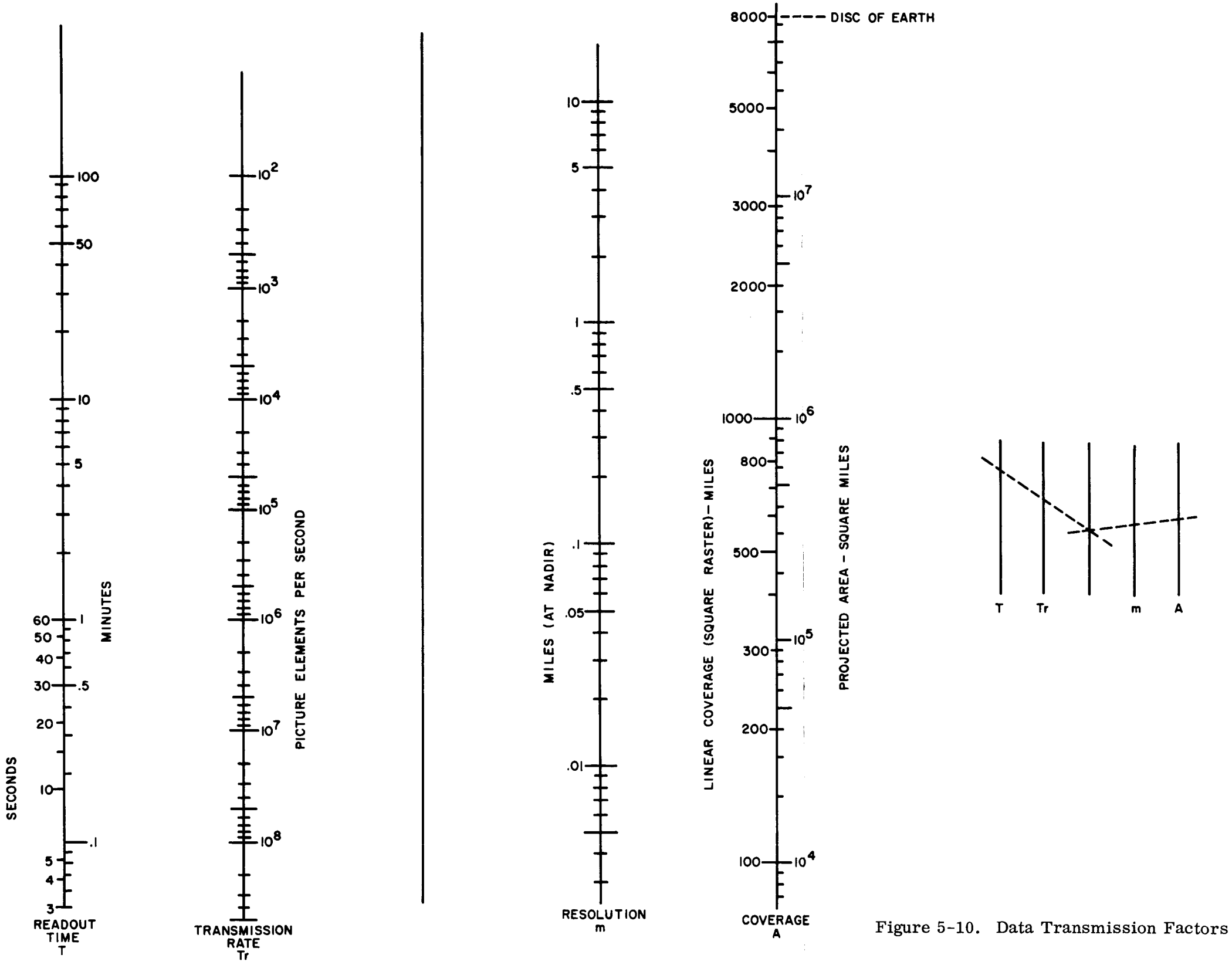

Figure 5-10. Data Transmission Factors

long-term unattended operation. It is possible to add remote control through telemetry to existing Image Orthicon systems, but this would not result in an optimum package. On the other hand, Vidicon camera systems are used in Tiros and are in an advanced state of development for Nimbus. It is quite likely that even these cameras can be miniaturized, perhaps using thin-film techniques and integrated modules.

There are several sizes and types of Vidicons and Image Orthicons, and, while specific size, weight, and power are difficult to ascertain with a fair degree of accuracy, it is possible to assess their positions on a relative scale. In the Vidicon category, the 1/2-in. type (as used in Tiros) is most compact and least complex. The 1-in. and 1-1/2-in. tubes rank next. A considerable savings in power, weight, and size can be achieved in the electrostatic versions of these tubes. Even in the electrostatic types, there are further subclasses of electrostatic versions.

Image Orthicons are available in 2-in., 3-in., and 4-1/2-in. diameters with both electrostatic and magnetic versions in some classes. Potentially, the most compact Image Orthicon camera is one built around the GE 2-in. electrostatic tube. Both Hazeltine and GE are building camera systems using this tube. The next most compact, low power camera would use the RCA 2-in. magnetic Image Orthicon. A camera system using this tube is under development by Raytronics. The Hazeltine and Raytronics cameras are intended for use in Nimbus and will therefore contain control circuits for unattended operation. GE's camera is a general purpose engineering model. Company plans are to modify the camera for unattended operation by late 1964. The 3-in. and 4-1/2-in. Image Orthicons are available only in the full magnetic type, are larger, and need more power. However, their performance exceeds that of the smaller tubes.

Table 5-1 contains data on cameras which are either operational or under development. All figures exclude the optical systems.

2. Typical Example

This subsection applies the considerations described above to implement typical camera systems. The example presented is believed to be typical of expected performance, although no formal optimization or error analysis is executed. The performance guidelines within which the system is constrained are as follows:

Medium Capability Vehicle

- Full Earth disc coverage, low resolution
- Selected area, high resolution pictures, 25 frames maximum
- Cycle time, once every 30 minutes
- Vehicle stabilization, 0.003 degree per second, 3-axis stabilized
- Moderate size, weight, and power

TABLE 5-1
SUMMARY CHARACTERISTICS OF TYPICAL CAMERA SYSTEMS

Manufacturer	Camera Tube Type	Camera Tube Number	Total Weight (lb)	Average Power Watts	Volume cu. in.
General Electric	2 in. E.S. I.O.	ZL-7804 (GE)	14	25	367
Hazeltine	2 in. E.S. I.O.	ZL-7804 (GE)	15	30	320
Raytronics	2 in. Mag. I.O.	C-74081 (RCA)	18	36	450
RCA (Tiros)	1/2 in. Mag. Vid.	C-73496 (RCA)	9.7 (Includes Lens)	9	184
RCA (Nimbus-APTS)	1 in. Mag. Vid.	-	20.6	19	482
RCA (Ranger)	1 in. Mag. Vid.	-	14 (Includes Lens)	19	300

This system requires both full Earth coverage (assumed low resolution) in one frame and multiple-frame pictures at high resolution. With a 3-axis stabilized vehicle whose stabilization rate is 0.003 degree per second, Figure 5-2 shows that an exposure time of 1 second will produce a 1-mile ground smear. A 2-in. Image Orthicon presently capable of a 625-line resolution (square raster) should resolve about 1000 lines at slow scan rates. From Figure 5-8 it can be determined that a 14-in. lens permits a 1280-mile coverage at a 1.3-mile nadir resolution. Maximum ground smear is about 3/4 of a resolution element. At standard scan rates, the RCA 2-in. Image Orthicon C-74081 produces 200 lines of resolution at 3×10^{-6} foot-candle and 625 lines at 10^{-2} foot-candle on the photocathode. Under slow scan operation, at a 10-second frame time, the tube should be capable of 1000 lines at 10^{-3} foot-candle and 320 lines at 3×10^{-7} foot-candle, assuming continuous imaging and readout. For a 1-second exposure and 10-second readout, the illumination requirements become 10^{-2} foot-candle for 1000 lines and 3×10^{-6} foot-candle for 320 lines. Using Figure 5-7 and assuming an f/4 lens and 60% scene reflectivity, it can be determined that a 1000-line resolution occurs at 1 foot-candle on the scene and a 320-line resolution occurs at 3×10^{-4} foot-candle. This latter illumination corresponds to that obtained on the Earth under conditions between clear starlight and quarter Moon. These values are for highlight illumination, so that details within the scene at lower light levels will be seen at reduced resolution, although the tube's dynamic range decreases with reduced illumination. To achieve optimum performance under high illumination levels, it is necessary to attenuate the illumination so that the photocathode level is maintained at 10^{-2} foot-candle. Table 2-14, found in Volume 3, shows that 8080 foot-candles would be incident upon the sensor photocathode for a high-altitude (40,000 ft), high-reflectivity (0.7) cloud when the Sun is over the nadir. The calculations were made using an f/0.5 lens. Assuming that the worst conditions resulted in 10,000 foot-candles with an f/0.5 lens, the photocathode illumination with an f/4 lens would be approximately 160 foot-candles. The range of light control required is then 1.6×10^4:1. This is well within the range obtainable with neutral density filter wheels (see Volume 3). For illumination levels below the control range, the optical system is operating at maximum efficiency, and tube parameters should be adjusted to accommodate varying illuminations. The methods given in Volume 3 can be used to obtain maximum performance within the restrictions of limited light levels.

With the aid of Figure 5-10 it can be determined that a readout time of 10 seconds requires a transmission rate of 100,000 picture elements per second. A frame time of 10 seconds is judged to be a good compromise between transmission rate (and therefore transmitter power), circuit complexity, number of pictures in a sequence, and conservative design with reasonable expansion capability.

Having selected a Vidicon suitable for slow scan operation and an exposure time, we can predict the illumination levels over which the system will operate to obtain a full Earth disc coverage in one picture. A typical high-sensitivity Vidicon (Machlett 7351A) produces a 500-line resolution at 5×10^{-2} foot-candle on the photocathode. Another high-sensitivity Vidicon (Westinghouse WX-5915) is capable of 200 lines at 10^{-3} foot-candle. With increased accelerating potentials and magnetic fields, the resolution increases by about 60%, corresponding to 800 lines and 300 lines, respectively. These figures are for normal scan rates. Following the procedure outlined in Volume 3, the illumination required is reduced by 10, and resolution is increased by 50% when a 10-second slow scan

system is used. Thus, 1200 lines should be obtained at 5×10^{-3} foot-candle, and 450 lines at 1×10^{-4} foot-candle for slow scan operation with continuous imaging. With the aid of Figure 5-8 it can be determined that 1200 lines, using a 1-in. Vidicon, will require a 1.25-in. focal length lens to cover the disc of the Earth with less than a 7-mile nadir resolution. From Figure 5-7, assuming an f/1.5 lens and 60% scene reflectivity, it can be determined that the scene illumination is about 3750 foot-candles for 250 foot-candles on the photocathode, and 75 foot-candles for 5 foot-candles on the photocathode. These values correspond to 1200 and 450 lines of resolution, respectively. The maximum illumination incident upon the photocathode during daylight hours is about 1000 foot-candles. To operate the Vidicon at its optimum illumination level (about 250 foot-candles), light control over a range of 4:1 is required. However, if no light control is employed, the maximum illumination will be equivalent to two f-stops above the knee of the transfer characteristic. This is tolerable because the knee is not well defined and also because typical commercial operation is one f-stop above the knee.

The optical exposure is achieved with either a curtain-type focal plane shutter or a rotary focal plane shutter. By using a slow scan Vidicon, long frame readout times can be employed with a resultant reduction in video bandwidth and transmitter power. Figure 5-10 shows that a transmission rate of 140,000 picture elements per second corresponds to a 10-second readout. The resulting video bandwidth is about 70 KC. Because of the slow readout time, it may be necessary to use a digital sweep generator to obtain good linearity.

In operation, the wide-angle Vidicon camera system will present a coarse (7 mile), overall view of the cloud cover. The high resolution (1.3 miles at the nadir) system gives usable pictures at close to starlight illumination. At least 25 such pictures can be transmitted in a 30-minute period. High resolution pictures are obtained for the complete disc of the Earth with a 10% overlap between pictures. More overlap would, of course, reduce the area coverage. A fixed program of sequenced pictures can be used with ground override capability through the telemetry link. This feature is useful when continued observation of a specific area is of interest.

During the 10-second frame time interval, the lenses of both camera systems are capped. The wielding mirror can be repositioned during this time. There is adequate time allotted to the light control systems to stabilize and thus ensure 25 optimum pictures within a 30-minute interval.

Reference to Figure 5-9 shows that the high resolution lens system (14-in. focal length, f/4 lens) will weigh between 5 and 10 lb. Figure 5-11 gives an approximate weight of the overall sensor system, for a given resolution. This figure can be used for the preliminary design evaluation.

3. Heat Budget Sensor

In the design of a heat budget sensor, the usual practice is to specify the desired resolution, A, and sensitivity, NET, of the system. In the example described these were chosen as follows:

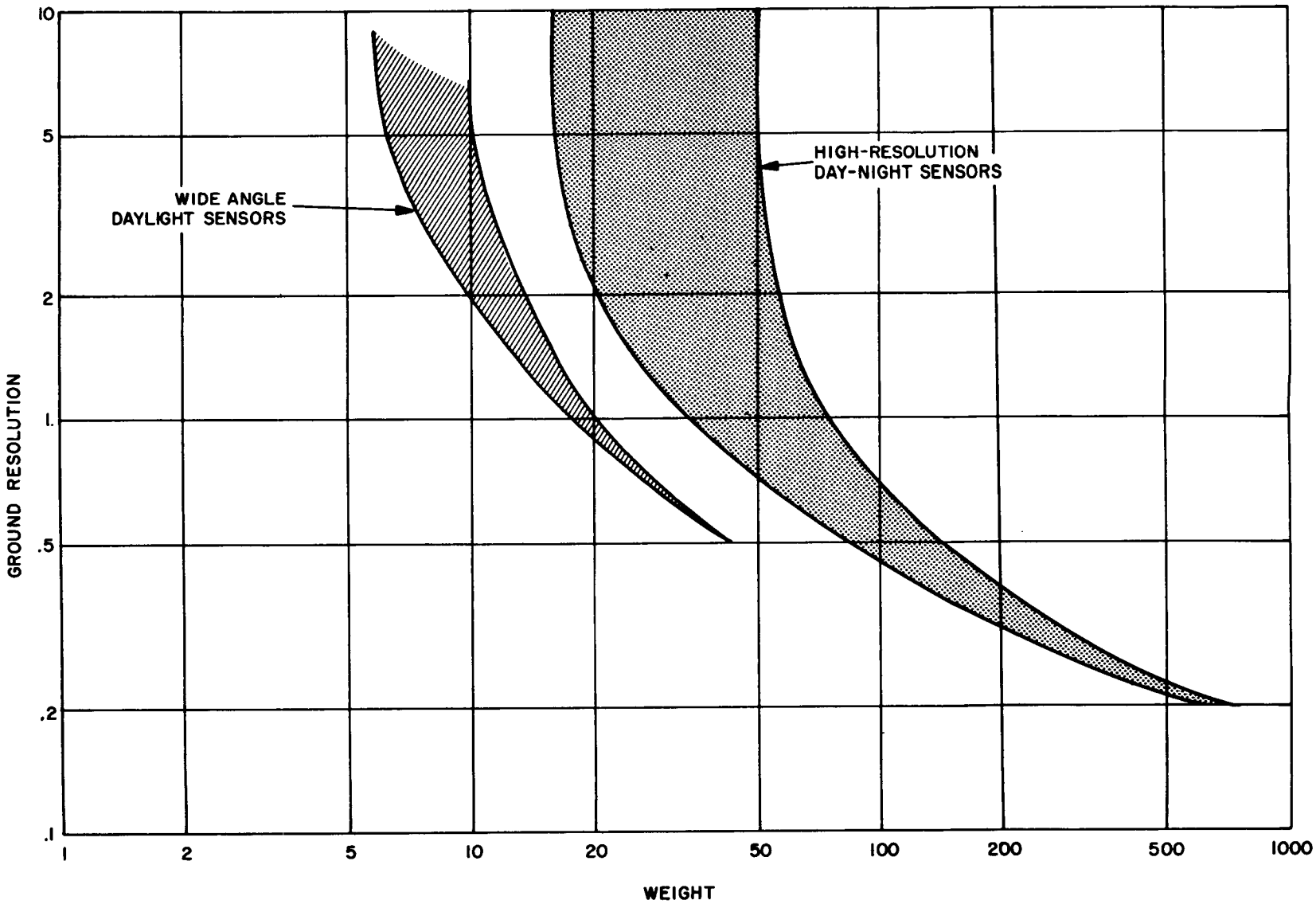

Figure 5-11. Sensor Weight vs Resolution

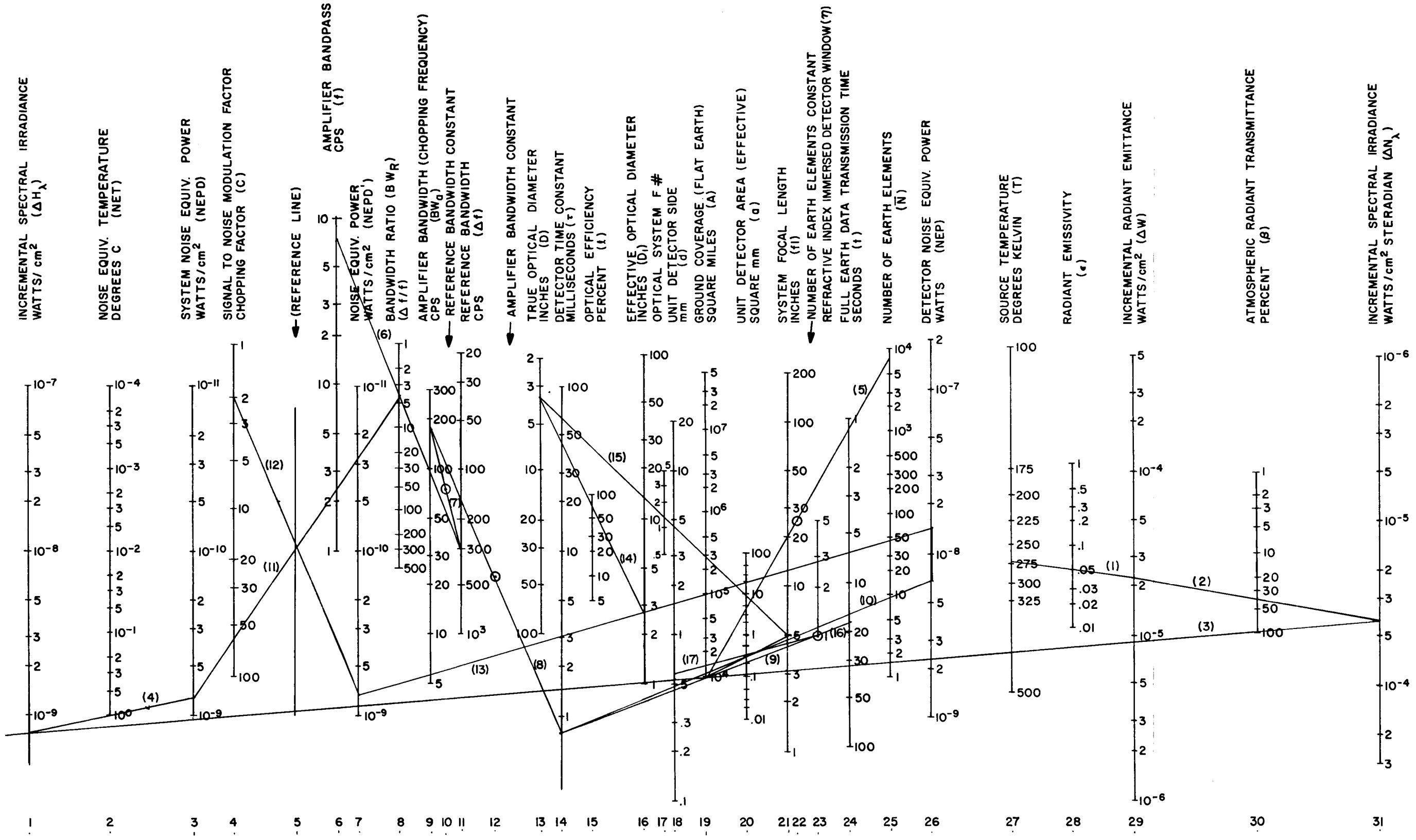

RESTRICTIONS:
a) THERMISTOR TYPE BOLOMETER
b) WAVE LENGTH – 4 TO 40 MICRONS
c) SPATIAL SCANNING SYSTEM
d) REFERENCE RETICLE FOR s/n IMPROVEMENT

$$NET = \frac{k\ell^2 C f l \sqrt{f}}{T^3 \epsilon \beta D^2 A \sqrt{t}}$$

$k = 8.63 \times 10^9$ FOR 20° SQUARE RASTER AT 22,240 MILES

Figure 5-12. Parametric Relationship Nomograph

Area at nadir = 100 x 100 miles
Noise Equivalent Temperature (NET) = 1° C

The lowest expected incremental radiant emittance will also affect the design parameters. The energy reacing the system will vary with both absolute temperature and emissivity. For example, from Figure 5-12:

at 200° K and $\epsilon = 0.9$, $\Delta W = 1.62 \times 10^{-4}$ watts/cm^2
at 273° K and $\epsilon = 0.1$, $\Delta W = 4.65 \times 10^{-5}$ watts/cm^2
at 300° K and $\epsilon = 0.2$, $\Delta W = 1.21 \times 10^{-4}$ watts/cm^2

The lower values of radiant emittance correspond to conditions on the Earth's surface wherein snow and cold temperature are not simultaneous. A very low value of ΔW would be in the order of 2×10^{-5} watts/cm^2. A temperature (T) of 273° K and an emissivity (ϵ) of 0.05 are assumed for the example. From Figure 5-13, an atmospheric transmission (β) of 34% is obtained for a 273° K target area temperature. It is assumed that the variation in thickness of the atmosphere has negligible effect for this case at the nadir.

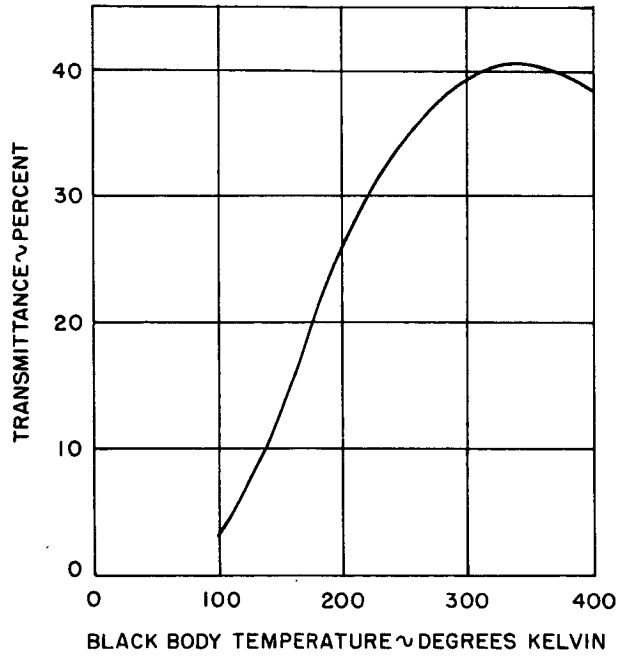

Figure 5-13. Percent of Atmospheric Transmittance as a Function of Terrestrial Black Body Temperature

From the above data, a system noise equivalent power (NEPD) can be obtained by drawing lines No. 1, No. 2, No. 3, and No. 4.

The next parameter which should be selected is the total data transmission time, t. This time should be as long as possible for high resolution systems. A reasonable maximum time can be obtained from the stability criteria of the vehicle

and the desired geometric fidelity. A rule of thumb which can be used is to divide the desired angular resolution by the maximum of the roll, pitch, and yaw rates. The maximum transmission time can be assumed to be one-half, or less (dependent upon the desired geometric fidelity), of the maximum time so obtained. In the example, for a 100-mile resolution element (4.5 milliradians) and a maximum angular rate of 0.003 degree per sec and a maximum transmission time of 43.3 seconds is obtained. The resolution element of 100 x 100 miles corresponds to 6400 Earth elements per frame (line No. 5) when the frame is a 20° angular square. With a 43.3-second transmission time, 73.5 elements must be transmitted each second. If it is assumed that 73.5 elements are transmitted each second, an amplifier bandpass of 37 cps is required when no chopping reticle exists. If a chopping reticle is incorporated, the amplifier bandpass must be increased to the element rate, or approximately 74 cps.

In order for a "reticle use payoff" in obtaining the NET to exist (disregarding the requirement for absolute temperature measurement), the value of $C/\sqrt{\Delta f/f}$ must be equal to or less than one. The use of an obscuration type of chopper results in a C equal to 2. Therefore, $\Delta f/f$ must be equal to or greater than 4 (line No. 6). With f equal to 74 cps, then Δf must be equal to or greater than 286 cps. With Δf equal to 286 cps, line No. 7 is drawn and a bandwidth (center frequency of bandpass) of 200 cps is obtained. Line No. 8 indicates that a detector time constant of 0.8 millisecond is required. Although this time constant is feasible, it is difficult to obtain. The trade-off required to increase the detector time constant would be to increase the size of the resolution element or increase the stability of the vehicle. Either of these trade-offs would tend to decrease the elements per second to be transmitted.

The selection of the system focal length permits many additional parameters to be obtained. Assuming a 5-inch focal length, line No. 9 is used to determine the detector area and line No. 10 gives the theoretical NEP of the detector. By drawing lines No. 11 and No. 12 and degrading the thermister theoretical NEP by a factor of 2 for a realizable thermister design, line No. 13 can be drawn and the effective optical diameter obtained. Lines No. 14 and No. 15 relate the true diameter, F#, and optical efficiency when any one of three parameters are known or selected.

Line No. 16 is used to determine the transmission time required when a chopping reticle is not required. Line No. 17 is used to determine the physical size of an immersed detector from its effective area.

One method of utilizing the nomograph in Figure 5-12 to design a heat budget sensor would be to enter on the nomograph all known and/or desired parameters. Lines can be drawn connecting these parameters and solving for other parameters as follows (disregarding order of lines and order in lines):

Line No. in Example	Ordinates Line No.			Equations of Line	
4	1	2	3	$NET \times \Delta H_\lambda = NEPD$	
3	1	19	31	$\Delta H_\lambda = Z \times 10^{-9} \times A \times \Delta N_\lambda$	
11	3	5	8	$NEPD \times \sqrt{BW_R} = K$ $\frac{NEPD}{NEPD'} = \frac{C}{\sqrt{BW_R}}$	
12	4	5	7	$NEPD' \times C = K$	
6	6	8	11	$BW_R = \Delta f / f$	
13	7	16	26	$D_1^2 \times NEPD' = 3.9 \times 10^{-3} \times NEP$	
7	9	10	11	$\Delta f = 1.58 \times BW_a$	
8	9	12	14	$158 = \tau \times BW_a$	
14	13	15	16	$D_1 = D \times \ell$	
15	13	17	21	$f \ell = D \times F\#$	
16	14	19	24	$\tau \times 0.2 \times 10^6 = tA$	(no chopping reticle)
10	14	20	26	$\tau \times NEP = 10^{-8} \sqrt{a}$	(theoretical)
17	18	20	23	$\sqrt{a} = d \times \eta$	η = index of refraction of immersion lens
5	19	22	25	$6.4 \times 10^6 = A \times \bar{N}$	N = Number of elements on equivalent flat Earth
9	19	20	21	$A \times f\ell^2 = 0.76 \times 10^6 \times a$	
1	27	28	29	$\Delta W = 22.4 \times 10^{-12} \times T^3 \times \epsilon$	
2	29	30	31	$\Delta N_\lambda = 0.317 \times \Delta W \times \beta$	β from Figure 5-13

The weight of an optical scanning heat budget sensor is basically dependent upon two factors, the weight of the electronics, and the weight of the optics and its supporting structure.

The weight of the heat budget electronics will be essentially constant for any type of scanning system. It is estimated that the electronics will weigh between 5 and 10 lb depending upon the type of electronics constructed, i.e., microminiature (solid state), printed circuits, etc.

The weight of the optics and its supporting structure is dependent upon the size of the optics, which in turn is dependent upon the required sensitivity of the system and the method of scanning. A 2-in. diameter F#2, single mirror, two-axis scanning system is estimated at 10 lb. The weight of the optical system would follow a curve similar to that estimated for the visible imaging system.

The reliability of the system is expected to be quite high under normal circumstances, except for certain items as follows:

(1) Particular care must be taken in the moving portions of the system to prevent cold welding after extended operation in space.

(2) The system can have a catastrophic detector failure through an inadvertent look at the Sun. It is therefore recommended that additional redundant detectors be incorporated into the system. These detectors should be shielded from all solar radiations until their use is required.

B. STABILIZATION AND STATION KEEPING SUBSYSTEM

The following is a listing of the important considerations in the design of a 3-axis stabilization system:

(1) Required stabilization rates

(2) Required pointing accuracy

(3) Reaction wheel divergence in sizing wheels and gas jets

(4) Cross coupling effects for Earth-oriented satellites using momentum-type control torquers

(5) Orbit injection velocity error and its effect on sizing the gas system's stored gas, thrust, etc.

(6) Acquisition time and its effect on electric power supply sizing

(7) Stabilization system sizing depends on the disturbance torque model which should be accurately determined

(8) Basic performance is determined by the attitude sensor characteristics

Resolution requirements of the SMS have little effect on the 3-axis stabilization system's weight, power, reliability, and feasibility as long as the pointing accuracy is not required to be better than 0.5° and the stabilization rates are less than 3×10^{-3} degrees/sec. These limits are assumed for the purposes of this volume.

The characteristics of the stabilization system are affected by the characteristics of the horizon sensor. The effect of horizon sensor noise on roll and roll rate and yaw and yaw rate are shown in Figure 5-14. The effect of the sensor dead zone on pointing accuracy has a one to one relationship, as shown in Figure 5-15.

A listing of the physical characteristics of typical 3-axis stabilization systems for 500-and 1000-lb vehicles is given in Table 5-2.

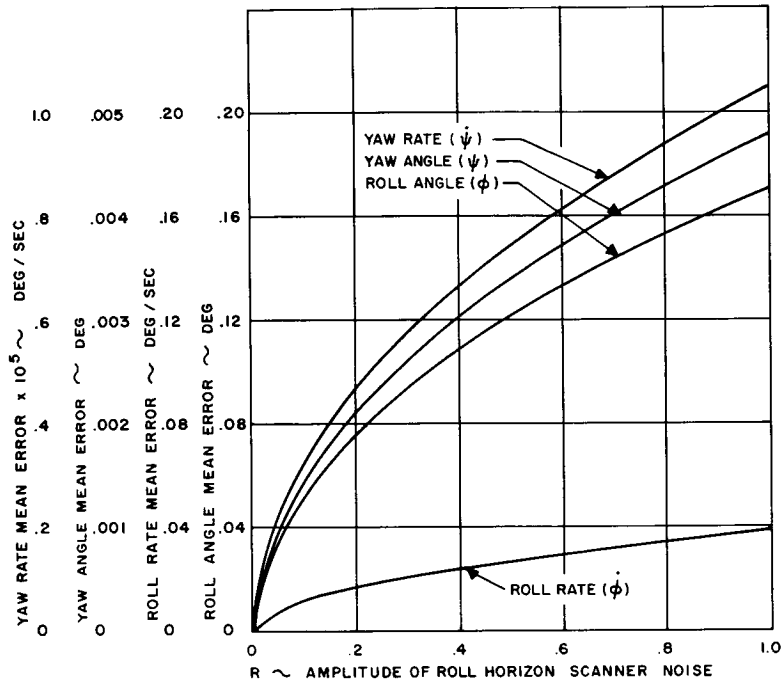

Figure 5-14. Gyrocompass System - Horizon Scanner Noise Effect on Tracking Accuracy

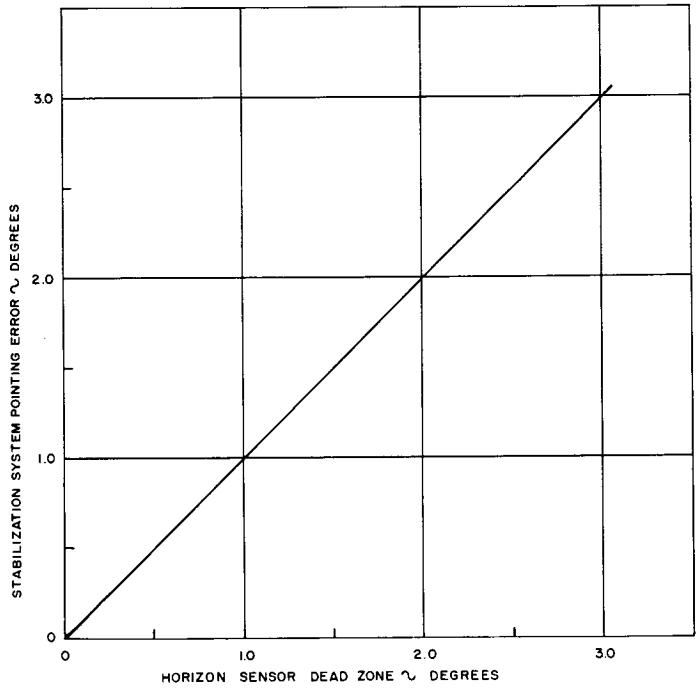

Figure 5-15. Effect of Horizon Sensor Dead Zone on Pointing Accuracy

TABLE 5-2
TYPICAL 3-AXIS STABILIZATION SYSTEM

All Size Vehicles	Size	Peak Power	Average Power	Weight
Variable Speed Wheels (2)	8.75 in. dia x 3.75 in.	9 watts each	4.5 watts each	5 lb each
Constant Speed Wheel	10.75 in. dia x 3.75 in.	36 watts	18 watts	10 lb
Horizon Sensor	6 in. x 6 in. x 6 in.	4 watts	4 watts	4 lb
Sun Sensor	2 in. dia x 1.9 in.	-	-	0.2 lb
Rate Gyros (3)	2.25 in. dia x 3.1 in. each	28 watts each	8 watts each	0.85 lb each
Electronics	8 in. x 8 in. x 5 in.	75 watts	26 watts	12 lb
500 lb Vehicle				
Cold Gas System-Nitrogen (3000 psi*)	-	-	-	24.0 lb
Titanium Tank	2587 cu in.	-	-	30 lb
Valves and Nozzles (7)	1/2 cu in. each	6 watts each	-	1.0 lb
Total	3961 cu in.	259 watts	81 watts	93.75 lb
1000 lb Vehicle				
Cold Gas System-Nitrogen (3000 psi*)	-	-	-	41.5 lb
Titanium Tank	4474 cu in.	-	-	50.0 lb
Valves and Nozzles (7)	1/2 cu in. each	6 watts each	-	1.0 lb
Total	5848 cu in.	259 watts	81 watts	131.25 lb

* Includes 50% safety factor plus 0.5 lb for leakage

Optimizing the wheel sizes for specific vehicles would change the wheel characteristics slightly. However, in general, the sensors, wheels, and electronics would not be affected by vehicle weight. The cold gas system is affected by the weight of the vehicle, since the major portion of stored gas is used for velocity correction and station keeping. The curve of stabilization system weight as a function of vehicle weight is shown in Figure 5-16. For the heavier vehicles, the major weight contribution comes from the gas system. A cold gas system rather than a hot gas one is selected because of its reliability

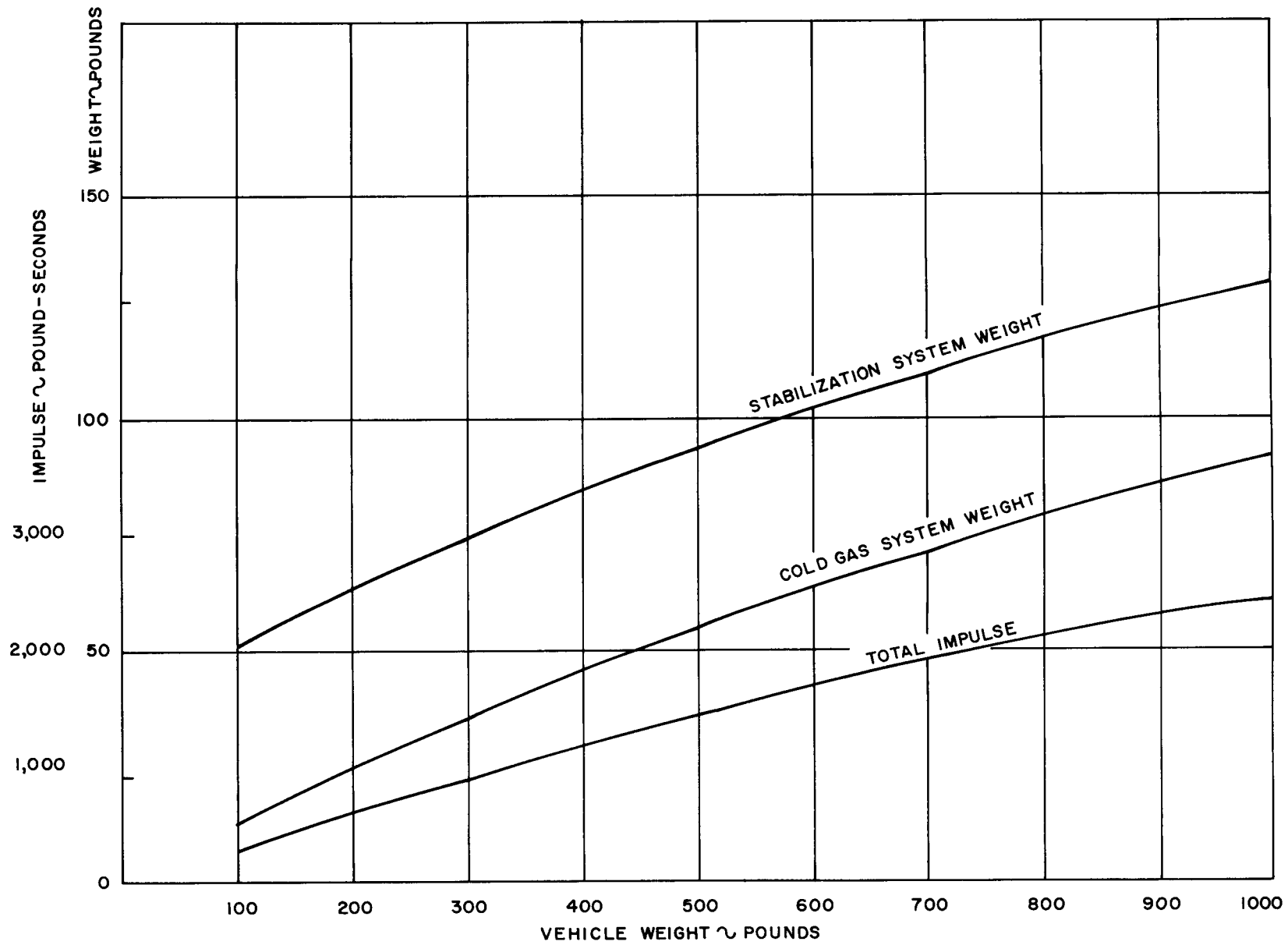

Figure 5-16. 3-Axis Stabilization System Weight

and low thrust levels. Figure 5-17, which was furnished by Walter Kidde and Company, shown the regions of thrust and total impulse normally provided by the different thrust systems. The low thrust requirements of SMS place it in the stored gaseous systems area or in the electric propulsion area for the higher total impulse.

Figure 5-18, supplied by Rocket Research Corporation, shows the relative weight advantage of their solid subliming system over the conventional cold gas system. When this system is further developed it can be used instead of the cold gas system with a considerable weight savings.

Redundancy in the stabilization system can be provided by adding redundant components, such as sensors, wheels, electronic amplifiers, etc. A more efficient method is by providing redundant functions. The use of the ground command to unload the reaction wheels, in addition to the normal automatic means, is an example of this method. The same ground command can also be used to operate the 3-axis control jets as a backup system in case of a wheel failure. Ground command control of the vehicle rates in a rate mode of control can be used in case of a horizon sensor or gyrocompass failure. This again is a functional type of redundancy.

C. POWER SUBSYSTEM

The mission of a satellite and its duration establish the duties for the various subsystems on the vehicle, such as stabilization and control, environmental control, communications, sensors, etc. Since all these subsystems require electrical power in one form or another which usually varies from one instant to the next, a power profile is essential to the determination of the power supply configuration.

An approximate relation between the power level required, the duration of the mission, and the power system to be used is shown in Figure 5-19.

For the purposes of this volume, the power range of 100 to 1000 watts is considered. It is also assumed that the vehicle configuration is a 3-axis stabilized, Sun-oriented system operating in a synchronous orbit about the Earth for a life duration of one year. Solar cell panels are used and are designed to provide time average power during the vehicle mission, and batteries are used to meet acquisition, occult, and peak load requirements.

The solar cell panels must meet the following provisions:

(1) Provide a given power output over a specified voltage range

(2) Operate reliably under the stated orbit and space environment conditions

The solar cell characteristics vary approximately with the cosine of the angle of incidence of the Sun's rays. The effect of temperature on current is relatively small, but power and voltage decrease rapidly with increasing temperature.

It is usual to allow 15% additional capacity to account for uncertainties in orbit precession and attitude (or aspect ratio) variations. If weight and size are

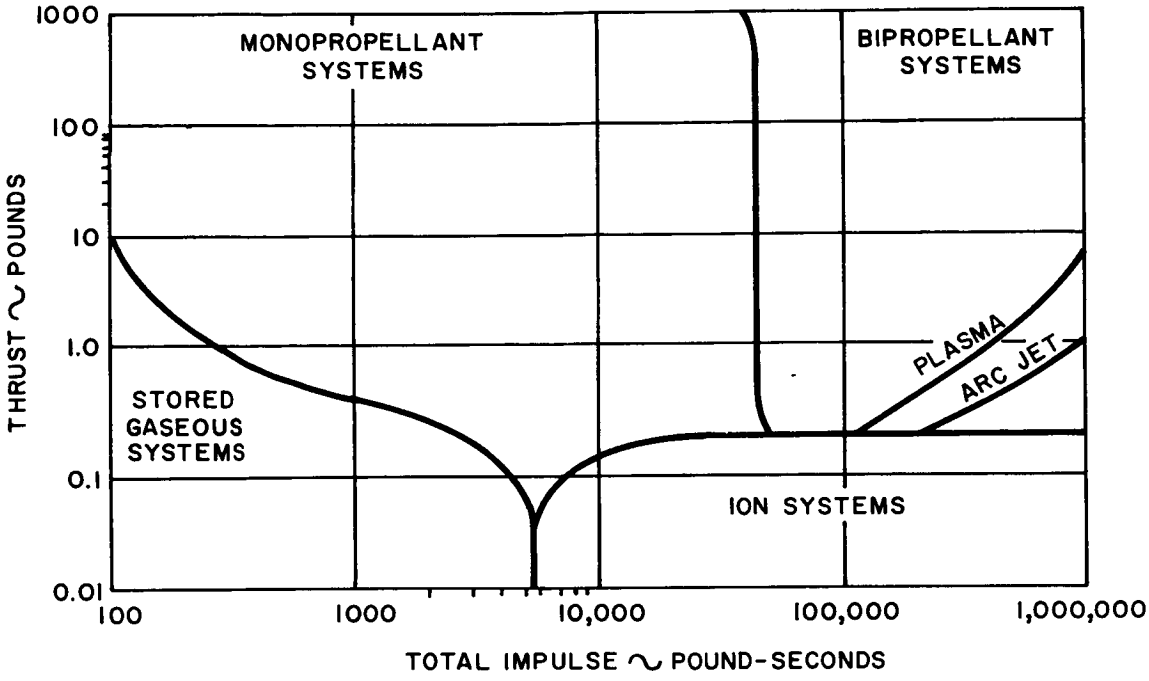

Figure 5-17. Optimum Regimes for Various Systems

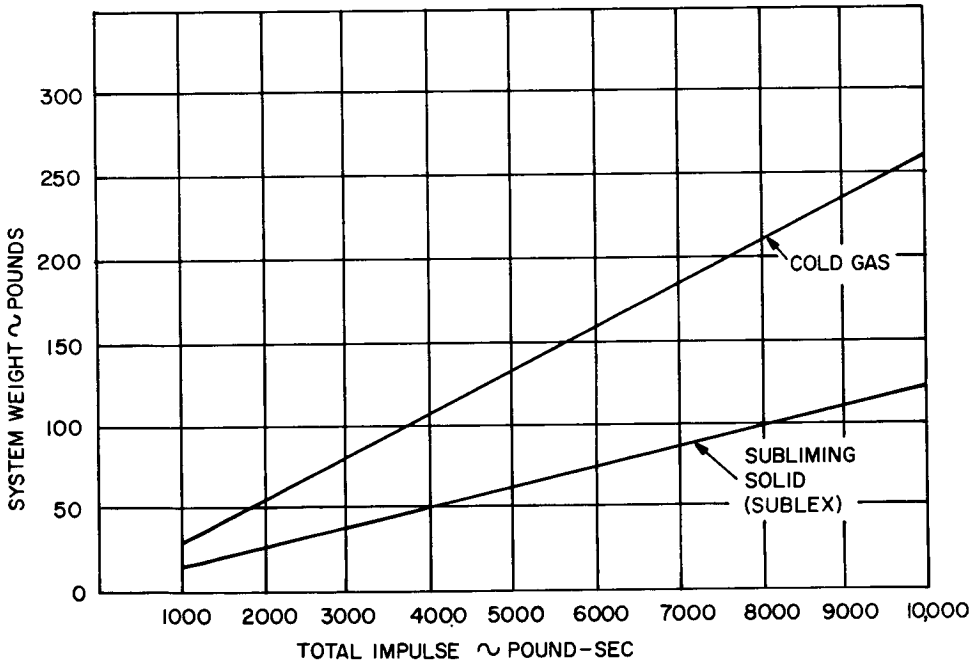

Figure 5-18. System Weight Including Propellant, Tanks, Valves, Regulators, and Six Thrusters

of prime importance, consideration must be given to the use of the most efficient cells available. At the present time, silicon solar cells of 12% conversion efficiency are available in quantity.

In the usual case, the operating voltage per cell is obtained primarily from temperature conditions. Referring to Figure 5-20 for cells over a temperature range of -100°C to + 100°C, with a design center of 0°C, the optimum cell voltage would be approximately 0.5 V.

The design will take into consideration the degradation of solar cell efficiency with, for example, a ± 100°C temperature variation from 0°C. The silicon cell efficiency goes down about 50% with a 100°C rise in temperature. Thus, it shall be necessary to assume that the efficiency of solar energy conversion is only 6%, though the cells used are of the 12% efficiency type at 0°C. Since the solar power available at the Earth, and with slight variation at the synchronous orbit, is 130 watts/ft^2, the solar cell output will therefore yield 6% of 130 or 7.8 watts/ft^2. Reducing this figure to include the loss of solar cell area due to contact "shingling," it can be assumed that the power density of the solar array is 7.5 watts/ft^2.

Protection from Van Allen radiation and micrometeoroidal damage at the synchronous orbit altitude may be provided by protecting the solar cells with a 6-mil quartz cover. If solar flares are anticipated, it would be wise to increase the solar cell area capacity by approximately 30% to allow for solar cell system degradation.

The weight of the solar cell array, which includes the protective quartz glass top, the bonding layers, solar cells, and aluminum honeycomb base, is approximately 1.5 lb/ft^2. Therefore, the specific power of the solar array is essentially $\frac{7.5}{1.5}$ = 5 watts/lb.

Two basic parameters govern the circuit configurations of solar cell arrays. The required output voltage establishes the number of cells which must be connected in series, and the load current requirement establishes the number of parallel banks of series strings which must be provided. The number of cells to be connected in series is obtained by dividing the system time average load voltage requirement by the cell operating voltage (as determined from the temperature range of operation). Having determined the number of cells in series, it is then necessary to fix the required number to be connected in parallel from considerations of illumination and power (current) requirements. The illumination will depend upon the orbit and the degree of array orientation.

Though the output voltage and current requirements control the overall number of series and parallel cells, for increased reliability purposes, the solar cells may be interconnected into series-parallel groups. For a given panel array, the optimum number of cells to be paralleled in a primary group unit depends upon:

(1) The required number of series and parallel units

(2) The probability of a solar cell open, short, or intermediate short to ground

(3) Solar voltage-current characteristics

(4) Load characteristics

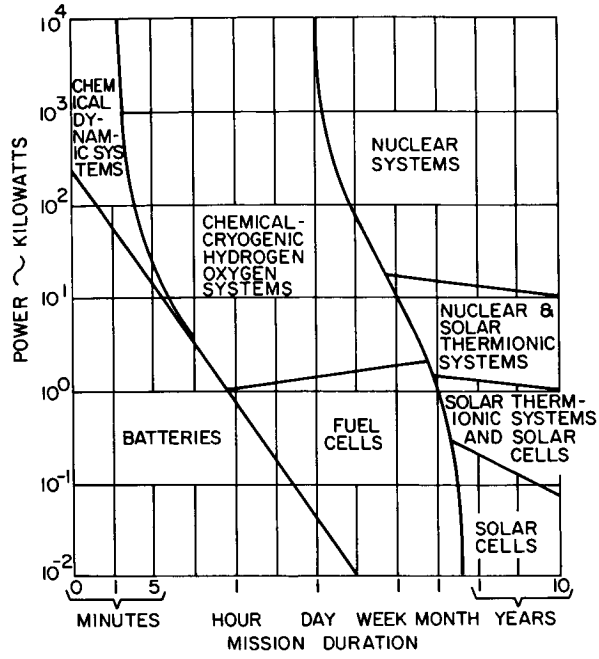

Figure 5-19. Application of Space Power Systems

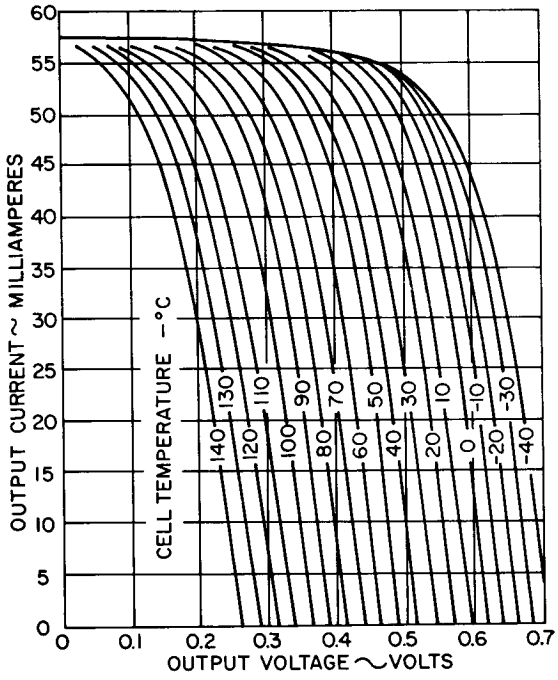

Figure 5-20. Effect of Temperature on Current-Voltage Characteristic of Solar Irradiated Cell (1x2 cm)

The exact configuration must be deduced from a thorough statistical analysis of the probability of multiple failures and the resultant effect on array characteristics.

The primary load to the solar array is the electrochemical storage battery, and this presents a special kind of panel design problem; namely, protection of battery life. An over-designed solar panel can significantly shorten battery life. Since battery life is affected by the depth of the charge-discharge cycle and by overcharging, accurate control of solar cell voltage is essential. A voltage-limiting characteristic should generally be incorporated into the battery charge circuit.

For the SMS orbit, the shadow period is roughly 70 minutes out of 24 hours at most. Therefore, a deep discharge of 65% is possible for the battery because of the slower charge rates which can be used with negligible possibility of damage to the cells. Since the power profile is such that there is an occurrence of peak ($<10\%$) drains on the battery during normal operation, it will be necessary to use a variable-type charge rate circuit rather than a slow constant current taper. This type of charging will in effect charge the battery at a rapid rate immediately after an occult period and at a slower rate during normal operation. The effects of a rapid charge to the battery when it is in its lower state of charge are not only not harmful, but beneficial; the slower rate of charge takes place when the battery is almost up to its full state of charge. In this state, the heating effects of rapid charging could be damaging to the battery, and caution must be taken.

The voltage-current characteristic of the ideal solar cell is almost rectangular. The nearly constant current characteristic on the short-circuit side of maximum power is well suited to the ideal charge condition for a battery, whereas the nearly constant voltage characteristic on the open circuit voltage side of maximum power is well suited to terminal voltage limitation as the fully charged condition of the battery is approached.

It is assumed that the solar array-battery combination will feed the load through a voltage regulator circuit. Those subsystems requiring uncommon power, i.e., increased or decreased voltage or AC voltages, etc., will have their individual conversion systems at, or within, the consuming equipment.

The following represents a typical design procedure and shows the application of the principles outlined in the discussion. Table 5-3 gives a resume of the power requirements for the medium capability 3-axis stabilized satellite configuration.

TABLE 5-3
3-AXIS STABILIZED MEDIUM CAPABILITY VEHICLE (Random Operation)

System Requirements	Acquisition (watt-hr)	Track	
		Average (watts)	Peak (watts)
Attitude Control	79 x 1	105	241
Communication	60 x 6	50	75
Data Handling	31.1 x 6	33.1	33.1
Power Supply	7 x 6	7.0	7.0
Sensor Equipments	10 x 6	77.1	131.0
Total	727.6 watt-hr	272.2 watts	487.1 watts

In order to compute the solar array and battery requirements, the following parameters will be assumed:

(1) The power density of the solar array is 7.5 watts/ft^2

(2) The weight of the solar array (with mounting) is 1.5 lb/ft^2

(3) The depth of discharge of the secondary battery (Ni-Cd) is 65%

(4) The specific energy of the secondary battery (Ni-Cd) is 12 watt-hr/lb

(5) The specific energy of the primary battery (Ag-Zn) is 40 watt-hr/lb

Once the power requirement has been established from the selection of equipment, the design will consider two alternatives; one in which all normal operations are carried on during the period in which the satellite is in eclipse of the Sun's energy and the other in which only the equipment which is on during acquisition, such as telemetering, command, and heating units, is in operation during the dark period while the sensor equipment is shut down.

- Normal Operation During the Dark Period

(1) During acquisition, 727.6 watt-hr are consumed.

(2) During track, 272.2 watts (average) and 487.1 watts (peak) are required of the power supply.

(3) Using Ag-Zn primary batteries for the acquisition, $\frac{727.6}{40} = 18.2$ lb.

(4) The solar array supplies 7.5 watts/ft^2 at a weight of 1.5 lb/ft^2. Hence, the specific power of the solar array is $\frac{7.5}{1.5} = 5$ watts/lb

(5) The weight of the solar array (mounting included) required to supply 272.2 watts is $\frac{272.2}{5} = 54.5$ lb + 15% = 63 lb.

(6) The solar array area is $\frac{63}{1.5} = 42$ ft^2. An allowance of 15% was made for variation of angle between the direction of solar radiation and the normal to the solar cell array.

(7) The maximum total dark period (umbra) in the synchronous orbit is approximately 67.4 minutes; in addition, there is a period of partial darkness (penumbra) which has a value of approximately 6.5% of the umbra.

(8) Considering the dark period as 70 minutes, the secondary battery would be required to supply $272 \times \frac{70}{60} = 320$ watt-hr.

(9) Assuming that the depth of discharge of the batteries during the occult period is 65%, the secondary battery size $= \frac{320}{0.65} = 493$ watt-hr.

(10) Ni-Cd has a specific power of 12 watt-hr/lb.

(11) The size of the secondary battery $= \frac{493}{12} = 41$ lb.

(12) A Sun-sensored solar paddle orientation system = 3 lb.

(13) A battery-solar paddle charge regulator circuit for the power supply system weighs approximately 12 lb.

The total system weight is therefore:

Primary Batteries	18.2 lb	
Secondary Batteries	41 lb	
Solar Array	63 lb	(42 ft^2)
Regulator-Selector Unit	12 lb	
Solar Paddle Drive	3 lb	
Total	137.2 lb	

The peak power, which occurs for about 5 minutes each half-hour cycle, will cause a $\frac{1}{6}\frac{(487.1-272.2)}{(493)} = 0.073$ or 7.3% depth of discharge.

- Limited Operation During the Dark Period

(1) 272 watts are required during normal operation.

(2) Solar array weight $= \frac{272}{3} = 54.8$ lb + 15% = 63 lb.

(3) 727.6 watt-hr are required during acquisition.

Therefore, $\frac{727.6}{40} = 18.2$ lb is the weight of the required primary batteries. Let us assume that the secondary batteries will be designed for a 10% depth of discharge to cover peak wattage requirements during normal sunlight operations and a 65% depth of discharge to cover occult period power requirements. The secondary battery capacity is therefore, $\frac{(1/6)\ (487.1 - 272)}{\text{Secondary Battery Capacity}} = 0.10$, or secondary battery capacity = 358 watt-hr; secondary battery weight = $\frac{350}{12} = 30.0$ lb.

During darkness, the vehicle requires approximately 82 watt-hr to carry on command, telemetering, heat control, etc. As a result, during the maximum eclipse period of 70 minutes, the secondary battery will have to supply $82.0 \times \frac{70}{60} = 96$ watt-hr. Assuming that a peak wattage period occurs just previously to the maximum eclipse period, the secondary battery would have to have a capacity of only $\frac{(1/6)(487.1 - 272) + 96}{0.63} = 203$ watt-hr. Hence, assume the higher energy requirements, i.e., a 358 watt-hr secondary battery capacity.

The total system weight is therefore:

Primary Batteries	18.2 lb	
Secondary Batteries	30 lb	
Solar Array	63 lb	(42 ft^2)
Regulator-Selector Unit	12 lb	
Solar Paddle Drive	3 lb	
Total	126.2 lb	

There is therefore a difference of 11 lb in battery savings in utilizing the alternative, i.e., working with limited operation during the dark period. It is usual, where weight is not a severe restriction, to overdesign the computed solar array by a 50% margin of safety. This will give the array the necessary 30% to encounter solar flare degradation plus an additional margin for redundancy in the event of unanticipated solar cell degradation. The solar array for the above examples will then become 63 ft^2.

Figure 5-21 is a rough curve of subsystem weight versus power requirements in terms of solar cell, battery, and solar cell array weight. It can be used for preliminary evaluation of system size.

D. STRUCTURE

For determining the final weight of the spacecraft, it is necessary to arrive at a procedure based on experience which will provide a method of estimating the weight of the structure required to house the equipment within the spacecraft. A number of existing spacecraft were investigated to determine the percent of the total weight allocated to structure. Figure 5-22 shows a plot of structural weight as a percent of orbital weight for known spacecraft and substantiates the conclusion that the structure will be approximately 20% of the orbital weight. For the procedure detailed in Section 6, this structural weight includes an allowance for thermal control. A discussion of thermal design is given in Appendix A.

Other factors entering into the consideration of spacecraft weight are:

(1) Solar paddle weight versus total weight (Figure 5-23)

(2) Wiring weight versus electronic system weight (Figure 5-24)

(3) Electronic system weight versus satellite orbit weight (Figure 5-25)

(4) Weight of liquid apogee kick motor versus orbital weight (Figure 5-26)

(5) Weight of solid apogee kick motor versus orbital weight (Figure 5-27)

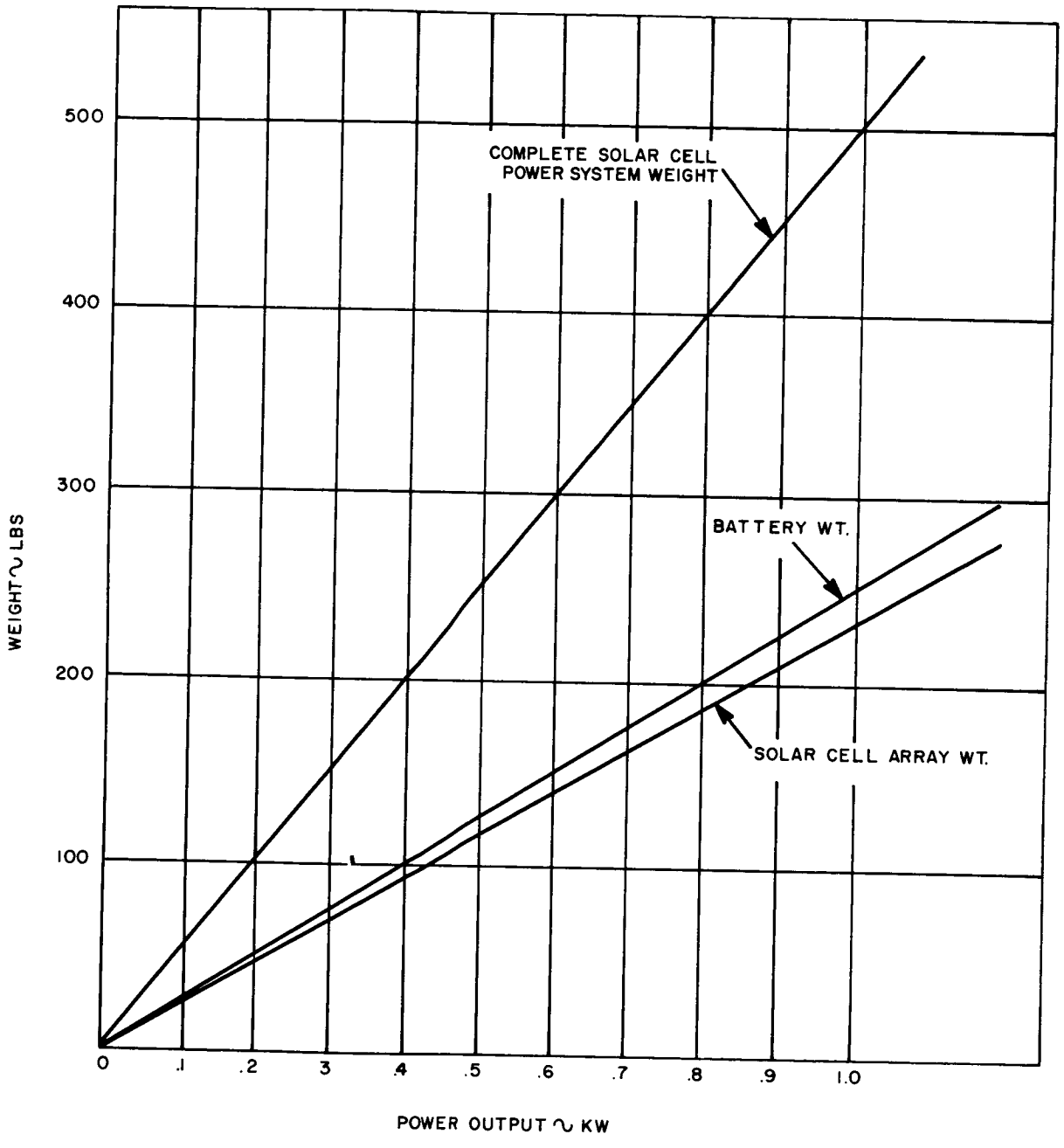

Figure 5-21. SMS Solar Cell Power System (Normal Operation During Occult)

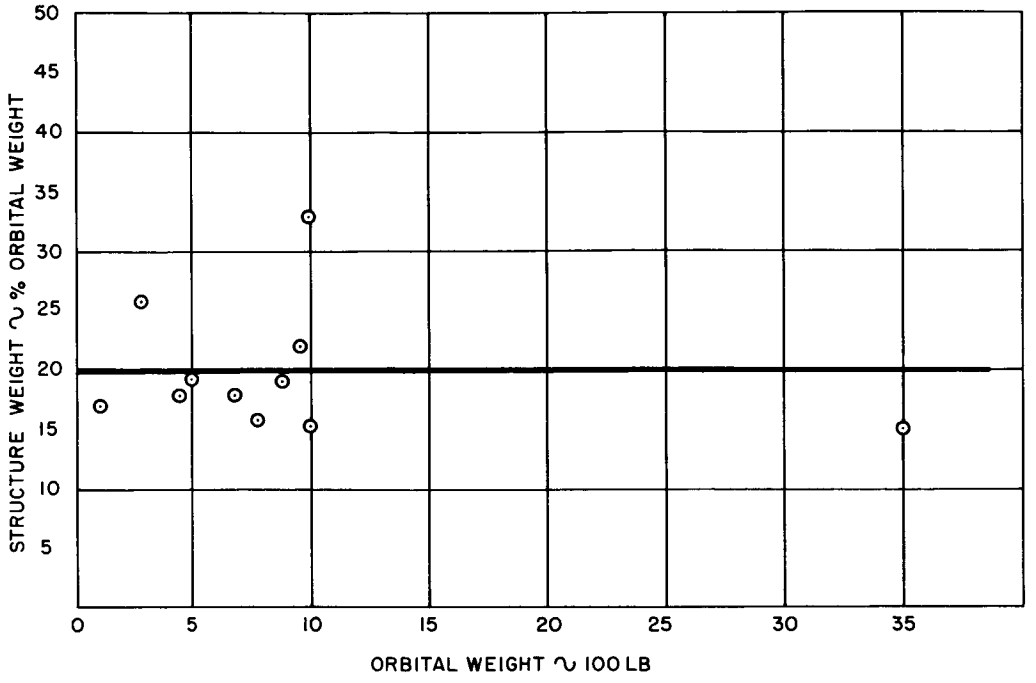

Figure 5-22. Satellite Structure Weight vs Orbital Weight - Existing Vehicles

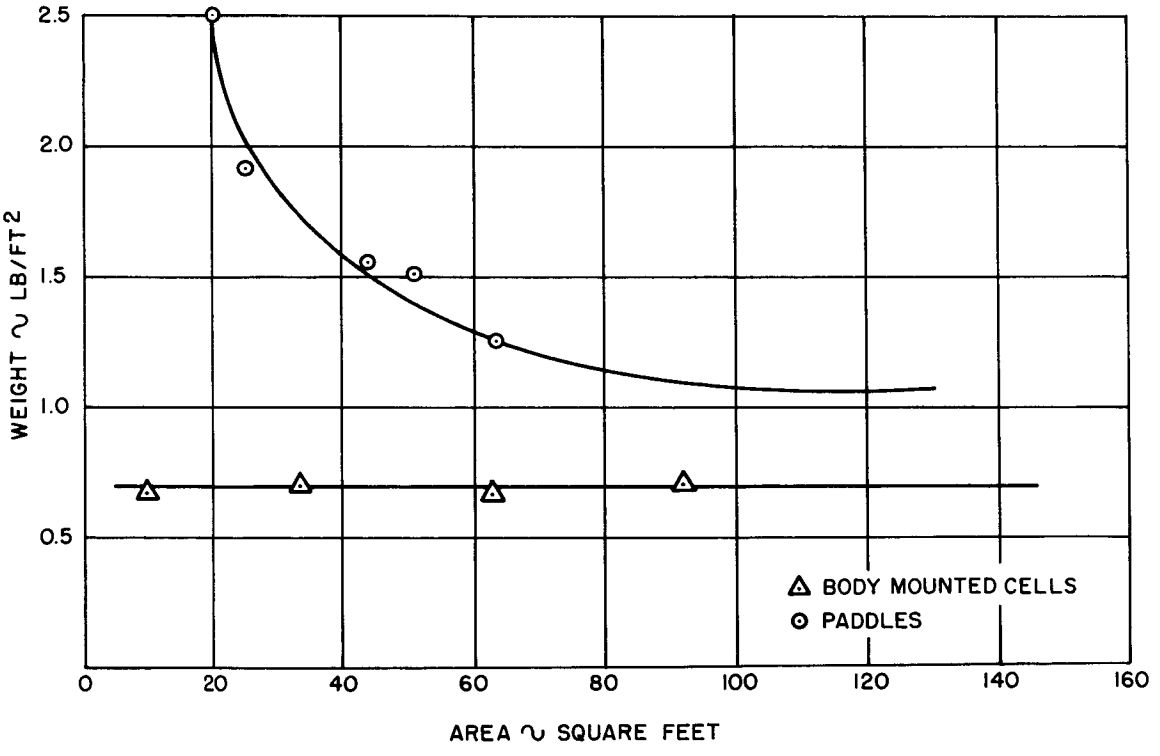

Figure 5-23. Solar Panels - Rigid Mounted - Existing Vehicles

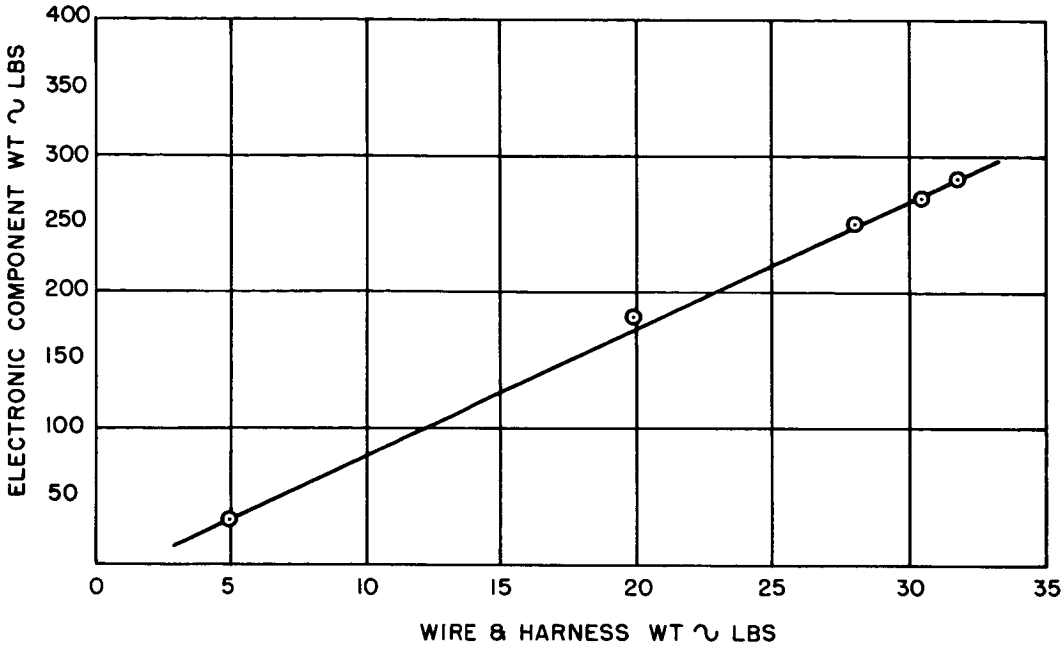

Figure 5-24. Satellite Wire and Harness - Existing Vehicles

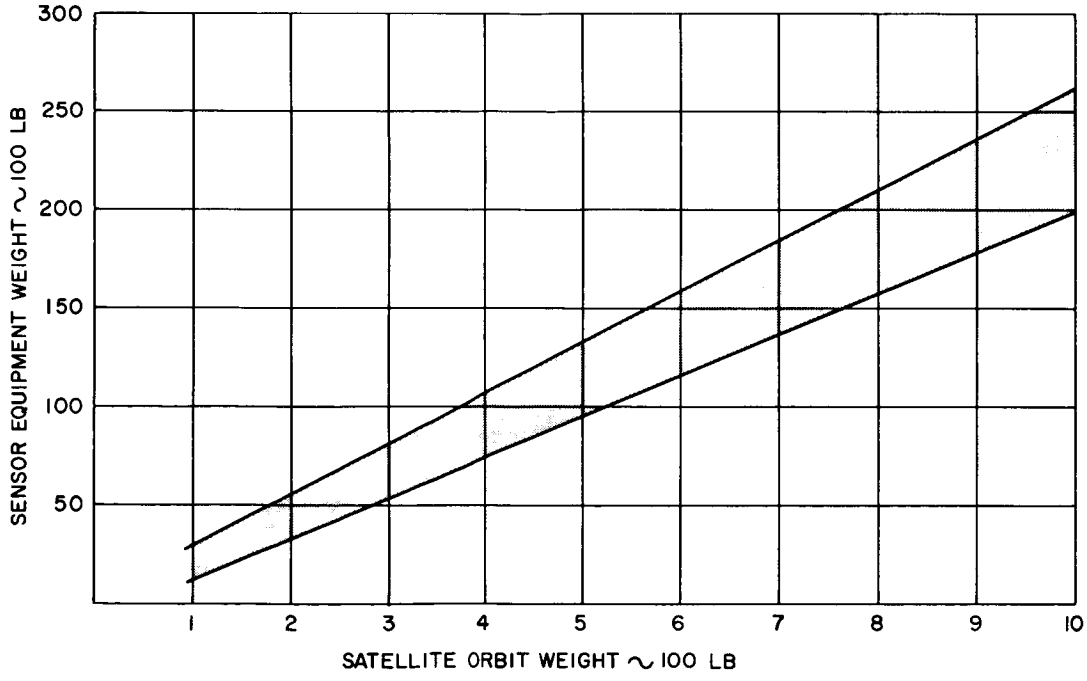

Figure 5-25. Electronic System Weight vs Satellite Orbit Weight

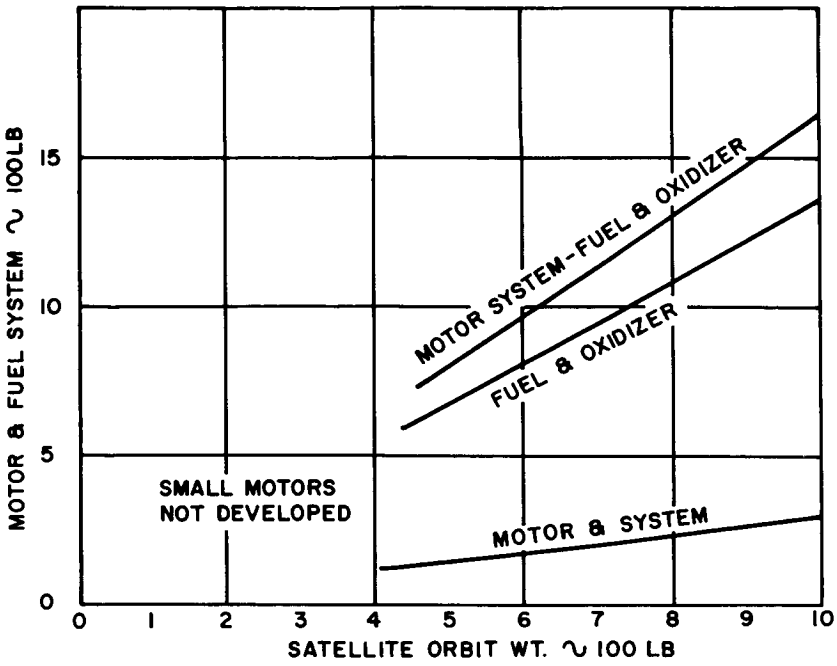

Figure 5-26. Liquid Apogee Motor Weight

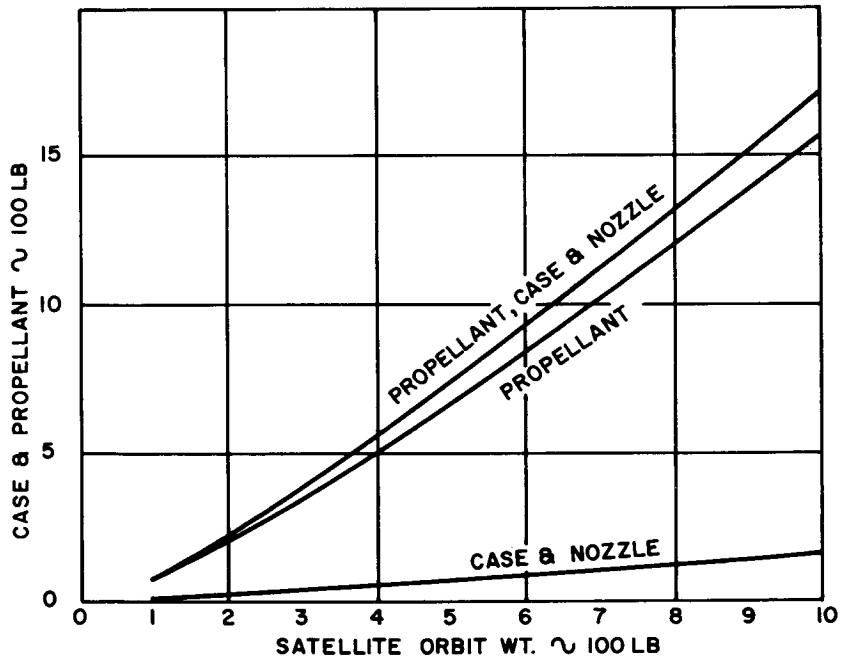

Figure 5-27. Solid Apogee Motor Weight

SECTION 6 - DESIGN PROCEDURES

This section presents a systematic procedure for arriving at an SMS system configuration. The design procedure is shown schematically in Figure 6-1. It involves nine steps culminating in a final system size. An iteration procedure can then be followed to bring the design within limits, or to compare various designs. In order to facilitate the design procedure, Figure 6-2 is provided. The performance specifications, important parameters, and computations can be tabulated on this sheet permitting evaluation of overall system effectiveness.

A. PERFORMANCE SPECIFICATIONS

In order to set the basic ground work for system design, a set of system performance specifications must be generated. First, a decision must be made as to the sensors to be included. For the selected sensors, the following information should be ascertained and listed, as shown in Figure 6-2.

(1) Full Earth Disc Sensor
- Resolution required
- Reporting cycle

(2) High Resolution Sensor
- Resolution required
- Reporting cycle
- Maximum number of pictures

(3) Heat Budget Sensor
- Resolution required
- Reporting cycle

In addition, a decision as to whether a communications relay should be incorporated into the spacecraft, and, if so, the type of information to be relayed, should be selected.

This information constitutes the basic system requirements and permits the user to fill in the performance evaluation criteria 1 to 4 and arrive at a performance figure for those assumed specifications.

With the foregoing information, the design procedure can then be performed.

B. SELECTION AND TABULATION

A study of the spacecraft equipment reveals the simplifying fact that many subsystems are quite insensitive to system performance specifications. In addition, these subsystems contribute only a small percentage to the weight, are readily available, and have a fairly high level of reliability. For these reasons, the design procedure narrows down to the following major areas:

(1) Selection of the sensors

(2) Selection of an attitude-station keeping system

(3) Selection of a power supply

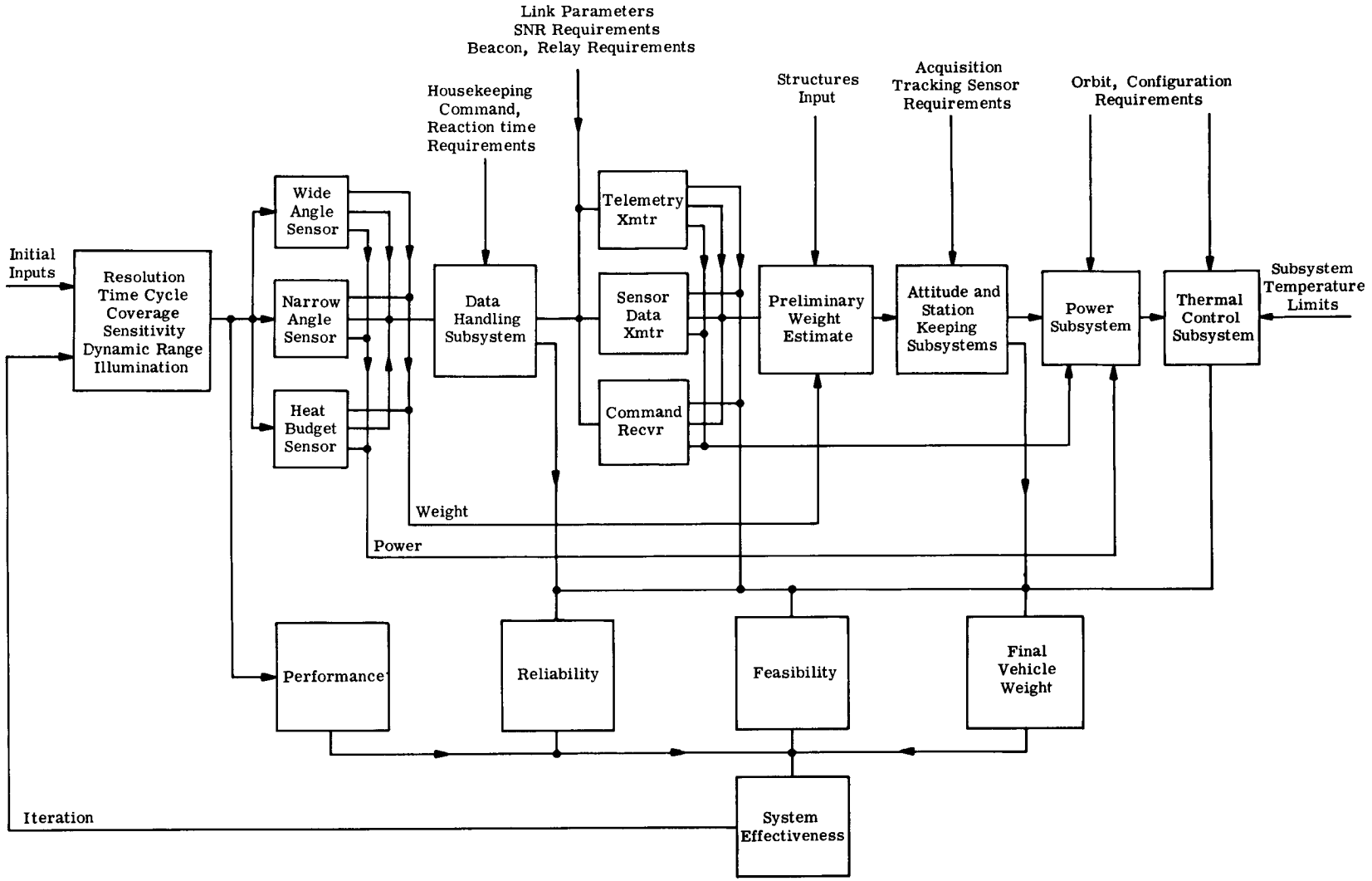

Figure 6-1. SMS Design Flow Chart

Performance Evaluation Criteria	Resolution (miles)	Reporting Cycle (hr)
1. Full Earth Disc Sensor a. Resolution b. Reporting Cycle		
2. High Resolution a. Resolution b. Reporting Cycle		
3. Heat Budget a. Resolution b. Reporting Cycle		
4. Relay or Other Secondary Function		

Vehicle Performance Class

HIGH	Same as medium Performance with Subsystem Redundancy
MEDIUM	Full Earth Disc, High Resolution, Heat Budget, and Relay Function
LOW	Full Earth Disc and Heat Budget

	Equipment	Weight (lb)	POWER Peak	POWER Average	POWER Duty Cycle	Feasibility (1)	Reliability (2)
1	Full Earth Disc Sensor						
2	Heat Budget Sensor						
3	High Resolution Sensor						
4	Data Handling for Telemetry a Command b Sensor c Telemetry Trans. d Command Receiver e Beacon f Relay-RARR						
5	Sensor Data Trans.						
6	Preliminary Wt. Total						
7	Attitude and SK Subsystem						
8	Power Totals						
9	Power Subsystem						
10	Thermal Control						
11	Structure						

(1) For Feasibility Use the Following Set of Numbers

Off-the-Shelf Item	3
Available in 1967	2
Available in 1970	1
No Apparent Availability	0

(2) For Reliability Use the Following Set of Numbers

Triple or More Redundancy	3
Double Redundancy	2
No Redundancy	1

Summary of Evaulation Criteria

System	#1	#2	#3
Performance Weight Feasibility * Reliability*			

* Based on subsystem feasibility and reliability, assign an overall letter or number for the system.

Figure 6-2. SMS Design Working Sheet

(4) Correlation with the structure for final weight estimate (structures weight will incorporate thermal control subsystem weight)

Although the various subsystem design sections contain detailed design information, a rough preliminary design evaluation can be carried out based on simplified evaluation criteria. To accomplish this, it is only necessary to do the following:

(1) List the weight of the various subsystems, taking account of the redundancy desired

(2) List the required power and duty cycle

(3) Assign a number for reliability and feasibility based on the design section's conclusions

(4) Sum up the various evaluation criteria, as shown in Figure 6-2, obtaining numbers for the various classes

(5) Iterate the sensitive subsystems, i.e., sensors, attitude-station keeping, and power, or varying the redundancy level of all subsystems

The non-sensitive subsystems, with weights, powers, reliability, and feasibility, are listed below and again in Figure 6-2. Note that the reliability and feasibility figures are merely a set of consistent numbers to show various levels. A full evaluation procedure would entail detailed reliability and feasibility calculations, which are beyond the scope of this study. However, Appendix B details methods of arriving at reliability numbers for redundant subsystems when the initial reliability figures are known. This appendix also incorporates a system reliability model for overall system reliability calculations.

Non-Sensitive Subsystems

		Notes	Weight	Peak	Avg.	Duty Cycle	Feasibility	Reliability
Data Handling		(1)	28.0	33	33	100%	3	1
Telecommunications	Telemetry	-	1.5	Telecommunications Subsystem Total 75 50 50%			3	1
	Command	(2)	1.0				3	2
	Beacon	(3)					-	-
	Relay	(4)	3.0				3	1
	Data Transmitter	(5)	13.25				3	1

(1) PCM system with tone-digital backup

(2) Redundant units

(3) Uses relay receiver and data transmitter

(4) Communications relay, using data transmitter and additional S-Band receiver

(5) Using 10 w transmitter

After listing the non-sensitive subsystems, proceed as follows:

(1) From Section 5.A, select a full disc sensor, a high resolution sensor, and a heat budget sensor. From the design considerations, assign a feasibility and reliability number. Determine the attitude rate required of the attitude system from Figure 5-2. Now, from Figure 5-11, determine the approximate weight of selected sensors. List all numbers in Figure 6-2

(2) Now, following the procedure outlined in Section 5.D, make a preliminary weight estimate using Figure 5-25

(3) Using Section 5.B it is now possible to select an attitude station-keeping subsystem. From the discussion in this section, a large degree of insensitivity of the various components is indicated. Although detailed design is a laborious procedure, a preliminary weight, feasibility, and reliability estimate can be obtained. After determining the feasibility of the subsystem, subsystem weight can be determined from Figure 5-18, noting that the major sensitivity is derived from the cold gas weight. List the weight, power, feasibility, and reliability in Figure 6-2

(4) Tabulate the required system power

(5) Using the design steps of Section 5.C, select a power supply. There are several options here resulting in some weight savings. Having selected the particular option, list the weight, feasibility, and reliability in Figure 6-2

(6) Tabulate all the effectivity parameters as shown in Figure 6-2, and evaluate the design

(7) Vary the performance requirements and/or redundancy to arrive at new effectivity numbers

APPENDIX A - THERMAL CONTROL SUBSYSTEM

A. SUBSYSTEM CONSIDERATIONS

The important considerations in the design of satellite temperature control subsystems can be divided into three basic categories:

(1) Recognition and analysis of all possible heat sources, heat sinks and heat paths that affect the satellite throughout its lifetime in orbit, and discrimination between significant and negligible heat sources, sinks, and paths

(2) Development, improvement, optimization, and integration of the suitable surfaces, surface coatings, insulation, heat paths, heat sinks, heat storage devices, and heat pumps necessary to maintain the desired temperature level

(3) Experimental verification of the adequacy of the thermal design and the acceptability of the overall system concept. The primary purpose of this phase is to verify that the theory, thinking, and assumptions that form the basis of the design are correct in direction and degree

The temperature design objective for the SMS system is 25°C ±10°C. However, the parametric curves included in this appendix show the operating temperature range as a parameter without being restricted to 25°C ±10°C.

B. SUBSYSTEM TYPES APPLICABLE TO THE SMS

Three basic thermal control systems were studied for SMS application; passive, semiactive, and active. Because the definitions of these systems are not universely accepted, they will be restated for the purpose of this report. The systems are listed in order of their increasing complexity and their ability to maintain temperatures within narrow limits.

A passive thermal control system is one in which there are no moving parts and/or fluids effecting the control. In passive systems, temperature control is achieved by using surface coatings with an absorptivity-emissivity combination that will result in maintaining permissible temperature range during all exposures of the spacecraft. Judicious use of insulation, heat paths, radiation barriers, energy storage devices, and control of internal heat dissipation can often supplement the use of surface coatings to control the spacecraft temperature.

A semiactive thermal control system is defined as one containing moving parts and/or fluids, but the system specifically excludes a heat pump. In a semiactive thermal control system, heat is rejected at or below the source temperature.

An active thermal control system, by definition, contains a heat pump. In this system, heat may be rejected at a higher temperature than the source temperature. This can not be done with a semiactive or a passive thermal control system.

It can be shown that for a solar cell-powered synchronous satellite the optimum active thermal control system is one in which the mean radiator temperature is equal to the mean temperature within the equipment compartment. This condition constitutes a semiactive system. Therefore, an active system is not competitive for SMS application. The analysis leading toward this conclusion is presented in detail in Volume 5, Section 4.

C. SUBSYSTEM SELECTION

The choice between a passive or semiactive thermal control system depends on numerous factors, and it is difficult to arrive at a clear-cut boundary between passive and semiactive regimes. A trade-off trend for temperature control systems is shown in Figure A-1. The curve is based on state-of-the-art assumptions published in the literature and represents a first approximation to indicate the trade-off trend. Passive systems based on the thermal heat storage principle or on surface heating elements were not included in this curve.

D. PARAMETRIC PRESENTATION

1. Three-Axis Stabilized Spacecraft

Figures A-2 through A-7 present temperatures for a nonspinning satellite as a function of surface radiative properties and internal power dissipation. The satellite is exposed to solar radiation only (synchronous attitude). Each $\alpha = 0$ line represents the case where the surface receives no solar flux. For a given absorptivity, emissivity, and power density combination, it is thus possible to determine the temperature during sunlight exposure as well as when the surface does not see the Sun by dropping along a constant ϵ line to the $\alpha_s = 0$ line. Table A-1, based on Figures A-2 through A-7, summarizes the maintainable temperature range for a three-axis stabilized SMS with surface property control only.

TABLE A-1
ATTAINABLE TEMPERATURES FOR A 3-AXIS STABILIZED VEHICLE WITH SURFACE PROPERTY CONTROL ONLY

Power Density (watt/ft^2)	0	0.5	1.0	2.0	5.0	10.0
Max. Temperature (°F)	130	140	150	168	115	110
Min. Temperature (°F)	-453	-145	-85	-12	15	50
Δ T (°F)	583	285	235	180	100	60
Absorptivity	0.05	0.05	0.05	0.05	0.05	0.05
Emissivity	0.1	0.1	0.1	0.1	0.2	0.3

Thermal storage can be very effective in controlling cyclic temperatures such as those encountered with the three-axis stabilized configuration (Table A-1). Figures A-8 and A-9 give the parametric performance of various heat storage materials for plane and cylindrical surfaces, respectively. For a given absorptivity, α_s, the weight of material per square foot can be obtained

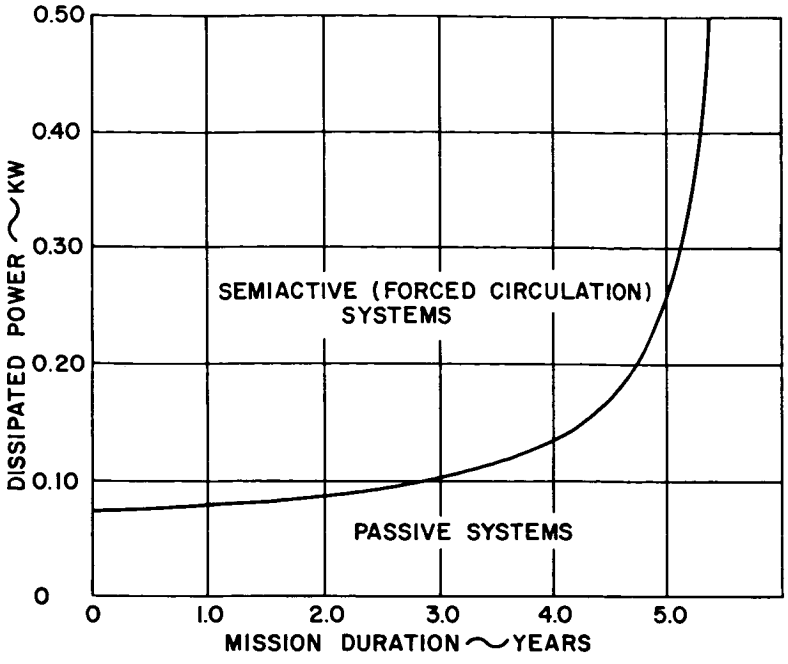

Figure A-1. Trade-Off Trend for Temperature Control Systems

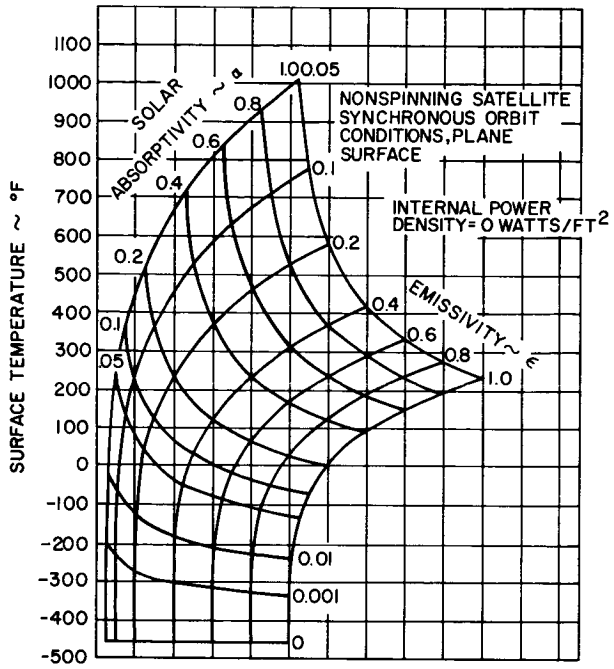

Figure A-2. Effect of Surface Characteristics and Internal Power Density (0 watts/ft^2) on Spacecraft Surface Temperature - Non-Spinning Satellite

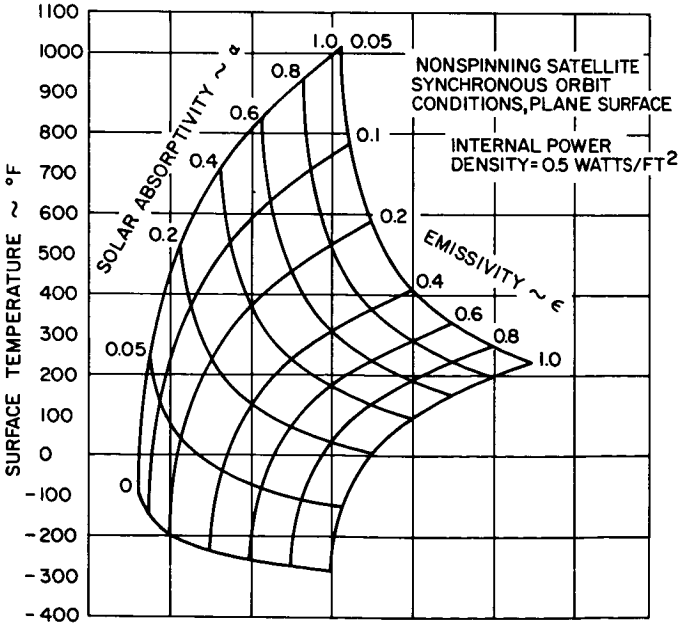

Figure A-3. Effect of Surface Characteristics and Internal Power Density (0.5 watts/ft^2) on Spacecraft Surface Temperature - Non-Spinning Satellite

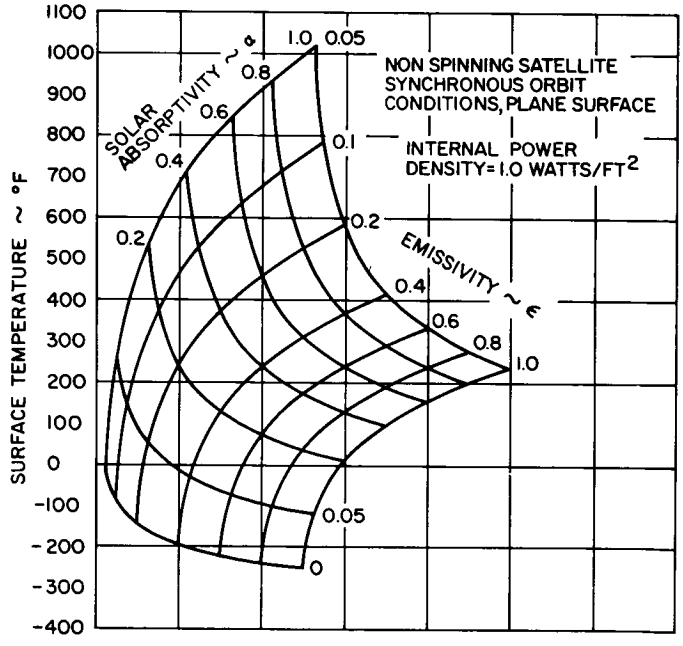

Figure A-4. Effect of Surface Characteristics and Internal Power Density (1.0 watts/ft^2) on Spacecraft Surface Temperature - Non-Spinning Satellite

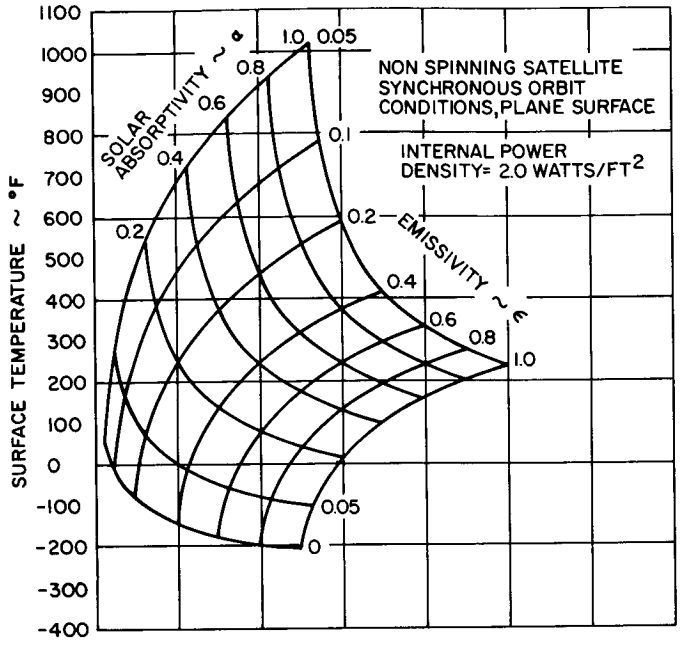

Figure A-5. Effect of Surface Characteristics and Internal Power Density (2.0 watts/ft^2) on Spacecraft Surface Temperature - Non-Spinning Satellite

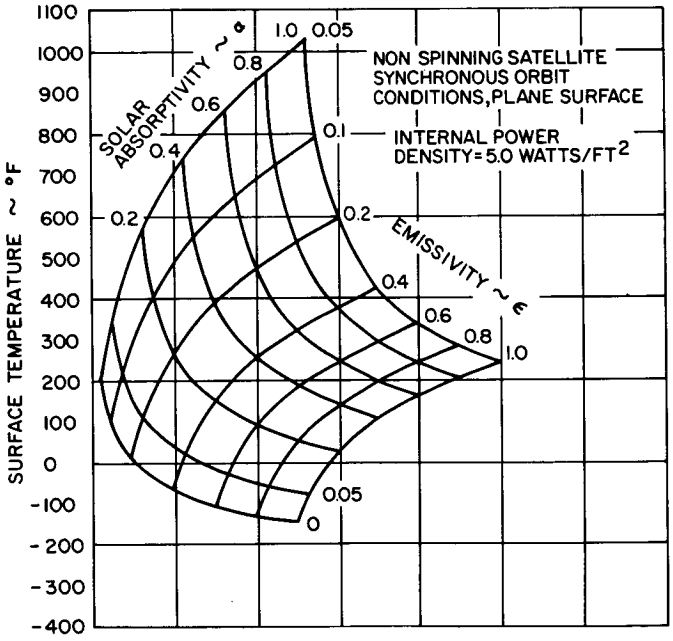

Figure A-6. Effect of Surface Characteristics and Internal Power Density (5.0 watts/ft^2) on Spacecraft Surface Temperature - Non-Spinning Satellite

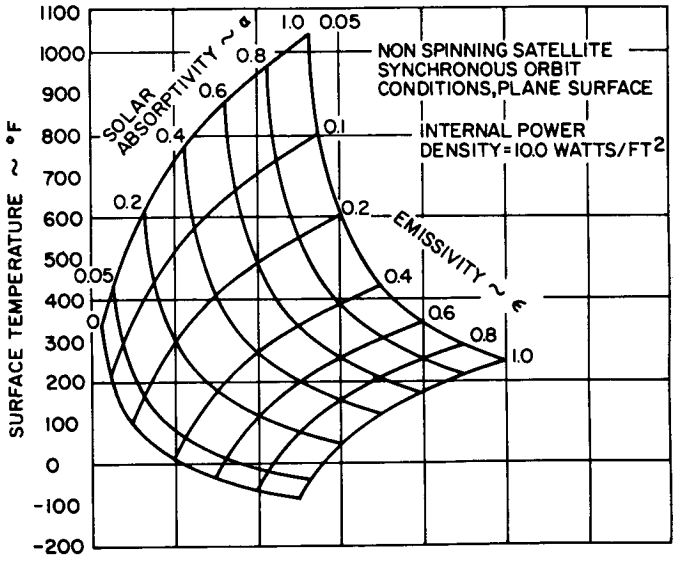

Figure A-7. Effect of Surface Characteristics and Internal Power Density (10.0 watts/ft^2) on Spacecraft Surface Temperature - Non-Spinning Satellite

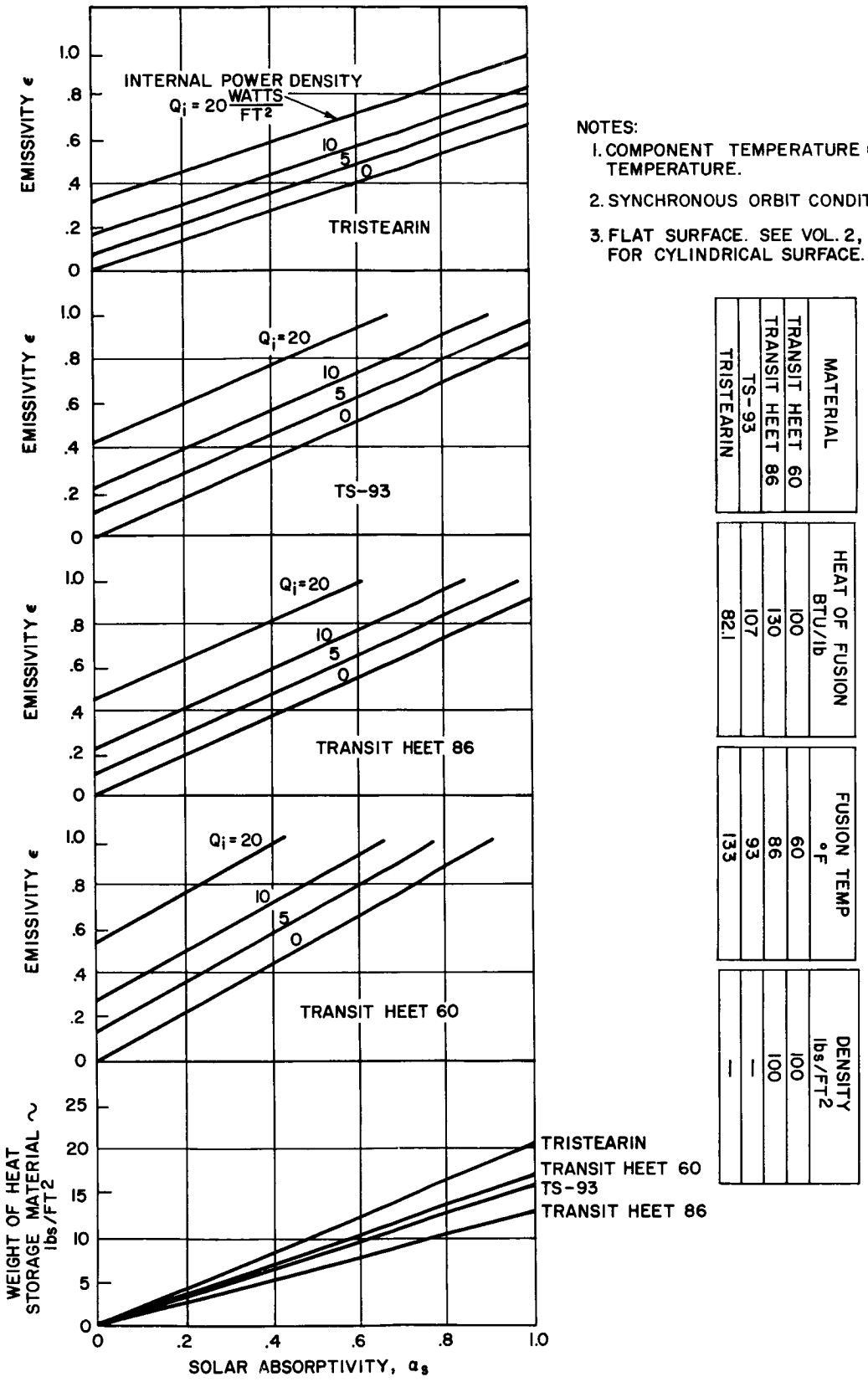

Figure A-8. Performance of Thermal-Storage Temperature Control Systems - Flat Surface

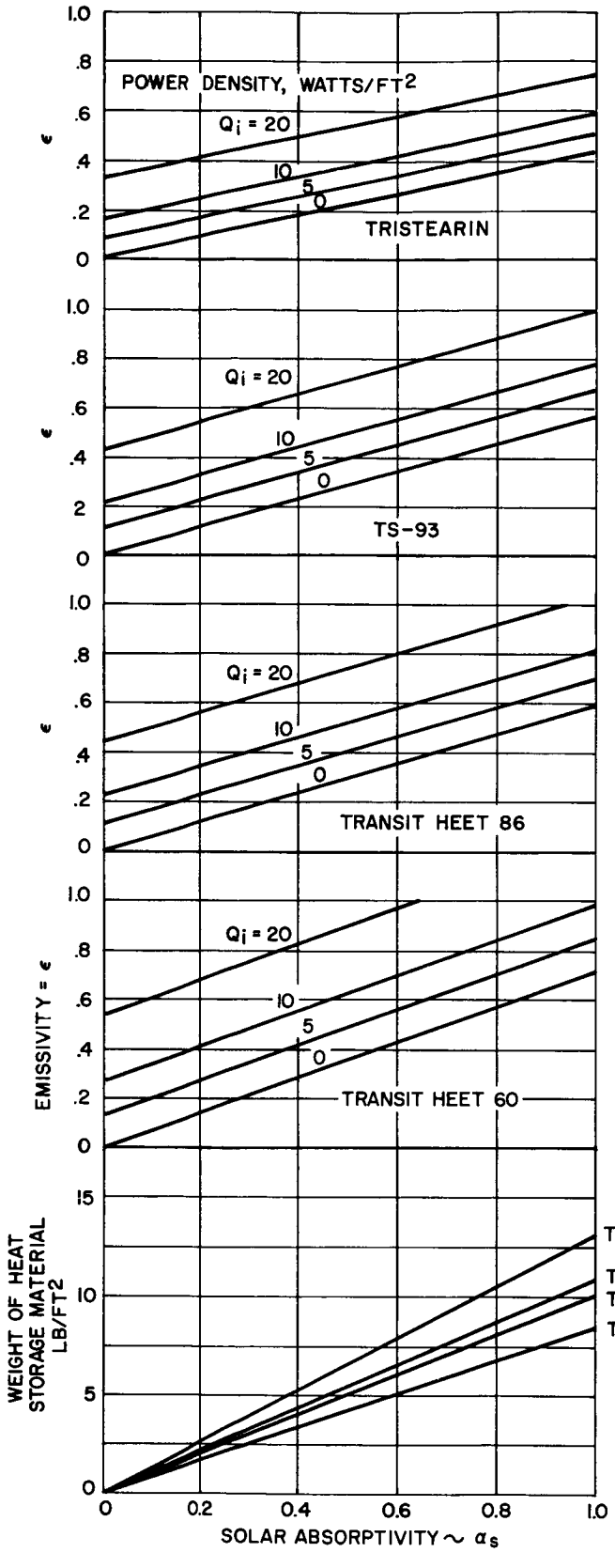

NOTES:

1. COMPONENT TEMPERATURE ≈ FUSION TEMPERATURE.
2. SYNCRONOUS ORBIT CONDITIONS.

MATERIAL	HEAT OF FUSION BTU/lb	FUSION TEMP °F	DENSITY lbs/FT2
TRANSIT HEET 60	100	60	100
TRANSIT HEET 86	130	86	100
TS-93	107	93	—
TRISTEARIN	82.1	133	—

Figure A-9. Performance of Thermal-Storage Temperature Control Systems - Cylindrical Surface

from the lower portions of the graphs. Then, at the same absorptivity and the corresponding emissivity, ϵ, the amount of watts that can be dissipated per square foot is given by the upper portions of the graphs.

2. Spin-Stabilized Spacecraft

The temperature distribution on a spin-stabilized cylindrical satellite as a function of rpm is shown in Figure A-10. Figures A-11 through A-16 give the mean temperatures of a spin-stabilized satellite as a function of surface properties and internal power dissipation. The satellite is exposed to full solar radiation. For a given combination of α_s, ϵ, and power dissipation, the mean temperature can be obtained. The temperature fluctuations about the mean for a given rpm can then be obtained from Figure A-10. (The power density has no appreciable effect on the amplitude for a given rpm.)

E. THERMAL CONTROL SURFACE PROPERTIES

In the parametric presentation above, the radiative surface properties, α_s and ϵ, have a predominant effect on the obtained results. Tables A-2 and A-3 list a summary of the tested surface properties of various thermal control materials.

F. SUBSYSTEM COMPARISON ON A WEIGHT BASIS

It is estimated that a typical radiator and conductive structure of a purely passive thermal control system would weigh 1.25 lb/ft^2. The heat storage material and containment for a thermal storage control system would weigh (present available stable α_s is not less than 0.1) 1.0 lb/ft^2. Together with the radiator and conductive structure, the thermal control-by-thermal storage material would weigh 2.25 lb/ft^2 of radiator. A semiactive control radiator for a forced circulation loop is expected to weigh 0.5 lb/ft^2 of radiating surface. In this system, there are additional weight penalties, such as the weight of pumps, tubing, coolant, and valving. These weights are a function of the individual design complexity. The weights quoted are for radiators integrated with the vehicle structure.

G. SUBSYSTEM COMPARISON ON A RELIABILITY BASIS

Of the thermal control subsystems considered, the purely passive (radiative-property controlled) system is the most reliable. The only component subject to damage (meteorite erosion) is the radiator. Local damage on the radiator does not appreciably affect the entire radiator or system. Redundancy is not recommended for purely passive thermal control systems.

The thermal storage control system, in addition to being subject to radiator erosion damage, is also subject to loss of thermal storage material due to meteorite penetration. Compartmentization of the thermal storage material would localize material losses due to meteorite impact. Redundancy is not practical with this scheme.

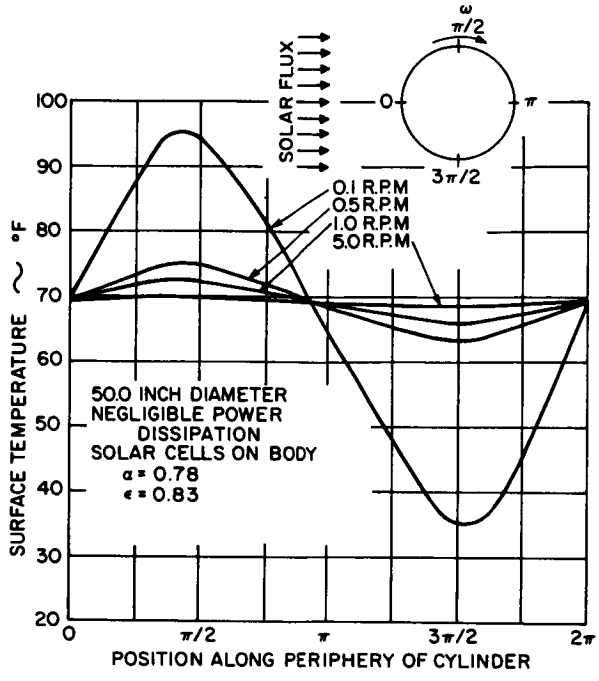

Figure A-10. Temperature Distribution on a Spin-Stabilized Cylindrical Satellite

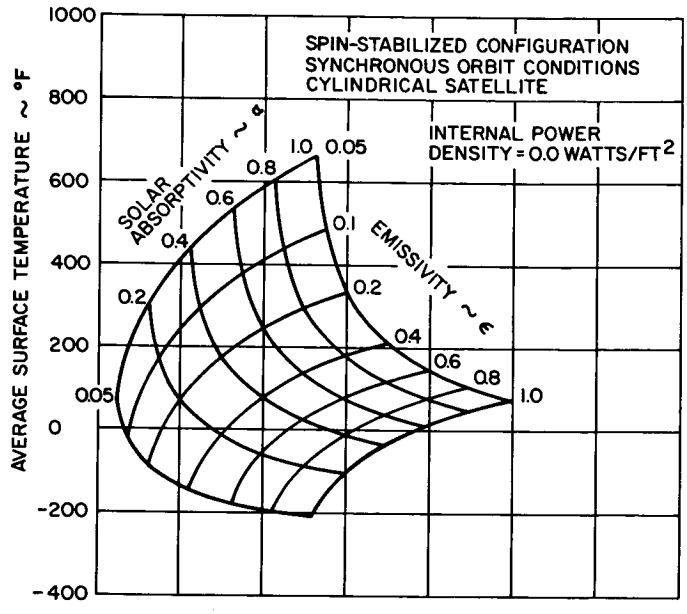

Figure A-11. Effect of Surface Characteristics and Internal Power Density (0.0 watts/ft^2) on Spacecraft Surface Temperature - Spin-Stabilized Configuration

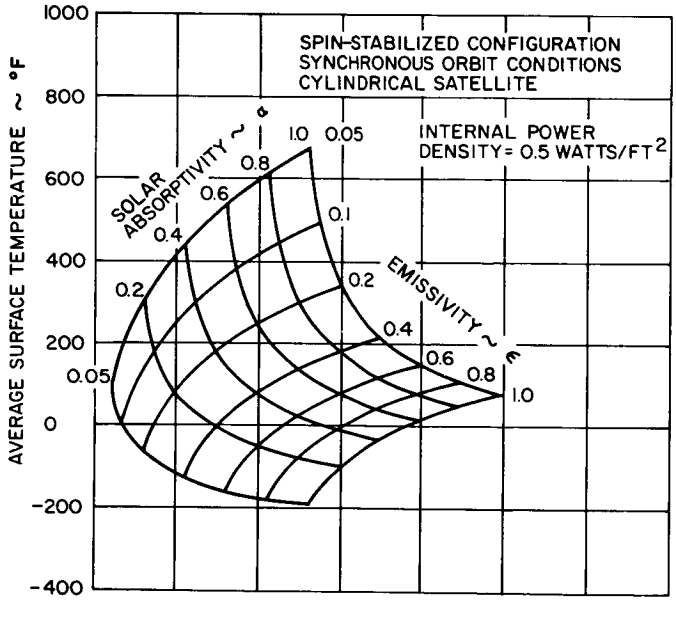

Figure A-12. Effect of Surface Characteristics and Internal Power Density (0.5 watts/ft^2) on Spacecraft Surface Temperature - Spin-Stabilized Configuration

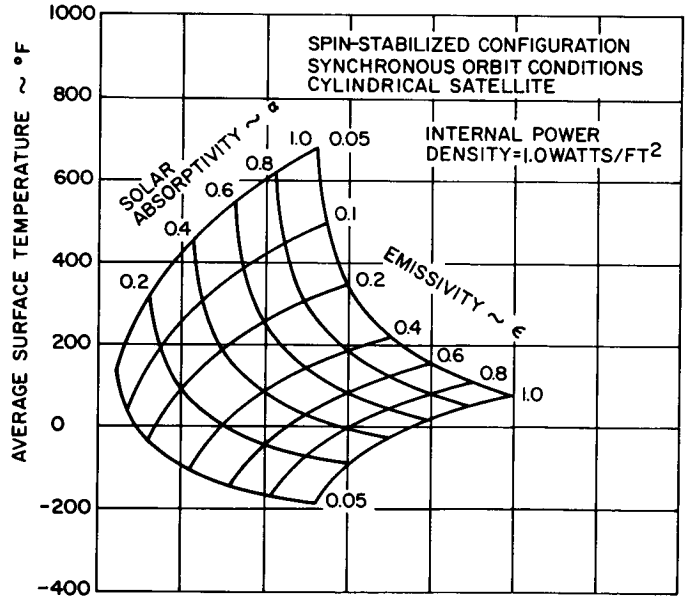

Figure A-13. Effect of Surface Characteristics and Internal Power Density (1.0 watts/ft^2) on Spacecraft Surface Temperature - Spin-Stabilized Configuration

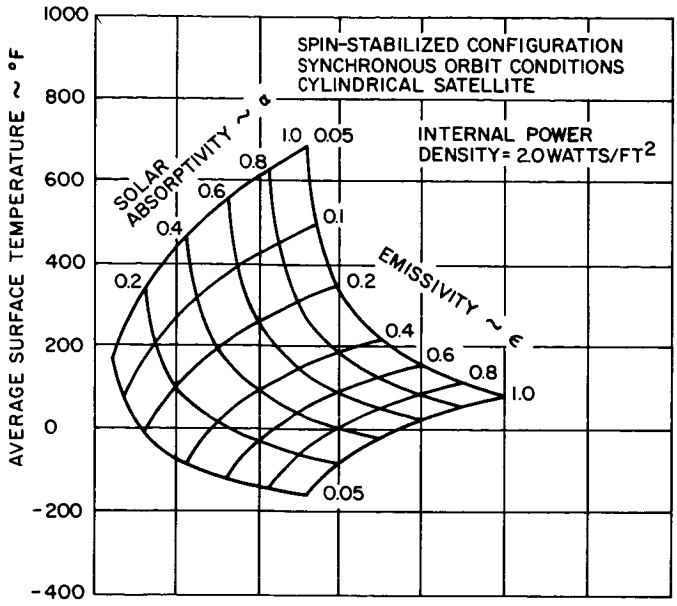

Figure A-14. Effect of Surface Characteristics and Internal Power Density (2.0 watts/ft^2) on Spacecraft Surface Temperature - Spin-Stabilized Configuration

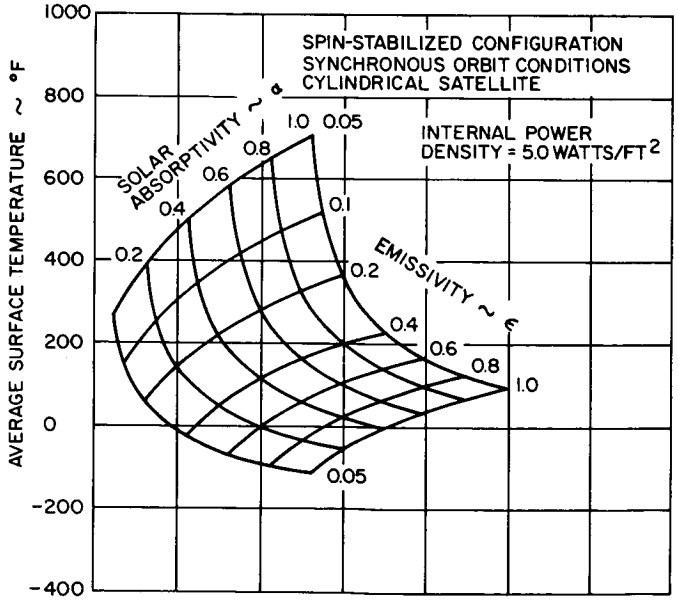

Figure A-15. Effect of Surface Characteristics and Internal Power Density (5.0 watts/ft^2) on Spacecraft Surface Temperature - Spin-Stabilized Configuration

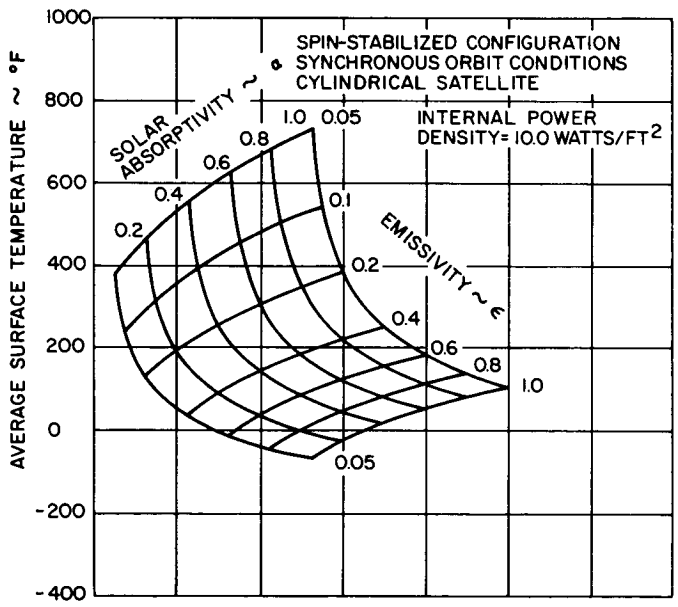

Figure A-16. Effect of Surface Characteristics and Internal Power Density (10.0 watts/ft^2) on Spacecraft Surface Temperature - Spin-Stabilized Configuration

TABLE A-2

RADIATION CHARACTERISTICS OF MATERIALS

Material	Tested by	Solar Absorptivity α_s	Infrared Emissivity ϵ	Comments
White Paint	STL	0.22	0.75 - 0.85	Zinc Sulphide - Silicon base - 4 coats req'd. Ultraviolet exposure raises $\alpha > 0.3$
Black Paint	STL	0.96	0.80 - 0.85	Carbon black pigment - Silicon base
Aluminum Paint	STL	0.20 - 0.24	0.20 - 0.24	Leafing Aluminum in Silicon base. Values vary up to 0.3 (NRL)
Evaporated Gold	STL	0.18	0.02	Must be clean - use strippable coating prior to launch
Evaporated Aluminum	STL	0.10	0.025	Must be clean - use strippable coating prior to launch
Polished Aluminum	STL	0.20 - 0.40	0.03 - 0.06	
Polished Stainless Steel	STL	0.30 - 0.50	0.10 - 0.20	
Electroplated Gold	STL	0.20 - 0.30	0.02 - 0.06	Contamination problem
Aluminized Mylar	STL	0.10	0.025	
Evaporated Gold with SiO Coating	STL	0.17 - 0.18	0.025 - 0.34	ϵ a function of SiO pigment
Magnesium Oxide		0.14	0.90	Plasma-sprayed
"Reflectal"	UCLA	0.19	0.05	Mechanical polish
"Reflectal"	UCLA	0.15	0.75	Mechanical polish, 15 min. anodize in 10% H_2SO_4
"Reflectal"	UCLA	0.15	0.05	Mechanical polish, Jacquet electropolish 15 min., 40F, 24V
1199 Al	UCLA	0.15	0.74	Mechanical polish, Brytal electropolish 15 min., anodize in 15% H_2SO_4
AZ31BMg	LAD/NAA	0.50	0.80	Sandpaper treated, white HAE 65V, 40 min.
AZ31BMg	LAD/NAA	0.70	0.60	Sandpaper treated, 1/2 strength white HAE 85V, 4 min.
Fused Silica		0.10	0.80	Developed by Corning Research Laboratory. Resistant to ultraviolet and particle radiation

TABLE A-3

RADIATION CHARACTERISTICS OF COATINGS ON SUBSTRATA

Substrate	Coating	Thickness (inches)	Tested by	Solar Absorptivity α_s	Infrared Emissivity ϵ	α_s/ϵ
321 SS	PR-2 Enamel (Allied Chem.)	0.003	LAD/NAA	0.20	0.90	0.22
321 SS	3385 Melamine (Allied Chem.)	0.010	LAD/NAA	0.17	0.94	0.17
1199 A1	B-66 Acryloid	0.002	LAD/NAA	0.24	0.85	0.28
1199 A1 Polished	B-72 Acryloid (Rohm & Hass)	0.001	LAD/NAA	0.20	0.60	0.33
1199 A1 Polished	B-82 Acryloid	0.005	LAD/NAA	0.23	0.80	0.29
321 SS	B-66 Acryloid TiO_2	0.006	LAD/NAA	0.21	0.80	0.26
321 SS	B-82 Acryloid TiO_2	0.003	LAD/NAA	0.23	0.80	0.29
321 SS	B-72 Acryloid TiO_2	0.002	LAD/NAA	0.24	0.85	0.28

The semiactive thermal control subsystem is the most complex of the subsystems considered applicable for the SMS. Its reliability is therefore the smallest. In this system, individual component damage has pronounced effects on the entire system. Key component redundancy is vital (and not too costly insofar as weight) for increased subsystem reliability.

APPENDIX B - SYSTEM RELIABILITY

A. ESTIMATING SYSTEM RELIABILITY REQUIREMENTS

At an early stage in the design of a satellite system, it will become necessary to estimate the major subsystem and component reliability values which must be attained in order to realize a specified minimum overall system reliability level. After this preliminary determination of subsystem reliability requirements, a prediction of attainable reliability should be made for each subsystem and principal component so that a fair estimate of the degree of development and of the redundancy requirements can be made.

As illustrated in Figure B-1, the reliability of the overall SMS system is equal to the product of the reliabilities of its major subsystems. The reliability of any device may be defined as the probability that it will render adequate performance for the period of time intended, under the operating conditions encountered. Sometimes, this probability is referred to as the "probability of survival."

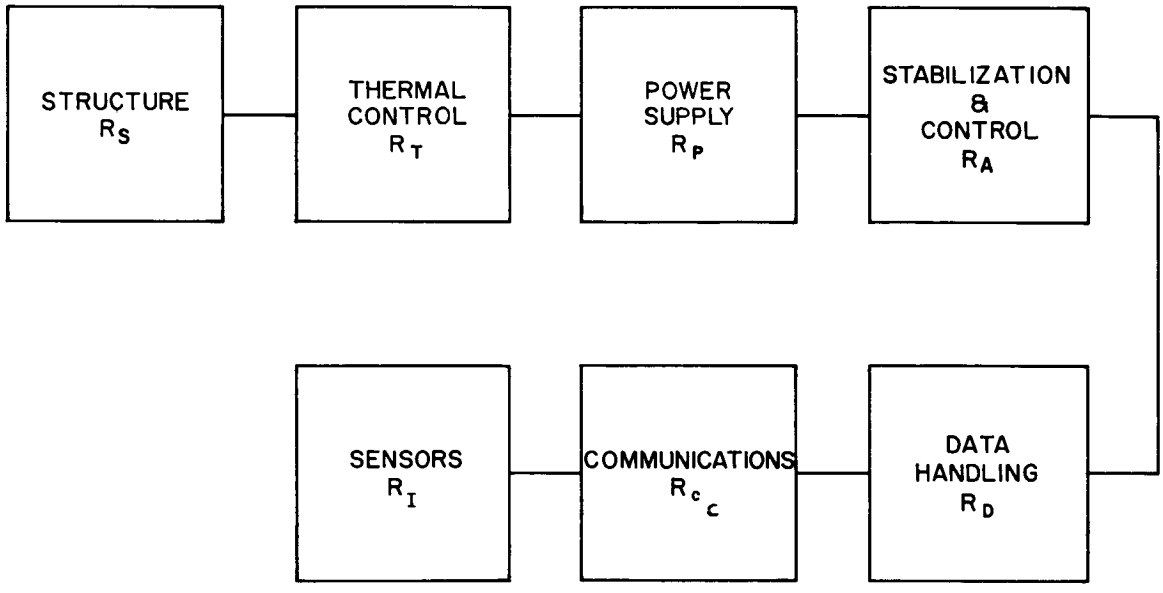

Figure B-1. System Reliability Model

The probability that a given device will render satisfactory performance at the time t, measured from the beginning of the mission, is given by the well known exponential law of reliability: $R(t) = e^{-\lambda t}$, where λ is the chance, or random, failure rate. Where several statistically independent subsystems are required to function jointly, the probability that all will function satisfactorily is the product of their individual reliabilities. Using the exponential formula, the

TABLE B-1
EXPONENTIAL FUNCTION e^{-x}

x	e^{-x}	x	e^{-x}	x	e^{-x}	x	e^{-x}
0.000	1.0000	0.260	0.7711	0.520	0.5945	0.780	0.4584
0.010	0.9900	0.270	0.7634	0.530	0.5886	0.790	0.4538
0.020	0.9802	0.280	0.7558	0.540	0.5827	0.800	0.4493
0.030	0.9704	0.290	0.7483	0.550	0.5769	0.810	0.4449
0.040	0.9608	0.300	0.7408	0.560	0.5712	0.820	0.4404
0.050	0.9512	0.310	0.7334	0.570	0.5655	0.830	0.4360
0.060	0.9418	0.320	0.7261	0.580	0.5599	0.840	0.4317
0.070	0.9324	0.330	0.7189	0.590	0.5543	0.850	0.4274
0.080	0.9231	0.340	0.7118	0.600	0.5488	0.860	0.4232
0.090	0.9139	0.350	0.7047	0.610	0.5434	0.870	0.4190
0.100	0.9048	0.360	0.6977	0.620	0.5379	0.880	0.4148
0.110	0.8958	0.370	0.6907	0.630	0.5326	0.890	0.4107
0.120	0.8869	0.380	0.6839	0.640	0.5273	0.900	0.4066
0.130	0.8781	0.390	0.6771	0.650	0.5220	0.910	0.4025
0.140	0.8694	0.400	0.6703	0.660	0.5169	0.920	0.3985
0.150	0.8607	0.410	0.6637	0.670	0.5117	0.930	0.3946
0.160	0.8521	0.420	0.6570	0.680	0.5066	0.940	0.3906
0.170	0.8437	0.430	0.6505	0.690	0.5016	0.950	0.3867
0.180	0.8353	0.440	0.6440	0.700	0.4966	0.960	0.3829
0.190	0.8270	0.450	0.6376	0.710	0.4916	0.970	0.3791
0.200	0.8187	0.460	0.6313	0.720	0.4868	0.980	0.3753
0.210	0.8106	0.470	0.6250	0.730	0.4819	0.990	0.3716
0.220	0.8025	0.480	0.6188	0.740	0.4771	1.000	0.3679
0.230	0.7945	0.490	0.6126	0.750	0.4724		
0.240	0.7866	0.500	0.6065	0.760	0.4677		
0.250	0.7788	0.510	0.6005	0.770	0.4630		

overall combined reliability may be expressed as $R_o(t) = e^{-\lambda_o t}$ where $\lambda_o = \sum_i^n \lambda_i$. The λ_i's represent the failure rates of the individual subsystems, numbered 1 through n. In equating the overall failure rate to the sum of the individual failure rates, there is an implicit restriction that the operating time, t, be common to all subsystems, since it is treated as a common factor in the exponent.

This procedure is also applicable to components and piece-parts within subsystems and modules, as well as to subsystems within an overall system. For convenience in estimating system, subsystem, component, and piece-part reliabilities, Table B-1 and Figures B-2 and B-3 have been prepared. In the table, the exponential function e^{-x} is tabulated for values of x ranging from 0 to 1.0. This function corresponds to the reliability function, $R(t) = e^{-\lambda t}$, where the general parameter x corresponds to the λt in the exponent. For a single system, subsystem, or component, the product of the failure rate and the operating time is directly equal to x. For multi-component subsystems, and subsystem combinations, x represents the product of the sum of the individual failure rates and the common operating time, $(\sum_{i=1}^n \lambda_i t)$.

To determine the total subsystem failure rates corresponding to given levels of overall system reliability, the value of x corresponding to the specified reliability is determined from either the graphs or the table. This value of x must be divided by the number of operating hours required (8760 hours for a one-year mission) to obtain the failure rate. For example, a reliability of 0.99 for one year corresponds to a value of 0.01 for the exponent, x. The failure rate, λ_o, is equal to 0.01 divided by 8760, or 1.142×10^{-6} failures per hour. The mean time before failure (MTBF), represented by m, is the reciprocal of the failure rate, or 876,000 hours per failure. Table B-2 shows the relation between overall satellite reliability, total failure rate, and MTBF for a one-year mission.

TABLE B-2
OVERALL SMS RELIABILITY VS. TOTAL FAILURE RATE AND MTBF REQUIRED FOR A ONE-YEAR MISSION

(8760 hours)

Overall SMS Reliability	$\lambda_o \left(\frac{\text{Failures}}{\text{Hour}}\right)$	m - MTBF $\left(\frac{\text{Hours}}{\text{Failure}}\right)$
0.99	1.14×10^{-6}	876,000
0.95	5.71×10^{-6}	175,200
0.90	11.42×10^{-6}	87,600
0.85	16.27×10^{-6}	54,800
0.80	25.11×10^{-6}	39,900
0.75	33.11×10^{-6}	30,000
0.70	40.81×10^{-6}	24,300
0.65	49.09×10^{-6}	20,400
0.60	58.22×10^{-6}	17,150
0.50	78.77×10^{-6}	12,700

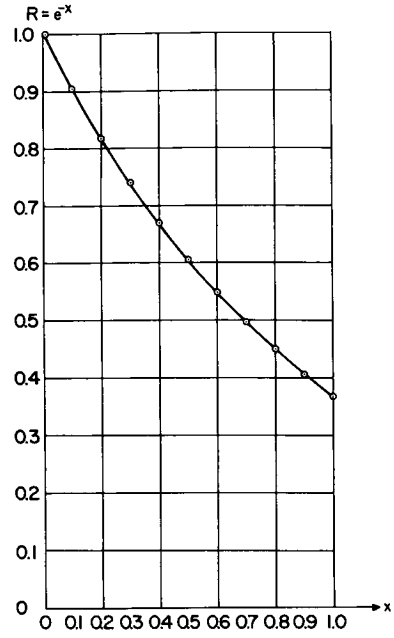

Figure B-2. Exponential Reliability Function - Range 0 to 1.0

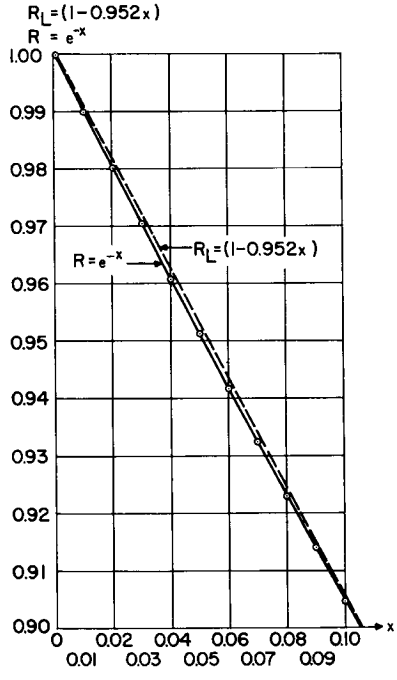

Figure B-3. Exponential Reliability Function - Range 0 to 0.1

Considering the overall SMS system as composed of seven major subsystems, all of which must function properly for a successful mission, the sum of these seven individual failure rates will determine the overall system failure rate, λ_o, and hence, the overall reliability. In the general case, the individual subsystem failure rates will differ from each other, depending upon subsystem configuration and component failure rates. To get a first estimate of the levels of subsystem reliability required for the overall system reliability range of 0.50 to 0.99, it can be assumed that six of the subsystems each have the same failure rate, and the seventh, corresponding to the structure, has a zero failure rate (reliability = 1). Thus, the individual failure rates will be equal to one-sixth of the overall failure rates. In terms of the parameter $x = \lambda t$, the value of $x_o = \lambda_o t$, corresponding to the overall system, is related to $x_i = \lambda_i t$, which represents the individual subsystems, according to $x_i = \frac{x_o}{6}$. Table B-3 expresses the relations between overall reliability and individual subsystem reliability for the case where $x_i = \frac{x_o}{6}$.

TABLE B-3

OVERALL SYSTEM RELIABILITY VS. INDIVIDUAL SUBSYSTEM RELIABILITY $\left(x_i = \frac{x_o}{6}\right)$

Overall SMS Reliability	x_o	x_i	Individual Subsystem	
			Reliability	Average Failure Rate (Failure/Hour)
0.99	0.01	0.00167	0.9983	0.190×10^{-6}
0.95	0.05	0.00833	0.9915	0.952×10^{-6}
0.90	0.10	0.0167	0.9826	1.903×10^{-6}
0.85	0.16	0.0267	0.9733	3.045×10^{-6}
0.80	0.22	0.0367	0.9635	4.185×10^{-6}
0.75	0.29	0.0483	0.9532	5.518×10^{-6}
0.70	0.36	0.0600	0.9423	6.801×10^{-6}
0.65	0.43	0.0716	0.9306	8.181×10^{-6}
0.50	0.69	0.1150	0.8905	13.128×10^{-6}

Although Table B-3 assumes a uniform level of reliability among six major subsystems, which may not conform exactly with the failure characteristics of the actual equipment, it does serve a useful purpose in illustrating the level of subsystem reliability and the average subsystem failure rate necessary to provide various specified levels of overall system reliability. A reliability of 0.8905 is required in each subsystem to produce even 0.50 reliability in the overall system. For higher overall system reliability levels, the required subsystem reliabilities increase rapidly. This table shows the need for maintaining a high level of reliability, and a corresponding low average failure rate among the subsystems.

It should be noted that the subsystem reliability range of 0.8905 to 0.9983, which corresponds to the respective overall system reliability range of 0.50 to 0.99, applies only to each composite subsystem, and not to the components and piece parts within any subsystem. While the overall system has been classified into seven major subsystems for convenience in handling the reliability study, each of these subsystems, excluding the structure, will be composed of a multitude of components and piece-parts which must have much higher individual reliabilities, and corresponding failure rates many orders of magnitude lower than those of the subsystems.

An estimate of the complexity of the SMS system has placed the number of individual components at approximately 10,000. On this basis, Table B-4 was formulated to show the average component failure rate needed to maintain specified levels of overall system reliability.

TABLE B-4
AVERAGE COMPONENT VS. OVERALL SMS SYSTEM RELIABILITIES REQUIRED AND FAILURE RATES FOR A 10,000-COMPONENT SYSTEM FOR A ONE-YEAR MISSION (8760 Hours of Operation)

Overall SMS System		Average Component	
Reliability	Failure Rate (Failures/Hour)	Reliability	Failure Rate (Failures/Hour)
0.99	1.14×10^{-6}	0.999999	1.14×10^{-10}
0.95	5.71×10^{-6}	0.999995	5.71×10^{-10}
0.90	11.42×10^{-6}	0.999990	11.42×10^{-10}
0.85	18.27×10^{-6}	0.999984	18.27×10^{-10}
0.80	25.11×10^{-6}	0.999978	25.11×10^{-10}
0.75	33.11×10^{-6}	0.999971	33.11×10^{-10}
0.70	40.81×10^{-6}	0.999964	40.81×10^{-10}
0.65	49.09×10^{-6}	0.999957	49.09×10^{-10}
0.60	58.22×10^{-6}	0.999949	58.22×10^{-10}
0.50	78.77×10^{-6}	0.999931	78.77×10^{-10}

B. SYSTEM RELIABILITY PREDICTIONS

When the design of a satellite system has progressed to the stage where the functional requirements of each major subsystem and component have been specified, and these functions can be performed by particular types of equipment, it is possible to make a quantitative prediction of subsystem and overall system reliability.

To make a prediction of overall system reliability, it is first necessary to make predictions of the reliability of each subsystem. Subsystem reliability can be predicted on the basis of failure rates and useful, maintenance-free life figures quoted by suppliers, and from analyses based upon component failure rates obtained from

manufacturers' data sheets and reliability handbooks. The failure rate of a subsystem is determined by adding the failure rates of all of its components. The failure rate of the overall system is then determined by adding the failure rates of all of its subsystems. Overall system and subsystem reliability can be determined from the formula: $R = e^{-\lambda t}$, where R is the reliability (or probability of successful performance), λ represents either the system or subsystem failure rate, and t represents the mission duration, usually specified in terms of hours. For a one year mission, t is 8760 hours.

It is suggested that the overall system reliability be computed from a tabulation of failure rates pertaining to the following subsystems:

(1) Structure

(2) Thermal Control

(3) Power Supply

(4) Stabilization and Control

(5) Sensors

(6) Communications

(7) Data Handling

For either the overall system or the individual subsystems, the reliability can be determined directly from the exponential function $R = e^{-\lambda t}$, where x represents the product λt. The value of R as a function of x can be found in Table B-1 or in Figures B-2 and B-3.

C. REDUNDANCY AND TRADE-OFF DECISIONS

By comparing the predicted overall system and subsystem reliability values with those required for a specified minimum overall system reliability level, those areas in which improvement is necessary will be revealed. Since overall system reliability is determined by the product of all the subsystem reliabilities, the most significant improvement will result from improvement of the least reliable subsystem. The least reliable subsystem or element within a subsystem imposes an inherent limitation upon the overall system reliability. For example, if six of the seven major subsystems in the SMS have reliability values of 0.9999 or better and the seventh has a reliability of 0.8000, no amount of improvement in the six high-reliability subsystems can raise the overall system reliability above 0.8000, the limit imposed by the least reliable subsystem.

When it comes to the question of reliability trade-off, raising the reliability of the least reliable element is generally preferable. Thus, in the foregoing example, it would be better to give up any redundancies which would raise 0.99-reliable elements to 0.9999 in order to have available sufficient weight, volume, and/or parametric allowances which would permit the addition of redundancy to a 0.8000-reliable system. Two elements which are each 0.8000 reliable will produce a parallel redundant combination having a 0.9600 reliability.

Figure B-4 shows the effect of redundancy upon the reliability of parallel redundant combinations of up to four elements as a function of the reliability of the common element. This graph is really a plot of the combined versus the common element failure probabilities, with reliability scale added. The failure probability of the combination, Q_S, varies as the Nth power of the common element failure probability, Q_I, according to the equation $Q_S = [\, Q_I \,]^N$, where N represents the number of elements in parallel redundancy. The reliability scale is simply $R_S = [\, 1-Q_S \,]$ for the combination and $R_I = [\, 1-Q_I \,]$ for the common elements.

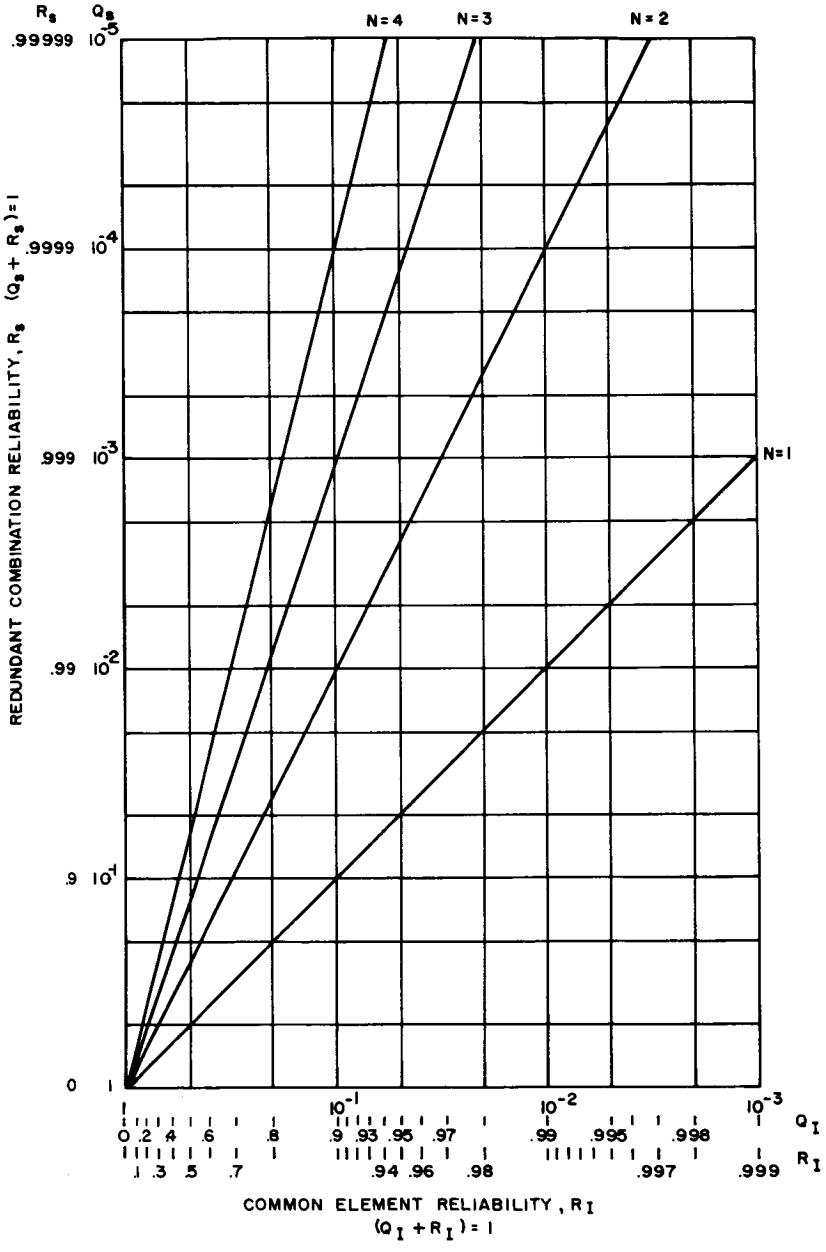

Figure B-4. Reliability Improvement of Redundancy